DYNAMIC MODELLING AND OPTIMIZATION OF POLYMERIZATION PROCESSES IN BATCH AND SEMI-BATCH REACTORS

W.H.B.W. IBRAHIM

PhD

UNIVERSITY OF BRADFORD

2011

DYNAMIC MODELLING AND OPTIMIZATION OF POLYMERIZATION PROCESSES IN BATCH AND SEMI-BATCH REACTORS

Dynamic Modelling and Optimization of Bulk Polymerization of Styrene, Solution Polymerization of MMA and Emulsion Copolymerization of Styrene and MMA in Batch and Semi-batch Reactors using Control Vector Parameterization Techniques

W.H.B.W. IBRAHIM

Submitted for the Degree of Doctor of Philosophy

School of Engineering, Design & Technology,

University of Bradford,

UK

2011

This thesis is dedicated to the memory of my late father, Wan Ibrahim.
My beloved father died peacefully during the course
of my study on 21 November 2008.
I miss him and will continue to miss him greatly, every day…

For my caring and lovely husband, Hasminizam,
and my wonderful children, Nur Aliya and Irfan.
They supported me throughout and waited patiently while I studied…

For my wonderful mother, Shamsiah.
Through thick and thin, always behind me…

Abstract

Keywords: Bulk polymerization, solution polymerization, emulsion copolymerization, batch reactor, temperature, modelling, optimization, gPROMS

Dynamic modelling and optimization of three different processes namely (a) bulk polymerization of styrene, (b) solution polymerization of methyl methacrylate (MMA) and (c) emulsion copolymerization of Styrene and MMA in batch and semi-batch reactors are the focus of this work. In this work, models are presented as sets of differential-algebraic equations describing the process. Different optimization problems such as (a) maximum conversion (X_n), (b) maximum number average molecular weight (M_n) and (c) minimum time to achieve the desired polymer molecular properties (defined as pre-specified values of monomer conversion and number average molecular weight) are formulated. Reactor temperature, jacket temperature, initial initiator concentration, monomer feed rate, initiator feed rate and surfactant feed rate are used as optimization variables in the optimization formulations. The dynamic optimization problems were converted into nonlinear programming problem using the CVP techniques which were solved using efficient SQP (Successive Quadratic Programming) method available within the gPROMS (general PROcess Modelling System) software.

The process model used for bulk polystyrene polymerization in batch reactors, using 2, 2 azobisisobutyronitrile catalyst (AIBN) as initiator was improved by including the gel and glass effects. The results obtained from this work when compared with the previous study by other researcher which disregarded the gel and glass effect in their study which show that the batch time operation are significantly reduced while the amount of the initial initiator concentration required increases. Also, the termination rate constant decreases as the concentration of the mixture increases, resulting rapid monomer conversion.

The process model used for solution polymerization of methyl methacrylate (MMA) in batch reactors, using AIBN as the initiator and Toluene as the solvent was improved by including the free volume theory to calculate the initiator efficiency, *f*. The effects of different *f* was examined and compared with previous work which used a constant value of *f* 0.53. The results of these studies show that initiator efficiency, *f* is not constant but decreases with the increase of monomer conversion along the process.

The determination of optimal control trajectories for emulsion copolymerization of Styrene and MMA with the objective of maximizing the number average molecular weight (M_n) and overall conversion (X_n) were carried out in batch and semi-batch reactors. The initiator used in this work is Persulfate $K_2S_2O_8$ and the surfactant is Sodium Dodecyl Sulfate (SDS). Reduction of the pre-batch time increases the M_n but decreases the conversion (X_n). The sooner the addition of monomer into the reactor, the earlier the growth of the polymer chain leading to higher M_n. Besides that, M_n also can be increased by decreasing the initial initiator concentration (C_{i0}). Less oligomeric radicals will be produced with low C_{i0}, leading to reduced polymerization loci thus lowering the overall conversion. On the other hand, increases of reaction temperature (T_r) will decrease the M_n since transfer coefficient is increased at higher T_r leading to increase of the monomeric radicals resulting in an increase in termination reaction.

Acknowledgements

I would like to express my sincere gratitude to Professor I.M. Mujtaba for his invaluable guidance and advice, continuous co-operation, valuable comments, suggestions, unlimited help and support throughout this work.

I would also want to extend my sincere gratitude to Dr. E. Ekpo and Dr. B. Alhamad for their wonderful cooperation and support in my study.

Thanks also go to all staff members of School of Engineering Design and Technology. In particular, I would like to thank John Purvis, Mick Cribb, Ian McKay, for their help and support.

I want to express my gratitude to my parents for their enormous love, brothers and sisters for their unconditional support and encouragement. My warmest thanks go to my husband, my daughter and my son for their love, understanding, and patience, during my study.

Above all, I am very much grateful to almighty Allah for giving me courage and good health for completing the venture.

Presentation and Publication From This Work

1. Optimisation of emulsion co-polymerization of styrene and MMA in semi-batch reactor, CAPE Ph.D. Poster Day 2010, Wednesday 12 May 2010, University of Leeds.

2. Optimisation of emulsion co-polymerization of styrene and MMA in semi-batch reactor, IChemE - PAPS III (Practical Aspects of Process Safety 3), 19 May 2010, Cedar Court Hotel, Bradford.

3. Optimisation of Emulsion Copolymerization of Styrene and MMA in Batch and Semi-batch Reactor, CAPE Forum, 21 – 22 March 2011, University of Bradford.

4. Optimisation of Emulsion Copolymerization of Styrene and MMA in Semi-batch Reactor, 14th International Conference on Process Integration, Modelling and Optimisation for Energy Saving and Pollution Reduction, 8 – 11 May 2011, Florence, Italy. *poster presentation

5. Wan Ibrahim W.H., Mujtaba I. and Alhamad B., (2011), Optimisation of Emulsion Co-polymerization of Styrene and MMA in Semi-batch Reactor, *Chemical Engineering Transaction*, 25, 249-254.

6. Optimisation of Emulsion Copolymerization of Styrene and MMA in Batch and Semi-batch Reactor, *Paper submitted to Chemical Product and Process Modelling.

TABLE OF CONTENT

Formatted: Font: Bold

Formatted: List Paragraph, Outline numbered + Level: 2 + Numbering Style: 1, 2, 3, … + Start at: 1 + Alignment: Left + Aligned at: 1.13 cm + Indent at: 1.9 cm

Formatted: Indent: Before: 2 cm

Formatted: Indent: Before: 1.9 cm, Hanging: 0.6 cm

Formatted: Indent: Before: 2.5 cm, First line: 0 cm

Formatted: Indent: Before: 1.9 cm, No bullets or numbering

LIST OF FIGURES

LIST OF TABLE

NOMENCLATURE

a	Density of reacting mixture
A	Area of reactor, m^2
A_d	Pre-exponential factor for initiator decomposition, s^{-1}
A_p	Pre-exponential factor for Propagation, *l/gmol-s*
A_t	Pre-exponential factor for termination, *l/gmol-s*
c	Initiator conversion used in styrene model
$C_{i,o}$	Initial concentration of initiator for MMA model, $kmol/m^3$
C_i	Initiator concentration for MMA model, $kmol/m^3$
$C_{m,o}$	Initial monomer concentration for MMA model, $kmol/m^3$
C_m	Monomer concentration for MMA model, $kmol/m^3$
C_p	specific heat of reaction, *cal/g-K* for styrene and *kJ/kg-K* for MMA
C_{pj}	Specific heat of cooling liquid, *cal/g-K* for styrene and *kJ/kg-K* for MMA
$C_{p,p}$	Specific heat capacity of polymer, *kJ/kg-K*
$C_{p,m}$	Specific heat capacity of monomer, *kJ/kg-K*
$C_{p,s}$	Specific heat capacity of solvent, *kJ/kg-K*
C_s	Solvent concentration, $kmol/m^3$
$C_{s,0}$	Initial solvent concentration, $kmol/m^3$
C_z	Inhibitor Concentration, $kmol/m^3$
D	Parameter in gel effect equation
E_d	Activation Energy for initiator decomposition, *cal/gmol*
E_p	Activation Energy for propagation, *cal/gmol*
E_t	Activation Energy for termination, *cal/gmol*
f	Initiator Efficiency
f_z	Number of radicals consumed per inhibitor molecule, dimensionless
F	Constant in heat transfer equation
$f_c(m)$	Ratio of the monomer conversion rate in the second stage to its initial value in styrene thermal model
F_j	Coolant flow rate, m^3/s
I_0	Initial Initiator Concentration for styrene model, *gmol/l*
I	Initiator Concentration for styrene model, *gmol/l*
k_d	Kinetic constant for initiator decomposition, s^{-1}
k_{fm}	Kinetic constant for transfer to monomer, $m^3/kmol\text{-}s$
k_{fs}	Kinetic constant for transfer to solvent, $m^3/kmol\text{-}s$

k_p	Kinetic constant for propagation, *l/gmol-s* (styrene) and m^3*/kmol-s* (MMA)
k_{po}	Initial kinetic constant for propagation, m^3*/kmol-s*
K_t	Rate constant for termination, *l/gmol-s* (styrene) and m^3*/kmol-s* (MMA)
k_{to}	Initial kinetic constant for termination, m^3*/kmol-s*
K_n	*(n=1,2..),* Rate expressions for styrene model equations
$K_{\theta p}$	Parameter in gel effect equation, s^{-1}
$k_{\theta t}$	Parameter in gel effect equation, s^{-1}
k_z	Kinetic constant for inhibition, m^3*/kmol-s*
m	Monomer conversion used in the styrene model
M_2	Number average molecular weight of polymer chains formed in the second stage for the styrene thermal model, *g/mol*
M_f	Final number average molecular weight in styrene thermal model, *g/mol*
M	Initial Monomer concentration for styrene model, *gmol/l*
$M_{mth,rad}$	Number average molecular weight of polymers formed at the end of the first stage for the thermal polymerisation model, *g/mol*
M_n	Number average molecular weight, *kg/kmol*
M_w	Weight average molecular weight, *kg/mol*
MW_i	Molecular weight of initiator, *kg/mol*
MW_m	Molecular weight of monomer, *kg/mol*
MW_s	Molecular weight of solvent, *kg/mol*
P_D	Poly-dispersity Ratio used in styrene model
P_{DI}	Poly-dispersity index used in MMA model
Q_W	Heat supplied by reactor heater, *cal/s*
Q_r	Heat generated by reaction, *cal/s* for styrene model and *kJ/s* for MMA
Q_j	Heat transferred to cooling liquid, *cal/s*
R_g	Universal Gas Constant, *cal/gmol-K* for styrene and *kJ/kmol-K* for MMA
R_p	Rate of polymerisation, *gmol/l-s* for styrene and *kmol/*m^3*s* for MMA
r_0	Rate of radical formation, *gmol/l-s* for styrene and *kmol/*m^3*s* for MMA
S	Constant in heat transfer equation
t_f	Final batch time, *s*
T	Reactor Temperature, *K*
T_J	Jacket of coolant temperature, *K*
T_{J0}	Inlet Temperature of cooling liquid, *K*
T_{JSP}	Jacket temperature set point, *K*
T_{rsp}	Reactor Temperature se point, *K*
U	Overall heat transfer coefficient, *cal/s-*m^2*-K* (styrene), *kJ/s-*m^2*-K* (MMA)

V	Volume of reactor, *litres* for styrene model and m^3 for MMA model
V_J	Volume of Coolant, *litres* for styrene model and m^3 for MMA model
X_i	Initiator conversation used in MMA model
X_n	Number average molecular weight
X_w	Weight Average Molecular Weight
X_m	Monomer conversion used in MMA model

Greek letters

ξ_n	*(n=0,1,2), nth* dead polymer moment for styrene model, dimensionless
	Also, *nth* living polymer moment for MMA model, $kmol/m^3$
ΔH_r	Heat of polymerisation, *cal/gmol* for styrene model and *kJ/kmol* for MMA model
ρ	Density of reaction for styrene model, *g/l*
ρ_{mix}	Density of reacting mixture for MMA model, kg/m^3
ρ_m	Density of MMA monomer, kg,m^3
ρ_J	Density of Cooling liquid, *g/l* for styrene and *kg/m3* for MMA model
ρ_p	Density of Polymer, kg/m^3
μ_r	Viscosity of initial reactor content, *cp*
φ_m	Volume fraction of monomer, dimensionless
φ_P	Volume fraction of polymer, dimensionless
μ_n	*(n=0,1,2),* nth moment of dead polymer chains for MMA model, $kmol/m^3$
τ_J	Jacket time constant, *s*

ABBREVIATION

AIBME	2,2' - azodiisobutyrate
AIBN	2-2 Azobisisobutyronitrile catalyst
AVN	2,2',4,4 - tetramethyl - 2,2'-azovaleronitrile
BA	Butyl Acrylate
CSTR	Continuous Stirred Tank Reactor
CTA	Chain Transfer Agent
CVP	Control Vector Parameterization
DAEs	Differential-Algebraic Equations
DAOP	Differential Algebraic Optimization Problem
DMP	Discrete Maximum Principle
EA	Evolutionary Algorithms
gPROMs	General Process Modelling System
GRG	Generalized Reduced Gradient
IDP	Iterative Dynamic Programming
jcrit	Critical Size For Homogeneous Nucleation
$K_2S_2O_8$	Potassium Persulfate Catalyst
KPS	Potassium Peroxodisulfate
M	Monomer
MMA	Methacrylate
Mn	Number Average Molecular Weight
MWD	Molecular Weight Distribution
Na-MMT	Sodium Montmorillonite
NLP	Nonlinear Program
OC	Orthogonal Collocation
P	Polymer
PMMA	Polymethyl Methacrylate
PMP	Pontryagin's Maximum Principle
PS	Polystyrene
PSD	Particle Size Distribution
QSSA	Quasi Steady State Assumption
S	Solvent
SLS	Sodium Laurylsulfate
SQP	Successive Quadratic Programming
T	Transfer Agent
TB	Tert-Butanol
TSPM	Three Stage Polymerization Model
VA	Vinyl Acetate
VAC	Vinyl Acetate

Chapter One

Introduction

1.1 Introduction

Batch processes occupy an important position in chemical industry, especially with regards to manufacturing specialty chemicals, pharmaceuticals, bio-products and polymers (Zhou and Yuan, 2004). Their flexibility and convenient operation ensure that batch reactors are often used in manufacturing of small volume products that have a high added value. Batch reactors are also helpful in the production of goods whose demands are seasonal as sometimes, only a few batches per annum are required to meet the demand for an unusual product.

Polystyrene is a widely used polymer with many day-to-day uses which is certainly in the interest of this billion-Euro-a-year business that production be optimized (Ekpo and Mujtaba, 2004). According to Lyulin and Michels (2002), polystyrene is probably only polyethylene which is more common in our daily life for its inexpensive and hard plastic. Some of the products made out of polystyrene are model cars and airplanes, the outside housing of the computer, clear plastic drinking cups and it also is made in the form of foam packaging and insulation. Besides that,

polystyrene is also used in toys, and the housings of things like hairdryers and kitchen appliances a lot of the moulded parts on the inside of a car, like the radio knobs.

Polymethyl methacrylate (PMMA) is a synthetic polymer of methyl methacrylate (MMA). It is often used as a light or shatter-resistant alternative to glass because of its transparent thermoplastic (Arora et al., 2010; Ekpo, 2006). It has a wide range of uses in medicine, being used as a component of implants, bone cement, in dentures and also implanted lens in the eyes.

Polymerization is basically the joining end to end of monomers. The distribution of these repeat units in the final product is defined as the molecular weight distribution (MWD) (Rudin, 1999). The MWD can be represented by its statistical properties, using moments of the distribution (Lorenzini et al., 1992). Materials with different MWD will have different properties. The width of the MWD also important, especially for the mechanical properties of the polymer produced. Certain desired mechanical and physical properties of a polymer product can be improved by controlling the molecular weight and its distribution (Kiparissides, 1996).

Molecular weight of a polymer is an important factor for determining its physical properties (Gilbert, 1995; Clay and Gilbert, 1995). Different molecular weight of polymer can have different properties, such as different temperatures for transition from liquids to waxes, different mechanical properties such as stiffness, strength, viscoelasticity, toughness and also viscosity of the polymer. A high molecular weight material exhibits a higher melt viscosity, which is above its crystalline melting point.

A higher molecular weight material also has a higher modulus of elasticity and thus, will give higher mechanical strength. A breadth of the MWD of a polymer may significantly affect its suitability for certain applications. For example, the best balance of processing characteristics and tensile strength for the process of extrusion can be achieved when the molecular weight distribution is as narrow as possible.

Monomer conversion is another important factor that can influence mechanical, physical and biocompatible properties of the resultant polymer (Holmes et al., 2007; Asmussen and Peutzfeldt, 2001). However, the monomer conversion is never complete when monomers in a resin composite polymerize to form a polymer (Asmussen and Peutzfeldt, 2001). This makes the resultant polymer still has numerous unreacted double bonds (Holmes et al., 2007).

Polymer structure and properties normally cannot be modified after it is produced, all required characteristics need to be clearly defined before the polymerization process begins. As the polymerization is under way, only few parameters can be controlled and one of this is the temperature of the reacting mixture.

The Gel Effect also known as Tromsdorff-Norrish-Smith Effect or auto acceleration, which only occur during polymerizations with high concentrations of monomer (Kalfas and Ray, 1993; Rudin, 1999; Chiu et al., 1983). During the early stage of the polymerizations, the kinetic rate constant for initiation is equal with initial kinetic rate constant for termination. As time proceeds the polymer concentration will increase. This high concentration hinders the diffusion of chains because of entanglements, so the rate of termination slows considerably. In diluted solutions, the

viscosity never builds up to the point where the diffusion of chains is slowed, so the gel effect does not occur. This auto acceleration phenomenon strongly affects the end-use properties of the produced polymer as it leads to broader molecular weight distribution (Verros et al., 2005).

The glass effect is related to the decrease in the propagation rate constant caused by a decreased in mobility of monomer molecules due to the 'freezing' of the reaction mixture at the glass transition temperature (Achilias and Kiparissides, 1992). It appears in the polymerization reactions taking place at a temperature below the glass transition temperature of the polymer. As a consequence from this phenomenon, the reaction mixture will freeze below 100% and for styrene it is around 95% (Wolff and Bos, 1997).

The decomposition of initiator molecules at the beginning of the process to form very active primary radicals are dependant on the initiator efficiency, *f*. The decomposition of the initiator does not form 100% primary radicals since some of them might either have self-terminate or react with other reactants in the systems (Medeiros et al., 2010; Kiparissides, 1996). The value of initiator efficiency is not constant and will decrease with the increase of viscosity inside the reactor (Capek, 2001, Medeiros et al., 2010).

The bulk polymerization is the simplest of all polymerization processes since the conversion of monomer into a polymer will occur without any solvent other than catalyst (Asua, 2007). Initiator will be added to the process to initiate the addition

polymerization by forming primary free radicals. The viscosity of the reaction mixture change as the concentration of the monomer decreases continuously.

Solution polymerization is a polymerization process which incorporates solvent in the reactor process to aid in efficient heat transfer (Odian, 2004). At the beginning of the process, initiator and solvent are added into the reactor. Initiator will initiate the polymerization process by decomposition to form primary free radicals. These free radicals then will react with the monomer added in the reactor in homogeneous solution until the end of the process.

Basic ingredients or recipe for emulsion polymerization are water, surfactant, monomer and initiator where the system is agitated to form emulsion (Gilbert, 1995). The monomer are dispersed and emulsified with the surfactant in the water phase. Micelles are created from the excess surfactant in the water. Then initiators are added to the reactor to initiate the free radical polymerization process. Initiator is decomposed to form free radical initiator in the water phase. These radicals then react with monomer in the aqueous phase forming oligomeric radicals. These oligomeric radicals then continue to propagate until it reaches a degree of polymerization z when they become *surface active* (Gilbert, 1995, Zeaiter et al., 2002, Coen et al., 2004). Besides continuing propagation, these oligomeric radical also can terminate in the aqueous phase by termination or radical transfer.

1.2 Scope of This Research

According to Ekpo and Mujtaba (2008), the optimization of batch reactors has been researched since the early work of Denbigh. It is necessary to operate them in optimal condition to produce as many profitable products as possible while minimizing the generation of waste or undesirable by products.

Focus of this report is the modeling and optimization of three different polymerization process namely bulk polymerization of styrene, solution polymerization of methyl methacrylate (MMA) and emulsion copolymerization of styrene and MMA. Method used for optimization is the Control Vector Parameterization (CVP) technique. Dynamic optimization method has been used in order to find the optimal control variable profile that will yield a desired level of monomer conversion (X_n) and number average molecular weight (M_n) in a batch and semi-batch reactor. The batch time is divided into a finite number of intervals, and a piecewise constant temperature is used in each interval. In each interval, the temperature and length of the interval are optimized. The objective of solving the dynamic optimization for batch polymerization in this work is to find optimal control variable profiles that can be used in the polymerization system for desired product properties.

The Control Vector Parameterization (CVP) technique is employed in this work for the dynamic optimization of the process. Different mathematical models are used for the dynamic optimization in order to find optimal profiles for control variables used in this work. The optimization process for this work is for minimization of

production time values, maximization of the number average molecular weight and maximization of overall monomer conversion. All of these are based on a desired and fixed level of monomer conversion, number average chain length, polydispersity and batch time.

The general Process Modelling System (gPROMS) software is employed in this work to carry out the dynamic optimization problems for the polymerization batch reactor of polystyrene. This software is a powerful tool and can be used to solve the simulation and optimizations problems. Among its other advantages are modelling and solution power, project environment, multiple activities using the same model, integrated steady state and dynamic capabilities, and also it has sophisticated optimization capabilities ((PSE), 2007). The users of this software are able to build high accuracy models of their production facilities, make significant savings in process capital and operating costs while improving safety and environmental compliance via optimisation. Due to the advantages listing above among many others, gPROMS is chosen for the modelling, simulation and optimization of processes in this work.

The research on the diffusion control in bulk polymerization was started by Balke (1973) and Balke and Hamielec (1973) for MMA polymerization with AIBN initiator (Cunningham and Mahabadi, 1996). Baillagou and Soong (1985b) developed gel effect model for the polymerization of MMA under nonisothermal condition. Arai (1986) studied the bulk thermal polymerization of styrene which introduced gel effect into each elementary reaction by considering the decrease of segmental jump frequency during the polymerization. Soots and Stanford (1991) studied the gel-

effect for the batch solution polymerization of styrene with toluene. They also used AIBN as the initiator. A new framework was proposed by Achilias and Kiparissides (1992) for modeling the diffusion-controlled free radical polymerization for solution MMA. Raja (1995) and Ekpo (2004) studied the bulk polymerization of styrene with AIBN, however, the gel and glass effect was not included in their model. In this work, the process model of bulk polymerization of styrene was improved by including the gel and glass effect.

The initiator efficiency is often considered to be constant (Achilias and Kiparissides, 1992). Wang and Matyjaszewski (1995) observed that the increase of initiator efficiency, f from 22% to 65% with the addition of 2 molar CuCl2 in the system for bulk styrene polymerization with AIBN initiator. The initiator efficiency decreases with the decrease of temperature (Xia and Matyjaszewski, 1997). A theoretical investigation of the initiator efficiency was undertaken by Kurdikar and Peppas (1994) and reported that the initiator efficiency at the start of the polymerization reaction is usually between 0.3 and 0.8 and decreases as the reaction proceeds until it reaches a limiting value of zero. Achilias (2007) used time varying initiator efficiency in his work and reported that initiation reaction could also be diffusion-controlled and should be decreased at higher conversion of bulk polymerization. Ghosh et al. (1998) improved the model of Ray et al. (1995) by allowing the value of *f* to decrease at high conversion. Ekpo and Mujtaba (2008) carried out a dynamic optimization of MMA in batch reactor and a constant value of initiator efficiency (0.53) was employed in their work. In this work, the process model is improved for the solution polymerization of MMA by using the free volume theory to calculate the initiator efficiency.

Zeaiter et al. (2002) developed the control of particle size and molecular weight distribution described by a population balance model of styrene emulsion polymerization in semi-batch process. The model developed by Saldivar (1996) was validated by Saldivar and Ray (1997) with the emulsion copolymerization of styrene and MMA. Mead and Poehlein (1989) developed a steady state model for emulsion copolymerization in a seed-fed continuous stirred tank reactor (CSTR) for Styrene-MMA and Styrene-Acrylonitrile. Another extensive kinetic model was developed by Coen et al. (1998) for the particle size distribution (PSD), particle number, particle size and amount of secondary nucleation in emulsion polymerizations. The extension of this model for zero-one system was undertaken later by Coen et al.(2004) where pseudo bulk kinetics was included in the time evolution of the particle size distribution. Alhamad et al. (2005a) developed a comprehensive model for emulsion copolymerization process of styrene and MMA. However, the model used one fixed time for the seed formation for *ab initio* system. The effect of different pre-batch time for seed formation in emulsion copolymerization of styrene and MMA is studied in this work. Besides that, the simulation was carried out in batch and semi-batch process without pre-batch time.

1.3 Aims and Objectives

The aim of this work is to study the modeling and optimization of bulk polymerization of Styrene, solution polymerization of MMA and emulsion copolymerization of Styrene and MMA in batch and semi-batch reactors.

The objectives of this work are:

A. Bulk Polymerization

i. To improve the process model used for bulk polymerization of styrene in batch reactors, using 2, 2 azobisisobutyronitrile catalyst (AIBN) as the initiator by including the gel and glass effects which was absent in the earlier work.

ii. To find an optimal temperature profile for bulk polymerization of styrene that will yield desired polymerization characteristics in minimum time.

iii. To compare the results for the dynamic optimization of the bulk polymerization of styrene with or without taking into account the gel and glass effect.

B. Solution Polymerization

i. To improve the process model used for solution polymerization of methyl methacrylate (MMA) in batch reactors, using 2, 2 azobisisobutyronitrile catalyst (AIBN) as the initiator by including the free volume theory to calculate the initiator efficiency.

ii. To find an optimal temperature profile for solution polymerization of MMA that will yield desired polymerization characteristics in minimum time.

iii. To compare the results for the dynamic optimization of the solution polymerization of MMA with using i) the free volume theory to calculate the initiator efficiency, f ii) a constant value of f.

C. Emulsion Copolymerization

i. To find an optimal temperature profile for emulsion copolymerization of styrene and MMA that will yield desired polymerization characteristics for maximization of the number average molecular weight and maximization of overall conversion with different pre-batch time in a semi-batch reactor.

ii. To find an optimal temperature profile for emulsion copolymerization of styrene and MMA that will yield desired polymerization characteristics for maximization of the number average molecular weight and maximization of overall conversion with fixed batch time and fixed the number average molecular weight in a batch reactor respectively.

1.4 Layout of the Thesis

This thesis is laid out as follows:

Chapter one presents overview on polymerization process, brief introduction on polymer and their uses, molecular weight and monomer conversion. Also the scope of this research, aim, objectives together with thesis layout have been stated.

Chapter Two gives literature reviews of past works in the field of modeling and dynamic optimization of batch and semi-batch polymerization for styrene and MMA. Furthermore, types of polymerization process namely bulk polymerization, solution polymerization, emulsion polymerization and suspension polymerization are discussed. Mechanism of free radical polymerization, gel and glass effect, initiator efficiency are also explained.

Chapter Three presents an overview of three main mathematical models for free radicals of bulk polymerization of styrene, solution polymerization of MMA and emulsion copolymerization of styrene and MMA in batch reactors. The models are discussed and presented in a way that will be used in dynamic optimization.

Chapter Four focuses on the dynamic optimization of the free radical bulk polymerization of styrene in a batch reactor using 2, 2 azobisisobutyronitrile catalyst (AIBN) as the initiator by taking into account the gel and glass effect. Two models were employed for the dynamic optimization namely simple kinetic model and detailed model, with the energy balance equation added to the simple model. The types of solutions for dynamic optimization problems and formulation for optimization of bulk polymerization of styrene in a batch reactor also discussed here.

Chapter Five focuses on the dynamic optimization of the free radical solution polymerization of MMA in a batch reactor using 2, 2 azobisisobutyronitrile catalyst (AIBN) as the initiator by using free volume theory to calculate the initiator efficiency. As before, two different models also used here; simple kinetic model and detailed model (with energy balance model). The types of solutions for dynamic

optimization problems and formulation for optimization of solution polymerization of MMA in a batch reactor are highlighted.

Chapter Six focuses on the dynamic optimization of the free radical emulsion polymerization of styrene and MMA in a batch reactor using potassium persulfate catalyst ($K_2S_2O_8$) as the initiator. Nine case studies were carried out for the maximization of the number average molecular weight and maximization of overall conversion with different problem formulation for batch and semi-batch process.

Chapter Seven concludes the thesis by discussing the achievement of this work and laying out suggestions for future work.

Chapter Two

Literature Reviews

2.1 Introduction

In this chapter, literature reviews of four most popular polymer process namely bulk polymerization, solution polymerization, emulsion polymerization and suspension polymerization will be discussed including the mechanism of free radical polymerization. There are two monomers used in this research, styrene and methyl methacrylate (MMA) for the bulk, solution and emulsion polymerization process in jacketed batch reactor. The properties and uses of styrene and methyl methacrylate are also discussed briefly. Mechanism of free radical polymerization namely chain initiation, chain propagation, chain termination and chain transfer are explained since all the polymerization processes in this work have free radical polymerization. Besides that, a review of previous works in the field of batch reactor modelling and optimization are also discussed here.

In this chapter, section 2.2 to 2.7 describe general knowledge required to carried out this research. Section 2.9 provides further review of previous work on batch polymerization which are the main focus of this research.

2.2 Polymerization Process

The most popular ways of the polymerization process in the industry today are bulk polymerization, solution polymerization, emulsion polymerization and suspension polymerization (Stevens, 1999). Each of the polymerization process has advantages and disadvantages. These polymerization processes can be carried out using different reactants, additives and reactors. Different parameters like temperatures, concentration, reaction process time, flow rate, etc control the desired end properties of the products.

2.2.1 Bulk Polymerization

Bulk polymerization is the simplest polymerization process which is carried out with the monomer itself without any addition of dilutent or carrier (Odian, 2004). However, small amounts of an initiator are present to initiate the polymerization process. Conversely, it is also the most difficult polymerization process to control as the reaction process is very exothermic. Further problem is added when the viscosity of the monomer-polymer solution is increased leading to heat transfer problem (Stevens, 1999). The major commercial uses of bulk vinyl polymerization are in casting formulation and low molecular weight polymers for use as adhesive, plasticizers and lubricant additives. Polystyrene for general purpose usually produce by bulk thermal polymerization in the temperature range from 100^{o}C to 200^{o}C (Arai et al., 1986).

Formatted: Normal, Line spacing: single

There are several advantages and disadvantages of bulk polymerization:

Advantages

- It is the simplest polymerization process
- The polymer product obtained at the end of the process is pure since no solvent added
- Large casting may be prepared directly from the polymer obtain by bulk polymerization process
- Chain transfer agent can be used to change the molecular weight distribution

Disadvantages

- The mixing becomes very difficult as the concentration of the reaction mixture inside the reactor is increased
- Heat transfer is a major problem for highly exothermic nature of free radical addition polymerization
- Broad molecular weight distribution will be obtained due to the high viscosity and no aid (solvent) for heat transfer
- Polymer with very low molecular weight will be obtained

2.2.2 Solution Polymerization

Solution polymerization incorporates solvent in the process to aid in efficient heat transfer (Stevens, 1999). However, solvent must be chosen vary carefully since it will have a big impact on the chain transfer reaction, otherwise it can limit the molecular weight (Odian, 2004). The difficulty to remove solvent completely from

the finished polymer becomes a major problem apart from the environmental concerns associated with the organic solvents (Stevens, 1999). Advantages and disadvantages of solution polymerization process are given below:

Advantages

- Better reactor temperature control compared to bulk process since the solvent used in the process will absorb the exothermic of the polymerization process.
- The viscosity of the reaction mixture will decrease and make the mixing process in the reactor easier so the autoacceleration can be avoided.
- The product can be used directly (paint, adhesive)

Disadvantages

- Molar mass of the mixture will reduce making this polymerization process not suitable for high molecular weight.
- The removal of solvent used at the end of process will raise the production cost
- Solvent used in solution polymerization must be carefully selected since it can create environmental pollution

2.2.3 Emulsion Polymerization

Emulsion polymerization has an efficient heat transfer since it has water as a medium in the polymerization process (Odian, 2004; Stevens, 1999). Water is used in emulsion process while in solution polymerization process, solvent is used to aid in

efficient heat transfer. Monomer in emulsion polymerization is dispersed in the continuous aqueous phase by emulsifier. Initiator is then added to the process to initiate the primary free radicals which then diffuses into micelles swollen with monomer molecules. As monomer is used up in the polymerization reaction, more monomers enter the micelles to continue the reaction. Termination by radical combination occurs when a new radical diffuses into the micelles. Extremely high molecular weight is achievable in this process because only one radical is present in the micelles due to termination (Gilbert, 1995). The overall process is very complex, with heterogeneous phase of the process and also the reaction kinetics significantly different from that of bulk and solution polymerization.

Emulsion copolymerization is a heterogeneous reaction of two monomers with very complex mechanisms (Saldivar and Ray, 1997). Emulsion copolymerization of Styrene and MMA based on zero-one kinetic was employed by Alhamad et al. (2005). For a zero-one model, the particle diameters (D_{mm}) are small (~100nm). Polymerization within a relatively large particle is known as pseudo-bulk kinetics where the cross over diameter of Styrene for zero-one to pseudo-bulk is reported between 100 nm – 120 nm (Gomes et al., 2009). In *ab initio* emulsion polymerization, pre-batch time is needed for the seed formation and to eliminate any dissolved oxygen from the system (Gilbert, 1995; Coen et al., 1998; Zeaiter et al., 2002).

Initially monomer, initiator and surfactant were added in the continuous phase of water. Surfactant molecules coat the monomer droplets to form stabilized emulsion before polymerization starts. Surfactants have hydrophilic and hydrophobic end in

order to stabilize and emulsify the polymer droplets. Other surfactants form small aggregates called micelles which are required for particle formation by micellar nucleation. Besides that these micelles also absorb monomer molecules.

At the beginning of the reaction process, the initiator decomposes in the aqueous phase to form free radicals of initiator. These free radicals then react with the dispersed monomer forming oligomeric radicals in the aqueous phase. These oligomeric radicals can further the propagation process or undergo termination.

While propagating in the aqueous phase, the monomer will develop enough hyrophobicity in order to enter into the micelles also known as *z-mer* when it becames *surface active* (Coen et al., 2004; Gilbert, 1995). In other word, when the oligomeric radicals achieves equal or greater than the critical degree of polymerization for entry, *z*, it can enter into the micelles. However, there are three routes for the *surface active* polymer as shown in Figure 2.1~~Figure 2.1~~~~Figure 2.1~~.

Three routes that are possible for those oligomeric radical either enter the pre-existing particle, enter the formed micelles or propagate further until it reaches its critical size for homogeneous nucleation (j_{crit}) and collapse to form a particle (Meadows et al., 2003; Arai et al., 1979; Coen et al., 2004). Concentration of monomer in the particles are higher than that in the aqueous phase since monomers are consumed and oligomeric radicals enclosed in the micelles propagate rapidly to produce polymer particle. The micelles now contain long polymer chain while particle formation is still taking place until all the micelles disappear.

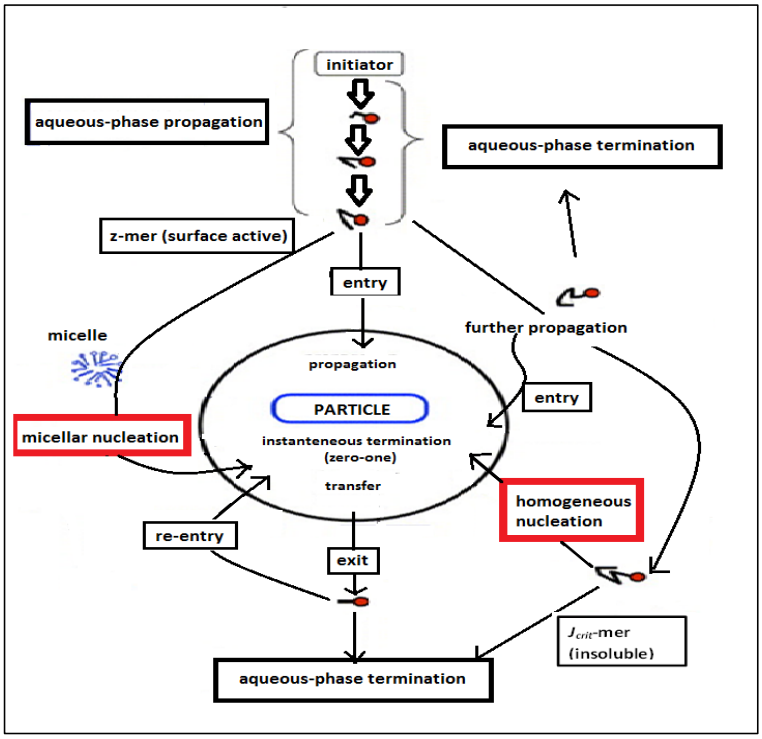

Figure 2.1: Some kinetic events in emulsion polymerization, including the competing paths for particle formation and for particle growth (adapted from Coen et al., 2004)

After the micelles disappear, no new particles are formed. Each free radical begins the polymerization within the micelles. Once a free radical has entered a micelle, the particles grow by chain propagation. Propagation, termination and radical transfer to monomer can occur inside the particles.

At the early stage of reaction process, the number average molecular weight (M_n) are very high because the particles formed are small in numbers, so monomers tend to enter the particles and increase the molecular chain in the particles. Then the molecular weight are decreased dramatically as the number of micelles capturing the

free radicals are increased. As time increases, all micelles are disappeared and no new particles are initiated.

The addition of monomer along the process increases the molecular weight of the produced polymer. Surfactant and initiator are fed to the reactor to cause the micellar nucleation and to initiate the radical process to form and allow entry of new particles. This will lead the addition monomer to enter into the existing growing particles to increase the molecular chain in the particles and also in the new particles.

Low monomer flow rates are used to ensure that all monomers are reacted in the micelles and the molecular weight are increased constantly afterward to reach the desired number average molecular weight. It has been observed that the reaction times are increased with the increase of molecular weight since more monomers are needed to increase the polymer chain.

The advantages and disadvantages of emulsion polymerization are given by Gilbert (1995) as below.

Advantages:

- The heat generated by the highly exothermic free radical polymerization process can be both readily absorbed by water and dissipated by the aqueous phase as the water has a high heat capacity. This is because the control of reactor temperature is easier compared to bulk process in order to prevent it from overheating.

- The rate of emulsion polymerization is usually considerably more rapid in an equivalent bulk process, thereby allowing faster throughput for a given capital cost.
- In the absence of modifier, the polymer that is formed usually has a considerably higher average molecular weight than that from an equivalent bulk process; as well it has a different molecular weight distribution.
- The final polymer product is formed in latex which makes it easier to handle compared to polymer product from the bulk and solution polymerization process which is a solid or is a viscous solution respectively.
- Molecular weight can be easily controlled by the addition of chain transfer agents which gives the additional control of the properties such as mechanical strength of the polymer and also the minimum film-forming temperature for latex.
- The process itself, and the resulting polymer latex, is water based rather than solvent based, which reduces both safety and environmental hazards.
- An emulsion polymerization can be carried through to relatively high conversion of monomer into polymer. This means the residual monomer are minimized while the monomer consumption is maximized.

Disadvantages:

- Generally initiator and surfactant used in emulsion polymerization product may impair the quality of the final product since it is difficult and/or expensive to be removed.

- The separation of the polymer from the water by coagulation or dewatering process might be necessary which increase the production cost for the further process.
- The mechanism for emulsion polymerization process is very complex and hard to understand and control since its heterogeneous process involves a minimum of two phases.

2.2.4 Suspension Polymerization

Suspension polymerization involves mechanically dispersing monomer in a noncompatible liquid, usually water (Odian, 2004; Stevens, 1999). Monomer soluble initiator is used for the polymerization process to occur. Monomer is kept in suspension by continuous agitation and the use of stabilizers such as poly vinyl alcohol or methyl cellulose. Polymer product obtained from this process will be in the form of granular beads if the process is carefully controlled (Odian, 2004). This polymer is easy to be handled and can be isolated by filtration or by spraying using spray dryer into a heated chamber (Stevens, 1999). Like emulsion, suspension polymerization allows efficient heat transfer and therefore the reaction is easily controlled. Suspension polymerization cannot be used for elastomer because it has a tendency for agglomeration of polymer particles.

2.3 Different Types of Polymers

2.3.1 Styrene

Styrene is an aromatic liquid monomer that is commercially manufactured from petroleum to make an aromatic polymer called polystyrene (PS). As a thermoplastic substance, this polymer normally is present in solid state at room temperature. Even though this hard plastic has a limited flexibility, it can melt if heated and becomes solid again when cooled.

Polystyrene is one of the most commonly used polymers because of its recyclable and can be cast into moulds with fine details. As a colourless polymer, it can be transparent or can be made into any favourable colour. Polystyrene products can easily be found in today's market like disposable cutlery, CD cases, the housing of the computer, smoke detector housing and most of the kitchen appliances. Some of the products of polystyrene is in the soft foam which is usually used for foam drinking cup, packaging materials, container and insulation among many others.

Polystyrene are made up of a long hydrocarbon chain from many styrene molecules. Chemical formula for Polystyrene is $(C_8H_9)_n$, which contains the chemical elements carbon and hydrogen. Figure 2.2 below show the formation of polystyrene from many molecule of styrene after undergoing a polymerization process.

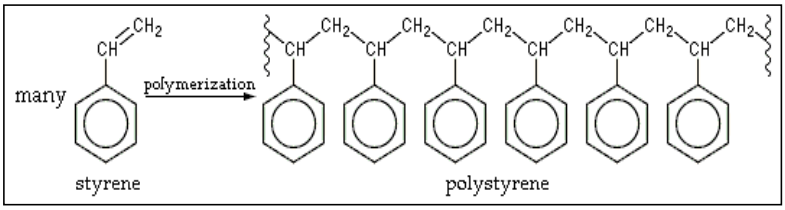

Figure 2.2: Chemical reaction for the formation of polystyrene

Polystyrene is commonly produced in three forms, extruded polystyrene, expanded polystyrene foam and extruded polystyrene foam. Each form of polystyrene has its variety of applications. Properties of Styrene are presented in Table 2.1~~Table 2.1~~Table 2.1 below.

Table 2.1: Properties of Styrene

Properties	
Molecular formula	C_8H_8
Molar mass	104.15 g/mol
Appearance	colorless oily liquid
Density	0.909 g/cm³
Melting point	-30 °C, 243 K
Boiling point	145 °C, 418 K
Solubility in water	< 1%
Viscosity	0.762 cP at 20 °C

2.3.2 Methyl Methacrylate (MMA)

Methyl methacrylate (MMA) is an organic compound used primarily for the production of polymethyl methacrylate (PMMA) by free radical polymerization. The chemical formula for MMA is $CH_2=C(CH_3)COOCH_3$ which then can produce PMMA by free radical vinyl polymerization as shown in Figure 2.3 below.

PMMA has been used in a wide range of fields and applications especially for transparent glass substitute like shatterproof, commercial aquarium and also motorcycle helmet visors. Besides that it is also used in medical technologies and implants (used for replacement lenses in the eye for cataract, bone cement and dentures); artistic and aesthetic uses (acrylic paints, substitute for a normal glass in picture framing); along many daily products (surface of hot tubs, shower units, sinks and also sheets for sign industry).

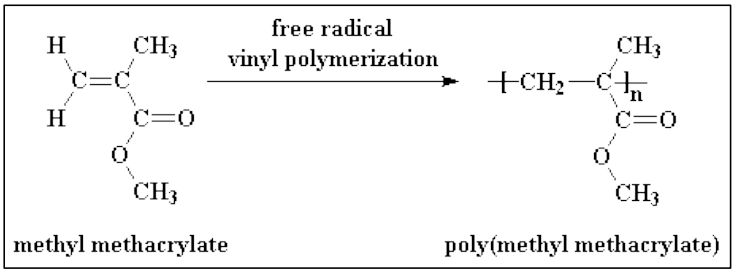

Figure 2.3: Chemical reaction for formation of PMMA

Properties of MMA are presented in Table 2.2 below. ~~Table 2.2 below.~~

Table 2.2: Properties of MMA

Properties	
Molecular formula	$C_5H_8O_2$
Molar mass	100.12 g/mol
Appearance	colourless liquid
Density	0.94 g/cm³
Melting point	-48 °C (225 K)
Boiling point	101 °C (374 K)
Solubility in water	1.5 g/100 ml (25 °C)
Viscosity	0.6 cP at 20 °C

2.4 Batch Reactor

Batch processes are widely used to produce small volume products with quite high value. Usually the production facilities used to carry out these processes are intended for multi-purpose use. In order to obtain the required product purity, cycle times, and to satisfy the commercial requirements and relevant regulatory authorities, achievements of stable and reproducible operating conditions are very important.

In a batch reactor, all reactants and the catalyst are charged into the reactor at the beginning of the process which is then closed to transport of substance and the reaction is allowed to proceed for a given time. The mixture of unreacted material together with the products is withdrawn at the end of the batch process. There is no

inflow or outflow of material during the process in the batch reactor. However, in semi-batch reactor, addition of reactants and catalyst are permitted along the process yet the product and unreacted material still will be withdrawn at the end of the process.

Modelling the batch reactor is more difficult since it is a dynamic process. It is also a very challenging task to control the process once it is underway as very little task can be done to change the reaction process in the reactor. The quality of end product can be controlled during the process to try to achieve the desired specifications of the product by controlling the external parameters like reactor temperature, jacket temperature, batch time or coolant flow rate.

A schematic diagram of a batch reactor system is shown in Figure 2.4 below. All reactants and catalysts are charged into the tank reactor using the inlet feed. A stirrer is used to agitate the reaction mixture inside the tank reactor. This is to ensure uniform mixing of the reactants for consistency of the process. Pressure building up inside the reactor is very dangerous since it could end up with disaster if explosion occurs. That is why a vent condenser is used for the batch reactor. The temperature inside the reactor can be controlled by using a jacket around the reactor with cooling or heating liquids to flow. Steam or cooling water is used to for the heating or cooling of the reactor temperature to follow the set point in the reactor respectively.

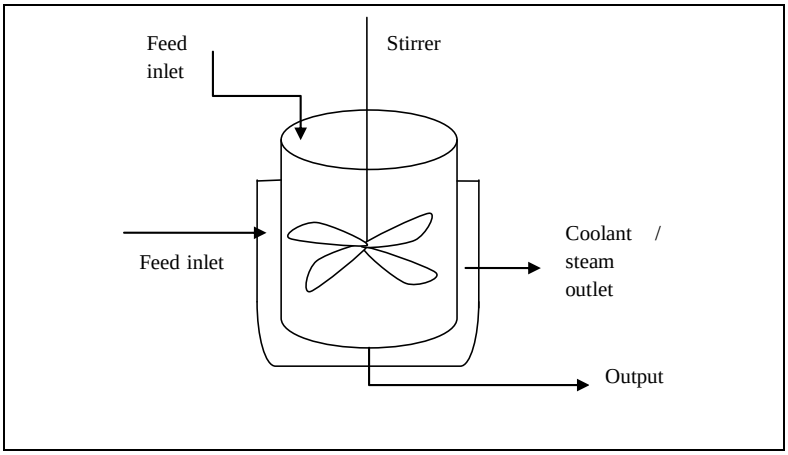

Figure 2.4: Schematic diagram of batch reactor system

2.5 Mechanism of Free Radical Polymerization

Free radical polymerization is the most common of all addition polymerization mechanisms. It is a chain polymerization in which each polymer molecule grows by addition of monomer to a terminal free radical reactive site which is known as active center.

Free-radical polymerization proceeds via multiple steps: chain initiation, chain propagation, chain termination, and chain transfer.

2.5.1 Chain initiation

Chain initiation involves formation of reactive radicals' active center. Initiating radicals may be provided via thermal decomposition of added initiators (I) in the first step and can be as:

$$I \xrightarrow{k_d} 2R^{\bullet} \quad (2.1)$$

There are some common thermal initiators: 2,2'-azo-bis-isobutyronitrile (AIBN); t-butyl hydroperoxide; cumyl peroxides; benzoyl peroxide (BPO); t-butyl peroxide; lauroyl peroxide, dipotassium persulfate.

Figure 2.5 shows the chemical reaction for the chain initiation process where AIBN was heated to form 2 free radical molecules which then initiate the process of polymerization.

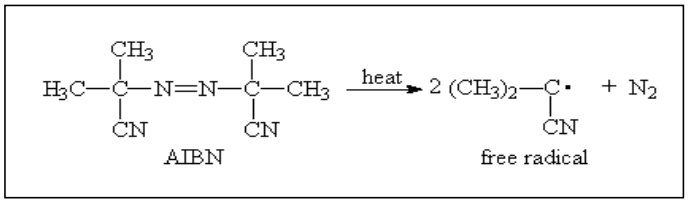

Figure 2.5: Chemical reaction for formation of free radicals molecules

Then in the second step, there will be addition of one of these free radicals to a molecule of monomer M and polymer P begins to grow as illustrated in the following steps:

$$R^{\bullet} + M \xrightarrow{k_i} RM^{\bullet} \quad (2.2)$$

$$R^{\bullet} + M \xrightarrow{k_i} P \quad (2.3)$$

Where $RM^{\bullet} = P$

Free radicals, $R^{\bullet}$ go on to react with monomer molecules, M, then polymer chains, P begins to grow.

Chemical reaction of this step as shown in Figure 2.6 below shows that the free radical formed earlier from the AIBN react with styrene monomer to form a styrene free radical. k_d and k_i in the equations are the rate constants for the decomposition and initiation step in the chain initiation.

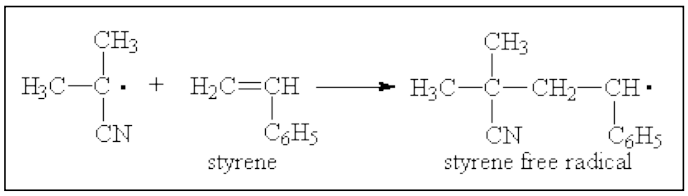

Figure 2.6: Chemical reaction for chain initiation of styrene free radical

2.5.2 Chain propagation

Chain propagation is where the monomer molecules are continuously added to the growing polymer chain. The equations for chain propagation steps can be written as:

$$RM^{\bullet} + M \xrightarrow{k_p} RMM^{\bullet} \quad (2.4)$$

$$P + M \xrightarrow{k_p} P_n \quad (2.5)$$

$$P_n + M \xrightarrow{k_p} P_{n+1} \quad (2.6)$$

k_p is the rate constant for propagation. Chemical reaction for chain propagation of styrene polymerization process is shown in Figure 2.7 below.

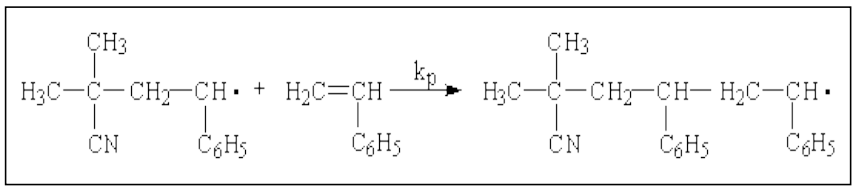

Figure 2.7: Chemical reaction for chain propagation of styrene polymerization process

2.5.3 Chain termination

Chain termination is when the growth of the polymer chain is terminated. There are two types of chain termination which is known as combination and disproportionation.

i. Combination:

Two growing polymer chains terminate by combining together to form a single bond. k_t is rate constant for termination with combination. Chemical reaction for chain termination by combination of styrene polymerization process is shown in Figure 2.8 below.

$$P_n + P_m \overset{k_t}{\rightarrow} M_{n+m} \tag{2.7}$$

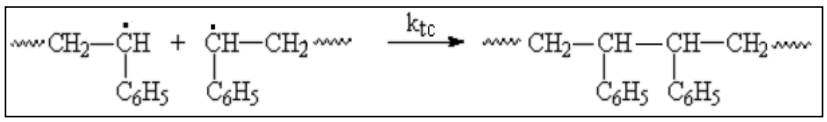

Figure 2.8: Chemical reaction for chain termination by combination of styrene polymerization process

ii. Disproportionation:

Termination by disproportionation gives two terminated chains. The radical at the end of one chain attacks a hydrogen atom at the second-to-last carbon atom in the second chain and the polymer chains terminate independently. In this case, one terminated chain will have an unsaturated carbon group while the other terminated end is saturated as shown in Figure 2.9. k_{td} is the rate constant for termination with disproportionation.

$$P_n + P_m \xrightarrow{k_{td}} M_n + M_m \tag{2.8}$$

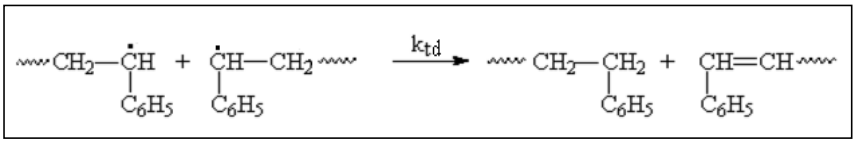

Figure 2.9: Chemical reaction for chain termination by disproportionation of styrene polymerization process

2.5.4 Chain transfer

Termination by chain transfer can be achieved when the free radical reacts with non radical species. The chain end radical attacks a weak bond and a hydrogen atom gets transfer to the end chain. When this is happened, the current chain terminates to yield a 'dead' polymer while a new 'living' polymer chain may start from the radical chain. The termination chain transfer can be occurred by a few chain transfer reactions, namely transfer to monomer *M*, transfer to polymer *P*, transfer to solvent agent *S*, or transfer to transfer agent *T*.

$$P_n + M \xrightarrow{k_{fm}} + M_n + P_1 \quad (2.9)$$

$$P_n + S \xrightarrow{k_{fs}} + M_n + S \quad (2.10)$$

$$P_n + P \xrightarrow{k_{fp}} + M_n + P_m \quad (2.11)$$

$$P_n + T \xrightarrow{k_{ft}} + M_n + T \quad (2.12)$$

k_{fm}, k_{fs}, k_{fp} and k_{ft} are the kinetic rate constants for transfer to monomer, transfer to solvent agent, transfer to polymer and transfer to transfer agent respectively. However, in bulk polymerization of Styrene, chain transfer to monomer and polymer do not take place in the process. Furthermore there are no solvent involved in the bulk and emulsion process. In solution polymerization of MMA, chain transfer to monomer and solvent are considered. In emulsion copolymerization of Styrene and MMA, transfer to each monomer is considered. No transfer agent involved in all polymerization process.

2.6 Gel and Glass Effect

There is a phenomenon which occurs during the polymerization process for high concentration of reactant mixture in the reactor which is called the gel effect (Ramteke and Gupta, 2011; Rudin, 1999; Kalfas and Ray, 1993). It is also known as Tromsdorff-Norrish-Smith Effect / or auto acceleration in recognition of the early workers in the field (Odian, 2004). The initiation kinetic rate constant and the initial kinetic rate constant for termination are equal at the beginning of the process. However, the viscosity of the reaction mixture in the reactor will increase as the time

proceeds which will leads to entanglement of the polymer chain. This is because the diffusion of chain is hindered which then slows down the termination process as it involves the reaction between the two chain ends. This phenomenon always occurs in bulk polymerization (Tulig and Tirrell, 1981).

However, for high concentration solution polymerization, gel effect might happen when the viscosity of the reaction mixture is increased as the polymer chain forms (O'Neil and Torkelson, 1999). This is when the rate of polymerization suddenly goes up drastically because of slow kinetic rate constant and produces a higher molecular weight than the chains that grew earlier. In contrary for dilute solutions, the gel effect does not occur. This is because the addition of solvent in the reaction mixture will hinder the build-up of the viscosity to slow down the chain diffusions. This auto acceleration phenomenon strongly affects the end-use properties of the produced polymer as it leads to broader molecular weight distribution (Verros et al., 2005; Achilias and Kiparissides, 1992).

These effects are undesirable in a polymerization reaction, as they can lead to reactor runaway which effect results in hot spots and erratic behavior, which worsens the quality of the end product, and even can lead to reactor explosion.

The problem of the gel effect is usually avoided by performing the free radical polymerization in solution by adding a solvent to the reactor which can limit the increase of the viscosity and eliminate the diffusion constraints (Ekpo, 2006). However, the use of considerable amounts of solvent implies much larger reactors and an extra separation step have to be taken. Besides that, the solvents are usually

hazardous chemicals and their usage is limited. Moreover the purity of the product decreases with the increase of solvent added to the reactor.

The graph in Figure 2.10 shows the free radical polymerization of MMA in Benzene solution at various initial monomer solutions. It can be clearly seen that the more concentrated the solution, the earlier the gel effect occurs. On the other hand its values are reduced when there is lower initial concentration of monomer in the solution. However, as already mentioned the addition of a solvent has many negative consequences and is not the most desirable solution to the problem.

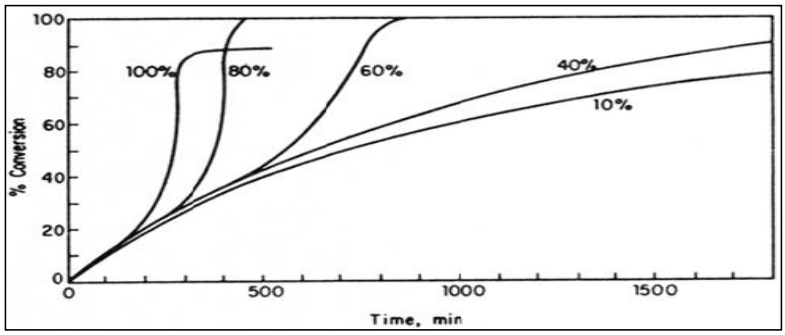

Figure 2.10: Autoacceleration in the free radical polymerization of MMA in benzene. The different curves refer to different initial concentrations of the monomer in the solvent (Odian, 2004)

The glass effect is related to the decrease in the propagation rate constant caused by a decreased in mobility of monomer molecules due to the 'freezing' of the reaction mixture at the glass transition temperature (Achilias and Kiparissides, 1992). This phenomenon occurs at much higher conversion (Ramteke and Gupta, 2011). It appears that the polymerization reactions taking place at temperature below the glass transition temperature of the polymer. As a consequence from this phenomenon, the

reaction mixture will freeze below 100% which for styrene it is around 95% (Wolff and Bos, 1997).

2.7 Initiator Efficiency

The decomposition of initiator molecules at the beginning of the process to form very active primary radicals depend on the initiator efficiency, *f*. Not all initiator molecules decompose to form primary radicals since some of them might either have self-terminate or react with other reactants in the system which make the initiator efficiency less than 100%.

Achilias and Kiparissides (1992) had reported that there are quite a lot of published paper which have treated the initiator efficiency, *f* as a constant value. Ekpo (2006) and Ekpo and Mujtaba (2008) was using a constant value of 0.53 for the initiator efficiency in solution polymerization of MMA. However, it is believed that the initiator efficiency is not constant and will decrease as the viscosity inside the reactor increases. Dube et al. (1997) have used the free volume theory to model the changing of initiator efficiency. Initiator efficiency should decrease at high conversion for bulk polymerization (Achilias, 2007).

2.8 Batch Polymerization

The dynamic optimization of batch polymerization reactors has not received much attention from researchers as much as the dynamic optimization of general batch

reactor. However, many solution techniques relating to general batch reactor can easily be extended in order to be emploed for polymerization batch reactor (Ekpo, 2006). This is due to the similarities between both systems which arise from the same batch mode operation.

2.8.1 Gel and Glass Effects

According to Cunningham and Mahabadi (1996), Balke (1972) and Balke and Hamielec (1973) carried out the first work to compare the experimental and theoretical distribution in the bulk polymerization of methyl methacrylate by using AIBN as the initiator. The results showed that the bulk polymerization of MMA to high conversion leads to a gel effect in which there is a sharp rise in both the monomer conversion and the polymer average molecular weight (Balke and Hamielec, 1973).

The viscosity of the reacting mixture inside a reactor increases by several orders of magnitude as the polymerization started until the conversions complete in free radical polymerization. This is due to autoacceleration or gel effect which begins at 30-50% of conversion (Andrzejewska and Bogacki, 1997) which caused a drastic decrease in the rate of termination because of limited mobility of polymer chains (Achilias, 2007) .

Baillagou and Soong (1985a) developed gel effect model for the free radical polymerization of poly methyl methacrylate (PMMA) under nonisothermal

conditions. It has been used to simulate profiles of various system parameters such as temperature, initiator concentration, and conversion. The results from his study show the radical and dead polymer molecular weight distributions give average consistent by those found by the method of moment.

A kinetic study has been performed by Arai et al. (1986) on the bulk thermal polymerization of styrene in the temperature range 100^{o}C to 180^{o}C. Rate equations were derived on the basis of a model which introduced the gel effect into each elementary reaction by considering the decrease of segmental jump frequency during polymerization. Jump frequency for bulk diffusion usually identified through the atomic jump and the spatial diffusion coefficient (Capasso, 2003). The model from this work could successfully simulate the conversion and the average molecular weight.

The gel-effect for the batch solution polymerization of styrene initiated by AIBN with toluene as the solvent was investigated by Soots and Stanford (1991). The study used a central composite experimental design in two variables and they are temperature and initial initiator concentration. The results show that the gel-effect correlates very well with the solution viscosity and reaction temperature. The resulting process model was found to simulate well the experiments carried out by others.

Penlidis et al. (1992) derived a detailed and complex mechanistic model for a batch solution polymerization of MMA. They showed how this complex model can be simplified using various assumptions and approximations. Five models of different

levels of complexity are presented and examined for their suitability for process optimization and control applications. They also discussed and compared the model responses in order to check whether the simplifications degrade the predictive capabilities of the original model.

A model for the simulation of suspension polymerization of MMA has been developed by Maschio et al. (1992) which allows to accounts for the effect of diffusive phenomena on reaction rate and to evaluate molecular weight distribution under non-isothermal conditions. Experiments were carried out in a laboratory reactor in order to validate the developed model. The results showed that an increase of the reaction temperature during the gel effect time had a favorable influence on the polymer quality. They also indicated that the control of temperature profiles in the reactor is an interesting operating strategy to be adopted in industrial units.

A new theoretical framework was proposed for modeling diffusion-controlled free-radical polymerization reactions by Achilias and Kiparissides (1992). The ability of the present model to explain the mechanism of diffusion-controlled reactions was demonstrated by analyzing the free-radical polymerizations of styrene and methyl methacrylate initiated by the thermal decomposition of AIBN, AIBME, AVN, and LPO chemical initiators. Termination rate constant, propagation rate constants and initiator efficiency were expressed in terms of a reaction-limited and a diffusion-limited. The diffusion limited was shown to depend on the diffusion coefficient of the corresponding species such as polymer, monomer, primary radicals and an effective reaction radius. It was shown that the proposed approach for modeling diffusion-controlled reactions did not require the introduction of critical break points

to mark the onset of various diffusional effects such as gel effect and glass effect. In this approach, the diffusion effects are taken as an integral part of the initiation, propagation and termination reactions from the beginning until the end of the polymerization process. It was shown that, at high conversions, initiator efficiency strongly depended on the size of initiator molecules.

Raja (1995) solved a minimum time problem for the batch polymerization of styrene using Lagrange multipliers with the Pontryagin's Maximum Principle to get the optimal temperature profiles for different fixed values of monomer conversion and number average chain lengths. He did not consider the gel and glass effect in his study.

Pinto and Ray (1996) calculated the molecular weight distribution (MWD) of a polymer from its mathematical model by using generating functions. The system used in his study was free-radical solution copolymerization of vinyl acetate (VA) and methyl methacrylate (MMA) in tert-butanol (TB). Besides that he also used the simplex method to determine the optimal temperature sequence for free radical polymerization to obtain desired monomer conversions and average molecular weights.

Loeblein et al. (1997) considered the parametric uncertainty for his study on the on-line optimization of batch reactors. The method of orthogonal collocation is employed to convert the differential algebraic optimization problem (DAOP) of the dynamic optimization into a nonlinear program (NLP) and determine the nominal optimum. The method of average deviation from optimum is developed for time

optimal problems in a semi batch reactor to produce 2-acetoacetyle pyrrole from pyrrole and diketene in minimum time.

A computational model for free-radical polymerization reactions for styrene and MMA in an ideally macromixed batch stirred tank reactor has been developed by Wolff and Bos (1997). In this research, they included a fundamental approach to account for the viscosity effects such as the cage effect, gel effect and glass effect as proposed by Achilias and Kiparissides (1992).

Asteasuain et al. (2000) introduced a dynamic model of the high pressure polymerization of ethylene in tubular reactor and a dynamic optimization problem is formulated for studying start-up strategies. The objective functions for this study are to maximize outlet conversion and optimize the time necessary for its stabilization while keeping product molecular properties within commercial ranges. Results from this work showed the time responses for temperature, number-average molecular weight and conversion along the reactor axial distance for different control variable profiles. The interface gOPT of the gPROMS simulator was used to resolve the optimization problem and to perform the simulations undertaken for this study.

The effect of operational conditions on the performance of a controlled batch polymerization reactor for solution polymerization of styrene was investigated experimentally by Erdogan et al. (2002). Besides that they also investigated the effect of agitation speed on conversion and heat transfer coefficient in free radical chain growth polymerization in this controlled, stirred, jacketed batch reactor. The experiments were conducted under optimal loading conditions calculated by using

Lagrange's multiplier method. The reactor temperature was controlled by manipulating the heat input to the reactor. A good agitation was found to improve the process control and efficiency of the control performance by improving heat transfer between the jacket and the reactor and quite promising in improving the heat transfer and temperature control.

The kinetics of bulk thermal polymerization of styrene over the range of 100-200 ^{o}C was studied based on three stage polymerization model (TSPM) in the research carried out by Qin et al. (2002). TSPM plots showed that the whole polymerization course only exhibits two stages, low conversion stage and gel effect stage, which is consistent with TSPM as the reaction temperature is higher than the glass transition temperature of polystyrene. From this research it was found that the critical conversion for the transition from low conversion stage to gel effect stage was independent of the reaction temperature and approximately equal to 0.5. In addition, the apparent reaction rate constants obtained from TSPM plots could be correlated to temperature by Arrhenius equation. Expressions predicting number-average molecular weight were also derived according to TSPM. Using the expressions, it was found that number-average molecular weight is independent of the conversion and relative to the reaction temperature at low conversion stage. However, it varied with the conversions at gel effect stage and the variations were more obvious as the reaction temperature rises.

Fan et al. (2003) worked on a pilot-scale tubular reactor fitted with in-line static mixers. It is experimentally and theoretically evaluated for the polymerization of concentrated MMA solution. A non-isothermal and non-adiabatic axially dispersed

plug-flow model was used to describe the flow characteristics of the reactor. Measured monomer conversions and polymer molecular weight were accurately predicted by model simulation. Studies also demonstrated the importance of inhibitor kinetics on the dynamic and steady-state performance of the reactor.

Ekpo and Mujtaba (2004) worked on the optimization of free radical polymerization of styrene using 2,2' azobisisobutyronitrile catalyst, (AIBN) as initiator in a batch reactor. A dynamic optimization method was used to find the optimal temperature profile that will yield a desired level of monomer conversion and number average molecular weight in minimum time. They used CVP technique in order to optimize the temperature and the length of the interval. Gel and glass effects were not considered in their work. However, Ekpo and Mujtaba (2008) also considered solution polymerization of MMA but included gel and glass effect into their model.

Verros et al. (2005) compared two different approaches to model diffusion controlled free radical polymerization, namely the free volume model and the entanglement theory. Both of the approaches were applied to MMA bulk polymerization in a batch reactor to calculate the conversion, total radical concentration, the number and weight average molecular weights as well as the entire molecular weight distribution as a function of the polymerization time and the process conditions. All the diffusion-controlled phenomena were taken into account, including gel, glass and cage effects as well as residual termination. Model predictions in this work were in good agreement with the available experimental data for conversion, number and weight average molecular weights as well as the entire molecular weight distribution.

A comprehensive mathematical framework for modeling the gel effect in branched polymer systems with application to the solution polymerization of vinyl acetate (VAC) was developed by Verros and Achilias (2009). The model is based on the free volume theory to describe the solution free radical homopolymerization of VAC. The model predictions for monomer conversion and number and weight average molecular weight were in good agreement with the data in the literature.

An experimental studies was carried out by Achilias and Verros (2010) for MMA bulk polymerization as well as the bulk and solution polymerization of VAC using the model developed in their previous study. Again the estimated parameters in the models were found to be in close agreement with literature. A detailed experimental study of diffusion-controlled reactions in free radical polymerization using differential scanning calorimetry (DSC) was carried out by Achilias and Verros (2010) at a wide range of experimental conditions including initial initiator concentration, reaction temperature, and type and amount of solvent for methyl methacrylate bulk polymerization as well as the solution and the bulk polymerization of vinyl acetate.

2.8.2 Initiator Efficiency

The initiator efficiency is often considered to be constant (Achilias and Kiparissides, 1992). However, the initiator efficiency may decrease significantly with the high viscosity of reaction mixture (Russell et al., 1988). Free radical polymerization is usually initiated by either thermal or photolytic dissociation of initiators. The rate of

primary radical formation is reflected by the initiator efficiency, *f*. For bulk styrene polymerization with AIBN initiator at 130^{o}C, Wang and Matyjaszewski (1995) observed the increase of initiator efficiency, *f* from 22% to 65% with the addition of 2 molar $CuCl_2$ in the system. Note, the initiator efficiency decreases with the decrease of temperature (Xia and Matyjaszewski, 1997).

Initiator efficiency at the start of the polymerization reaction is usually between 0.3 and 0.8 and decreases as the reaction proceeds until it reaches a limiting value of zero (Kurdikar and Peppas, 1994). A theoretical investigation of the initiator efficiency was undertaken by using 2,2-dimethoxy-2- phenylacetophenone as a model initiator. Expressions that allow for the prediction of the initiator efficiency at the onset and during the course of the polymerization were developed.

Initiation reaction could also be diffusion-controlled and should decrease at higher conversion of bulk polymerization (Achilias, 2007). The initiator decomposition rate constant, k_d, is not affected by viscosity of the reaction medium. The initiator efficiency was assumed to strongly depend on diffusion-controlled phenomena.

Ekpo and Mujtaba (2008) carried out a dynamic optimization of MMA in batch reactor to attain the desired polymer molecular and end point characteristics. A constant value of initiator efficiency 0.53 was employed in this work.

According to Ghosh et al. (1998) initiator efficiency, *f* decreases as the viscosity of the reaction medium increases. They improved the model of Ray et al. (1995) was improved by allowing the value of *f* to decrease at high conversion. A series of bulk

and solution polymerizations have been carried out at two different temperatures (50°C and 70°C) using benzoyl peroxide (BPO) as initiator.

2.8.3 Emulsion Polymerization

Many detailed studies have been reported in the literature on kinetic studies of batch emulsion copolymerization. Zeaiter et al. (2002) developed the control of particle size and molecular weight distribution described by a population balance model of styrene emulsion polymerization in semi-batch process. A bimodal distribution was observed at very low rate and a bigger particle size with higher feed.

Saldivar (1996) provided extensive information on developing a comprehensive mathematical model for emulsion copolymerization of several monomers in tank reactors. The developed model was validated by Saldivar and Ray (1997) with the emulsion copolymerization of styrene and MMA. A good agreement between the model predicted results for the effects of initiator and emulsifier initial concentrations and experimental data was obtained.

Another extensive kinetic model was develop by Coen et al. (1998) for the particle size distribution (PSD), particle number, particle size and amount of secondary nucleation in emulsion polymerizations. The model included the kinetic events such as the aqueous phase propagation, entry and re-entry, transfer, termination, diffusion, coagulation and particle formation by both micellar and homogeneous nucleation mechanisms for a zero-one system. The extension of this model which takes all the

complex events in emulsion polymerization into account for zero-one system was undertaken later by Coen et al. (2004). Pseudo bulk kinetics was included in the time evolution of the particle size distribution.

Alhamad et al. (2005a) developed a comprehensive model for emulsion copolymerization process of styrene and MMA which allowed the prediction of key polymer properties such as conversion, particle size distribution (PSD), molecular weight distribution (MWD), number average molecular weight (M_n), weight average molecular weight (M_w) and also average particle size. The model was used to maximize M_n for emulsion copolymerization of styrene with one fixed pre-batch time 1500s. They optimized temperatures, monomer flow rates, initiator flow rates and surfactant flow rates using 5 control intervals. Total monomer feed was used as constraint based on which the final batch time was calculated. Experimental works was also carried out to validate the results.

A steady-state model was developed by Mead and Poehlein (1989) for emulsion copolymerization in a seed-fed continuous stirred tank reactor (CSTR) for Styrene-MMA and Styrene-Acrylonitrile. The main reaction sites were considered to be the monomer-swollen polymer particles. The model was used to predict the steady-state PSD and rate of reaction for emulsion copolymerization in a seed-fed CSTR.

Bakhshi et al. (2010) carried out a semi-batch emulsion copolymerization to prepare poly(butyl acrylate-co-glycidylmethacrylate) latexes using potassium persulfate as an initiator, sodium dodecylbenzene sulfonate as an emulsifier and sodium bicarbonate as a buffer. According to them, high agitation speed reduced the

coagulation of polymer particles however had a negative effect on the monomer conversion.

The stability and kinetic behaviour of *ab-initio* emulsion copolymerizations of methyl methacrylate/butyl acrylate (MMA/BA) initiated by KPS (Potassium peroxodisulfate) in the presence of different amounts of sodium montmorillonite (Na-MMT) and different Sodium laurylsulfate (SLS) concentrations was studied by Bonnefond et al. (2011). The kinetics of the emulsion copolymerization of MMA/BA (MMA/BA = 50/50) in the presence of (Na-MMT) was investigated. SLS was used as surfactant at different concentrations and potassium persulfate as initiator.

Valappil (2002) formulated the control of end-use product properties as a nonlinear model predictive control problem of emulsion polymerization of styrene. Besides that an efficient numerical technique using successive linearization was utilized for the solution for this work. A parameter adaptive extended Kalman filter was used for state estimation of the molecular properties for the emulsion polymerization of styrene. The model developed by him can be used to predict the end-use properties, as a function of both the molecular weight and particle-size distributions of the product.

The development of a mathematical model for emulsion copolymerization of styrene and butyl acrylate carried out in the presence of *n*-dodecyl mercaptan as chain transfer agent (CTA) was carried out by Benyahia et al. (2009). This model is based on the kinetics of the complex elementary chemical reactions occurring both in the aqueous phase and in the particles. It takes into account the particles nucleation, the

radicals absorption and desorption, and the partition of each monomer, CTA and inhibitor between the monomers droplets, the aqueous phase and the polymer particles. A new approach was used to simplify the population balance by using two differential equations instead of the large number of differential equations generally used for the same purpose. This approach allowed reducing the corresponding simulation time.

Ginsburger et al.(2003) carried out the modeling and simulation of batch and semi-batch emulsion copolymerization of styrene and butyl acrylate. The key parameter of the data used to simulate in semi-batch process was taken from the basis of batch experimental data of emulsion copolymerization. Initiator used in the process is ammonium persulfate ($NH_4S_2O_8$) and surfactant composed of a mixture of anionic Texapon and non-ionic Genapol emulsifiers. A ten minutes pre-batch time for seed formation was used in the semi-batch process.

2.9 Dynamic Optimization Problems

Many engineering systems including polymerization in batch reactor are transient and are modelled by combinations of Differential-Algebraic Equations (DAEs) of varying complexities (Ekpo, 2006). The objective of dynamic optimization is to find the optimal control profile of one or more control variables or control parameters of a system. Today, there are large ranges of computational methods available for solving dynamic optimization problem.

Most popular methods used for optimization are presented here;

- Pontryagin's Maximum Principle (PMP) (Davisson et al., 1992)
- Discrete Maximum Principle (DMP) (Karátson and Korotov, 2005)
- Orthogonal collocation with successive quadratic programming (OC with SQP) (Xuemei et al., 2006)
- Orthogonal collocation (OC) (Gupta, 2006)
- Iterative dynamic programming (IDP) (Chen and Wang, 2007)
- Generalized reduced gradient (GRG) with golden search (GS) (Garcia et al., 1995)
- Nonlinear Programming with control vector parameterization (CVP) and successive quadratic programming (SQP) (Ekpo, 2006)

In the next sections Nonlinear Programming, CVP and SQP are briefly summarized.

2.9.1 Conversion of Dynamic optimization Problem to Non-Linear Programming Problem

The model equations used in the polymerization process (Chapter 3) results ~~to~~ in differential and algebraic equations (DAEs) due to the dynamic nature in batch reactor system. The DAEs can be represented in the compact form (~~Aziz, 2001~~Ekpo, 2006):

$$f(t, x'(t), x(t), u(t), v) = 0 \quad [t_0, t_f] \tag{2.13}$$

Where:

t is the independent variable,

$x(t) \in R^n$ is the set of all state variables ,

$x'(t)$ is the derivatives of $x(t)$ with respect to time,

$u(t) \in R^m$ is a vector of control variables such as reactor temperature,

v is a vector of time invariant parameters (design variables) such as volume of the reactor.

Suitable initial conditions $x(t)$ are defined at time $t = t_0$. The time interval of interest is $[t_0, t_f]$ and the function $f: R \times R^n \times R^n \times R^m \times R^p \rightarrow R^n$ is assumed to be continuously differentiable with respect to all its arguments.

The system is subject to bounds on the controls;

$$a^u(t) \leq u(t) \leq b^u(t), \quad t \in [t_0, t_f] \tag{2.14}$$

Where $a^u(t)$ and $b^u(t)$ are given continuous functions of time on $[t_0, t_f]$ and interior point or terminal constraints at time t_p of the form:

$$a^F \leq F(t_p, x'(t_p), x(t_p), u(t_p), v, x_0) \leq b^F \tag{2.15}$$

Where

$$F(t, x', x, u, v, x_0) \in R^n \tag{2.16}$$

At the terminal point where t_p equals t_f, the system performance is minimised in terms of a scalar objective function as:

Formatted: Font: (Asian) +Body, Superscript

Formatted: Font: (Asian) +Body, Superscript

$$J = (t_f, x'(t_f), x(t_f), u(t_f), v, x_0) \quad (2.17)$$

The optimal control problem is to choose to optimize set of control variables *u*(*t*) subject to constraints and bounds on the lower and upper limit in order to perform the dynamic optimization problems.

2.9.1.1 Control Vector Parameterization (CVP) Technique

Control vector parameterization is one of the most frequently used techniques for determining the optimal control profile in optimization of a batch process (Zhou and Yuan, 2004). According to Morison (1984), Vassiladis (1993) and, Mujtaba and Macchietto (1998), this technique applies parameterization to the control variable *u(t)* only and are approximated by a finite dimensional representation (Ekpo, 2006) to correct the dynamic optimization problem to a nonlinear programming problem. The technique is explained below.

The time interval $[t_0, t_f]$ is divided into a finite number of subintervals which contain a set of basis functions involving a finite number of parameters (Aziz, 2001):

$$u(t) = \Phi^j(t, z_j), \quad t \in (t_{j-1}, t_j), \quad j = 1,2, \ldots\ldots, J \quad (2.18)$$

Where t_J is equal to t_f, the function is assumed to be continuously differentiable with respect to *t* and z_j. The derivatives are uniformly bounded and the control is defined by the parameters z_j and the switching time t_j.

Then the constraints on the control become:

$$a^u(t) \leq \Phi^j(t, z_j) \leq b^u(t), \quad t \in (t_{j-1}, t_j), \quad j = 1,2, \ldots\ldots, J \tag{2.19}$$

The set of decision variables for the non-linear program can be written as:

$$y = \{x_0, z_1, z_2, \ldots, z_j, t_1, t_2, \ldots t_j\} \tag{2.20}$$

Where for this work, x_0 refers to the initial condition (e.g. initial initiator concentration), z_1, z_2, ...,z_j is refer to the control variables (e.g. reactor temperature), t_1, t_2,... is the switching time and t_j is the final batch time, t_f.

Fikar et al. (1998) compared the Iterative Dynamic Programming (IDP) and Control Vector Parametrisation (CVP) and come to the conclusion where CVP was significantly faster and within the framework of CVP methods, it is possible to investigate minimum time or sensitivity problems. Utilizing the nonlinear programming approach through discretization appears to be the most promising compared to evolutionary algorithms (EA) in the work of Balku et al. (2009).

2.9.1.2 NLP Optimization Problem

The optimization problem can now be presented as:

Minimize J(y)

Subject to	Equality constraint	(Eqn. 2.13)
	Inequality constraints	(Eqn. 2.15 and 2.19)

Successive Quadratic Programming (SQP) algorithm can be used to solve the nonlinearly constrained optimization problem using a sequence of quadratic programming (QP). The constraints of each QP problem are linearized of the constraints in the original problem. The resulting of QP problem is then used to find the direction which will specify the next step length of the decision variable. See Chen (1988) and Edgar et al. (2001) for further details.

2.10 Choice of gPROMS Sofware for Modelling and Optimization

2.10.1 Commercial Software

There are numbers of commercial simulators in the market today for developing process model such as Hysis, AspenPlus and ProII. Each of the software has its unique features for the developed process model and it seems all of them provide a wide range of application flexibility. Full comparison of these software are not available in the literature and was beyond the scope of this work.

Assessment of the parameters estimation capabilities of the gPROMS software compared with the Aspen Custom Modeler (ACM) software was carried out by Tijl (2005) using Sec-Butyl-Alcohol stripper for the case study. The physical and thermodynamics properties of the components in ACM are made available to the gPROMS model via the CAPE-OPEN interface. The CAPE-OPEN is a tool that allows the execution of any gPROMS model with a CAPE-OPEN compliant flowsheeting environment. Various aspects of parameter estimation are assessed such

as experiment data input, output interpretation, speed and accuracy of obtaining the solution. The author comes to the conclusion that the parameter estimation using gPROMS are better than using ACM.

2.10.2 Features of gPROMS

gPROMS (general Process Modelling Systems) has many advantages compared to other commercial software available in market today. The main applications of the software are in model-based engineering activities for process and equipment development and design, and optimization of process operations. Its equation oriented representation allows using one model for many different activities. According to Winkel et al. (1995), gPROMS has been widely used for the front end modeling and design of industrial process such as batch plants among others. The capability of this software package for modeling, simulation and optimization has been tested by Asteasuain et al. (2000), Ekpo (2006), and Sowgath (2007). Following are some advantages of gPROMS among many of them:

1. Modelling and solution power

- All solvers within gPROMS are specifically designed for large scale systems and there are no limits regarding problem size. This unparalleled modeling powers with the generality of the software means that it can be used for any processes that can be described by a mathematical model.

2. Project environment

- Project tree structure is a comprehensive project environment which all elements of a modeling project can be easily accessed and maintained. Besides that, a palette view can be used to access libraries of model icons when building a flowsheet.

3. Multiple activities using the same model

- Once a model is built in gPROMS, it can be used for steady-state and dynamic simulation**,** parameter estimation**,** optimization and experiment design. There are multiple activities can be done using the same model.

4. Integrated steady state and dynamic capabilities

- Models can be written to be steady-state or dynamic or both. It is not like steady state simulators which have added dynamic capabilities or dynamic simulator which have to iterate to steady state. gPROMS can always solve for a steady state providing the models and specifications allow this.

5. Sophisticated optimization capabilities

- gPROMS's optimisation facilities can be used for steady state or dynamic model to find the optimal answer to any design or operational questions directly rather than by trial-and-error iteration.

To summarize, gPROMS is a powerful general-purpose process modelling and optimization environment used to enhance design and operation that covers the full range of processes, from purely batch to purely continuous. With an accurate

gPROMS model of their process represented in equation form, engineers can simulate the system behavior, estimate unknown parameters from available data, optimize design and performance, and communicate with other applications and systems through sophisticated interfaces. Therefore, due to its strong modeling power among other advantages illustrated above, gPROMS is chosen for the modelling, simulation and optimization of processes to carry out the tasks in this thesis.

2.11 Summary

It is clear from the literature that the gel effect is occurs in bulk polymerization and concentrated solution polymerization. The research were carried out by Balke (1973), Balke and Hamielec (1973) for bulk polymerization of MMA initiated with AIBN shows the diffusion control of termination is dramatic in bulk process. Baillagou and Soong (1985b) developed gel effect model for the polymerization of PMMA. A kinetic study by Arai (1986) on the bulk polymerization of styrene also introduced the gel effect into the model. Soots and Stanford (1991) investigated the gel effect for the batch solution polymerization of styrene initiated by AIBN with toluene as the solvent. A new theoretical framework for modeling the diffusion-controlled free radical polymerization of styrene and MMA by the thermal decomposition of AIBN, AIBME, AVN and LPO chemical initiators was proposed by Achilias and Kiparissides (1992). Raja (1995) and Ekpo (2004) carried out the optimization of bulk styrene polymerization process with AIBN initiator, however, the gel and glass effect is not considered in his work. In this work, the process model

used by Raja (1995) and Ekpo (2004) for bulk polymerization of styrene was improved by including the gel and glass effect.

Many reported research used a constant value for initiator efficiency, f in polymerization process (Achilias and Kiparissides, 1992). However, the variable of initiator efficiency along the polymerization was also considered by other researcher (Wang and Matyjaszewski, 1995; Xia and Matyjaszewski, 1997; Kurdikar and Peppas, 1994; Achilias, 2007; Ghosh et al., 1998). In this work, the process model from the work of Ekpo (2004) is improved for the solution polymerization of MMA by using the free volume theory to calculate the initiator efficiency.

Mathematical model for styrene emulsion polymerization was developed by Zeaiter et al., (2002) which used 45 minutes for the seed formation. The model developed by Saldivar (1996) was validated by Saldivar and Ray (1997) with the emulsion copolymerization of styrene and MMA and no pre-batch time for seed formation is considered. Coen et al. (2004) extended her earlier model of zero-one to pseudo bulk kinetics and no pre-batch time is allocated in their *ab-initio* system. Alhamad et al. (2005a) developed a comprehensive model for emulsion copolymerization process of styrene and MMA using one fixed time for the seed formation for *ab initio* system. The effect of different pre-batch time for seed formation in emulsion copolymerization of styrene and MMA is studied in this work. Besides that, the process model was carried out in batch and semi-batch process without pre-batch time. Different optimization formulation is used in this work for maximize the number average molecular weight (M_n) in emulsion copolymerization process by

using the model developed by Alhamad (2005), where the total batch time is fixed, instead of free time.

The dynamic optimization problems were converted into nonlinear programming problem using the CVP techniques which were solved using efficient SQP (Successive Quadratic Programming) method available within the gPROMS software.

Chapter Three

Mathematical Modelling of Polymerization Process

3.1 Introduction

A model is an imitation of reality and a mathematical model is a particular form of representation consisting of mathematical objects, such as equations, graphs and rules (Hangos and Cameron, 2001). Mathematical modelling is a technique for understanding the dynamics of a system and for predicting future outcomes within the system. Mathematical models of chemical and polymer processes can be very complex due to their typical characteristics including non-linearity, stochastic behavior, time variation and also chemical reaction. By using the mathematical model to represent the real process will allows the model user to study and understand the relationships between the elements of the system without having to manipulate the actual system. So, use of a model to investigate the working of a process, certainly give many advantages rather than using the real process.

3.2 Modelling of Batch and Semi-batch Reactor

For this work, a polymerization batch reactor model has been developed using gPROMS for a process to be investigated. Simulations have taken place before performing any significant dynamic optimization. The model describes the working of the polymerization in batch and semi-batch reactor systems for bulk polymerization of styrene, solution polymerization of MMA and emulsion copolymerization of styrene and MMA.

A batch process is used to process a fixed amount of material each time it is operated where the product is removed after the processing of the reactants mixture in the reactor is complete. On the other hand, in a semi-batch process, material enters the process reactor during its operation, and no product is leaving the reactor until the processing time is finished.

3.3 Modelling Free Radical Bulk Polymerization of Styrene

In this work, an improvement of the process model used for polystyrene polymerization in batch reactors by Ekpo (2006) is first considered. Optimization of the process using the improved model is then considered. The process model for polymerization of styrene in batch reactors using 2, 2 azobisisobutyronitrile catalyst (AIBN) as initiator has been improved by including the gel and glass effects which was absent in the earlier work of Ekpo (2006). The model is essentially a set of differential equations that describe the changes taking place in the reactor.

3.3.1 Simple Kinetic Model

The model used was adopted from work of Ekpo (2006). They are presented in terms of first three moments of dead polymer and living polymer since this work is considering the gel and glass effects. Methods of moments of molecular weight distribution (MWD) are suitable for the purpose of controlling the MWD of the polymer (Begum and Simon, 2011; Baillagou and Soong, 1985b; Prasad et al., 2002). The first three moments are adequate to characterize the MWD where the zeroth moment refers of the mean of distribution, the first moment describe the standard deviation and the second moment describe the skewness of the distribution.

Polymer MWD can be characterized by means of ratios of dead polymer moment using methods of moments. The moments for the dead polymer moment are defined in this equation:

$$\sigma_k = \sum n^k P_n \tag{3.1}$$

Where P_n is the chain length, n is the number of molecules in the chain and k is the order of the moment. The rate of change of the zeroth, first and second moments of dead polymer molecular weight distribution (MWD) (Ray, 1972) can be given as:

$$\frac{d\sigma_0}{dt} = 0.5 k_t \mu_0^2 \tag{3.2}$$

$$\frac{d\sigma_1}{dt} = k_t \mu_0 \mu_1 \tag{3.3}$$

$$\frac{d\sigma_2}{dt} = k_t (\mu_2 \mu_0 + \mu_1^2) \tag{3.4}$$

Where k_t is the rate of termination reaction and μ_i is the i^{th} active polymer moment. Dimensionless form for monomer concentration, *M*, initiator concentration, *I* and dead polymer moments σ_0 can be defined as equation 3.5, 3.6 and 3.7. M_0 and I_0 in the equations are initial monomer concentration and initial initiator concentration respectively.

$$m = \xi_1 = 1 - \frac{M}{M_0} \tag{3.5}$$

$$c = 1 - \frac{I}{I_0} \tag{3.6}$$

$$\xi_n = \frac{\sigma_n}{M_0} \tag{3.7}$$

The rate of consumption of initiator concentration, *I* and the dimensionless form of rate of initiator conversion, *c* can be expressed as:

$$\frac{dI}{dt} = -k_d I \tag{3.8}$$

$$\frac{dc}{dt} = k_d(1 - c) \tag{3.9}$$

Quasi steady state assumption (QSSA) is a hypothesis saying that the rate of radical generation is approximately equal to the rate of radical destruction throughout the polymerization. By applying quasi steady state assumptions (QSSA) for this model, the equations for zeroth, first and second active polymer moment become:

$$\mu_0 = \left[\frac{2fk_dI}{k_t}\right]^{0.5} \tag{3.10}$$

$$\mu_1 = \left[\frac{2fk_dI + k_pM\mu_0}{k_t\mu_0}\right] \tag{3.11}$$

$$\mu_2 = \frac{2fk_dI + k_pM(2\mu_1 + \mu_0)}{k_t\mu_0} \tag{3.12}$$

Initiator concentration in the equation of zeroth active polymer moment is substituted with the initiator conversion in order to get the dimensionless form of zeroth active polymer moments which becomes:

$$\mu_0 = \left[\frac{2fk_dI_0(1-c)}{k_t}\right]^{0.5} \tag{3.13}$$

$$\mu_1 = \left[\frac{2fk_dI}{k_t\mu_0} + \frac{k_pM\mu_0}{k_t\mu_0}\right] \tag{3.14}$$

Rearrange the equation 3.10 for μ_0 to become:

$$\mu_0{}^2 = \left[\frac{2fk_dI}{k_t}\right] \tag{3.15}$$

Then substitute μ_0 from equation 3.15 into equation 3.11 with yield the dimensionless equation of the first active polymer moment:

$$\mu_1 = \left[\frac{\mu_0{}^2}{\mu_0} + \frac{k_pM\mu_0}{k_t\mu_0}\right] \tag{3.16}$$

$$\mu_1 = \left[\mu_0 + \frac{k_pM}{k_t}\right] \tag{3.17}$$

Rearrange and substitute equation 3.12 yield the dimensionless form for second active polymer moment:

$$\mu_2 = \mu_1 + \frac{2k_p M \mu_1}{k_t \mu_0} \tag{3.18}$$

To make the dead polymer moments of zeroth dead polymer moment of molecular weight distribution dimensionless, substitute σ_0 and μ_0 in equation 3.2 with rearranged equation 3.7 and equation 3.15. Then equation 3.2 becomes:

$$\frac{d\xi_0}{dt} = \frac{k_t f k_d I_0 (1-c)}{M_0 k_t} \tag{3.19}$$

$$\frac{d\xi_0}{dt} = a k_d (1-c) \tag{3.20}$$

Where *a* is defined from the equation:

$$a = f \frac{I_0}{M_0} \tag{3.21}$$

f in the equation is the initiator efficiency which is the fraction of primary free radicals that successfully initiate polymerization. Value for *f* is normally in the range of 0.3 to 0.8 due to side reaction where some of the radicals decompose to form compounds cannot decompose further to initiate the polymerization. For this system with AIBN as initiator, *f* is equal to 0.6 which is the same as previous work of Ekpo (2006) for bulk polymerization of Styrene.

Substitute μ_1 from equation 3.17 into equation 3.3 yield;

$$\frac{d\sigma_1}{dt} = k_t \mu_0 \left[\mu_0 + \frac{k_p M}{k_t}\right] \tag{3.22}$$

$$\frac{d\sigma_1}{dt} = k_t {\mu_0}^2 + k_p \mu_0 M \tag{3.23}$$

$$\frac{d\sigma_1}{dt} = 2fk_d I_0(1-c) + k_p M\left[\frac{2fk_d I_0(1-c)}{k_t}\right]^{0.5} \tag{3.24}$$

For the dimensionless form of first dead polymer moments, again the relation for ξ_n is used and the equation becomes:

$$\frac{d\xi_1 M_0}{dt} = 2fk_d I_0(1-c) + k_p M\left[\frac{2fk_d I_0(1-c)}{k_t}\right]^{0.5} \tag{3.25}$$

Equation 3.25 also can be written:

$$\frac{d\xi_1}{dt} = 2ak_d(1-c) + k_p\left[\frac{2fk_d I_0}{k_t}\right]^{0.5}(1-\xi_1)(1-\mathrm{c})^{0.5} \tag{3.26}$$

$$\frac{d\xi_1}{dt} = 2ak_d(1-c) + K_1(1-\xi_1)(1-\mathrm{c})^{0.5} \tag{3.27}$$

Where,

$$K_1 = k_p\left[\frac{2fk_d I_0}{k_t}\right]^{0.5} \tag{3.28}$$

Long chain hypothesis (LCH) is the assumption that the amount of monomer consumed in the initiation stage is negligible compared to that consumed by growing chain. By making long chain approximation, the first term on the right hand side of equation 3.28 can be neglected (Chen and Jeng, 1978). Therefore, the first dead polymer moment is:

$$\frac{d\xi_1}{dt} = K_1(1-\xi_1)(1-\mathrm{c})^{0.5} \tag{3.29}$$

By using the relation for ξ_n, the dimensionless form of the second dead polymer moment become:

$$\frac{d\xi_2}{dt} = \frac{k_t}{M_0}\left(\left(\frac{2k_pM\mu_1}{k_t\mu_0}\right)\mu_0 + \mu_1^2\right) \tag{3.30}$$

$$\frac{d\xi_2}{dt} = \frac{2k_pM\mu_1}{M_0} + \frac{k_t\mu_1^2}{M_0} \tag{3.31}$$

Substituting the μ_1 from 3.17, the above equation becomes:

$$\frac{d\xi_2}{dt} = \frac{2k_pM}{M_0}\left[\mu_0 + \frac{k_pM}{k_t}\right] + \frac{k_t}{M_0}\left[\mu_0 + \frac{k_pM}{k_t}\right]^2 \tag{3.32}$$

Rearranging and simplification gives:

$$\frac{d\xi_2}{dt} = \frac{2k_pM\mu_0}{M_0} + \frac{2{k_p}^2M^2}{k_tM_0} + \frac{k_t}{M_0}\left[\mu_0 + \frac{k_pM}{k_t}\right]^2 \tag{3.33}$$

$$\frac{d\xi_2}{dt} = \frac{2k_pM\mu_0}{M_0} + \frac{2{k_p}^2M^2}{k_tM_0} + \frac{k_t}{M_0}\left[{\mu_0}^2 + \frac{2\mu_0k_pM}{k_t} + \frac{{k_p}^2M^2}{{k_t}^2}\right] \tag{3.34}$$

$$\frac{d\xi_2}{dt} = \frac{2k_pM\mu_0}{M_0} + \frac{2{k_p}^2M^2}{k_tM_0} + \frac{k_t{\mu_0}^2}{M_0} + \frac{2\mu_0k_pM}{M_0} + \frac{{k_p}^2M^2}{k_tM_0} \tag{3.35}$$

$$\frac{d\xi_2}{dt} = \frac{4k_pM\mu_0}{M_0} + \frac{3{k_p}^2M^2}{k_tM_0} + \frac{k_t{\mu_0}^2}{M_0} \tag{3.36}$$

Substituting the μ_0 from equation 3.10, the above equation becomes:

$$\frac{d\xi_2}{dt} = \frac{4k_pM}{M_0}\left[\frac{2fk_dI_0(1-c)}{k_t}\right]^{0.5} + \frac{3{k_p}^2M^2}{k_tM_0} + \frac{k_t}{M_0}\left[\frac{2fk_dI_0(1-c)}{k_t}\right] \tag{3.37}$$

Simplifying the above equation from equation 3.29 and using

$$K_3 = M_0 \frac{{k_p}^2}{k_t} \tag{3.38}$$

the dimensionless equation for second moment of molecular weight distribution becomes:

$$\frac{d\xi_2}{dt} = 4K_1(1-\xi_1)(1-\mathrm{c})^{0.5} + 3K_3(1-\xi_1)^2 + 2ak_d I_0(1-c) \tag{3.39}$$

For the convenience of the readers, all the model equations are collected again and presented here.

First three dead polymer moments

$$\frac{d\xi_0}{dt} = ak_d(1-c) \tag{3.20}$$

$$\frac{dm}{dt} = \frac{d\xi_1}{dt} = K_1(1-c)^{0.5}(1-\xi_1) \tag{3.29}$$

$$\frac{d\xi_2}{dt} = 4K_1(1-\xi_1)(1-\mathrm{c})^{0.5} + 3K_3(1-\xi_1)^2 + 2ak_d I_0(1-c) \tag{3.39}$$

First three living polymer moments

$$\frac{d\sigma_0}{dt} = 0.5k_t\mu_0^2 \tag{3.2}$$

$$\frac{d\sigma_1}{dt} = k_t\mu_0\mu_1 \tag{3.3}$$

$$\frac{d\sigma_2}{dt} = k_t(\mu_2\mu_0 + \mu_1^2) \tag{3.4}$$

Initiator concentration and initiator conversion

$$\frac{dI}{dt} = -k_d I \tag{3.8}$$

$$\frac{dC}{dt} = k_d(1-c) \tag{3.9}$$

Number average molecular weight and weight average molecular weight

$$M_n = \xi_1/\xi_0 \tag{3.40}$$

$$M_w = \xi_2/\xi_1 \tag{3.41}$$

$$K_1 = k_p\left[\frac{2fk_dI_0}{k_t}\right]^{0.5} \tag{3.28}$$

$$K_3 = M_0\frac{{k_p}^2}{k_t} \tag{3.38}$$

Rate constant for decomposition, propagation and termination

$$k_d = A_d\, exp\left(\frac{-E_d}{RT}\right) \tag{3.42}$$

$$k_{p_0} = A_p\, exp\left(\frac{-E_p}{RT}\right) \tag{3.43}$$

$$k_{t_0} = A_t\, exp\left(\frac{-E_t}{RT}\right) \tag{3.44}$$

$$PD = \frac{X_w}{X_n} \tag{3.45}$$

$$a = f\frac{I_0}{M_0} \tag{3.21}$$

In this work, the gel and glass effect will take into account for the bulk free radical polymerization initiated by AIBN which was absent in early work of Ekpo and Mujtaba (2004).

The equations that will be used to calculate the gel and glass effects in polystyrene polymerisation for this work are the same as in Ekpo and Mujtaba (2008); Fan, Gretton-Watson et al. (2003) and Baillagou and Soong (1985b) which was used for MMA polymerization. However some parameters have been changed in order to fit the process of bulk free radical polystyrene process. The value for $k_{\theta p}$ and $k_{\theta t}$ are taken from Baillagou and Soong (1985b) with some amendment of the value of activation energy in calculation of $k_{\theta t}$. This value have been chosen based on the theory that the termination kinetic rate will decrease due to severe diffusion limitations. The result shows that the trend of k_p and k_t agreed with the theory of the diffusion limitation.

In order to calculate the diffusion coefficient of the polystyrene, the glass temperature, T_{gp} in the equation is referred to glass transition temperature (T_g) of the polystyrene. These equations express the changing volume fractions of consumed monomer and produced polymer during the polymerization reaction. Auto acceleration modifies the rate constants as the polymer fraction increases (Ekpo, 2006). The equations are presented below.

$$\varphi_m = \frac{C_m MW_m}{\rho_m} \tag{3.46}$$

$$\varphi_p = \frac{\mu_1 MW_m}{\rho_p} \tag{3.47}$$

$$k_t = \frac{k_{t_0}}{1 + \frac{k_{t_0}(\xi_0)}{D(k_{\theta t})}} \tag{3.48}$$

$$k_p = \frac{k_{p_0}}{1 + \frac{k_{p_0}(\xi_0)}{D(k_{\theta p})}} \tag{3.49}$$

$$k_{\theta p} = 2.5292 \times 10^{15} \exp\left(-2.8 \times 10^4 / RT\right) \tag{3.50}$$

$$k_{\theta t} = 4.4533 \times 10^{18} I_0 \exp(-2.8 \times 10^4 / RT) \tag{3.51}$$

$$D = exp\left[\frac{2.303\ (1 - \varphi_p)}{0.168 - 8.21 \times 10^{-6}\left(T - T_{gp}\right)^2 + 0.03(1 - \varphi_p)}\right] \tag{3.52}$$

A detailed treatment of all aspects of the model can be found in the referenced texts.

3.3.2 Energy Balance Model

Detailed model or energy balance model was developed by adding energy balance equations to the simple kinetic model. Energy balance equations for the free radical polymerization of styrene using jacket coolant flow and jacket temperature set point as the control variables are presented here

Type 1: jacket coolant flow (F_j) as control variable

$$\frac{dT}{dt} = \frac{Q_W + Q_r - Q_J}{Vc_P\rho} \tag{3.53}$$

$$\frac{dT_J}{dt} = \frac{F_J}{V_J}\left(T_{J0} - T_J\right) + \frac{Q_J}{V_J c_{pJ}\rho_J} \tag{3.54}$$

$$Q_r = (-\Delta H_r)R_P V \tag{3.55}$$

$$Q_J = UA(T - T_J) \tag{3.56}$$

Type 2: Jacket temperature set point (T_{jsp}) as control variable;

$$\frac{dT}{dt} = \frac{Q_r - Q_J}{Vc_P\rho} \tag{3.57}$$

$$\frac{dT_J}{dt} = \frac{T_{Jsp} - T_J}{\tau_J} + \frac{Q_J}{V_J c_{pJ}\rho_J} \tag{3.58}$$

R_p and r_0 are the rates of polymerization and radical formation respectively.

$$R_p = K_p M r_0 \tag{3.59}$$

$$r_0 = \left[\frac{2fk_d c}{k_t}\right]^{0.5} \tag{3.60}$$

3.4 Modelling Free Radical Solution Polymerization of MMA

This work is concerned with the improvement of the process model used for MMA polymerization in batch reactors by Ekpo (2006) and optimization the process using the improved model. The process model for solution polymerization of MMA in batch reactors using 2, 2 azobisisobutyronitrile catalyst (AIBN) as initiator has been improved by using the free volume theory to calculate the initiator efficiency,*f*. The

value of *f* in the earlier work of Ekpo (2006) was set at a constant value in order to avoid more complexity to the model.

The free radical solution polymerization of Methyl Methacrylate (MMA) with the initiator are feed into the tank reactor where the process of polymerization occurs. After the cycle batch time the product of Polymethyl Methacrylate (PMMA) can be taken out from batch reactor.

The free radicals solution polymerization of MMA in batch process proceeds in much the same as bulk process except the addition of solvent. Solvent is added to ensure that there is no heat build-up in the reactor and to aid an effective heat removal strategy. This eventually will hinder the occurrence of gel and glass effect in the reactor by reducing the viscosity of the reacting mixture.

The mechanism of the process also starts with the initiation of initiator at the beginning of the process. Simply put, the initiator breaks down in the presence of heat to produce free radicals which combine with the monomer to form growing polymer chains. However, chain termination for MMA is predominantly by disproportionation, where growing chains will terminate independently (Ekpo, 2006).

3.4.1 Simple Kinetic Model

The model equations adopted in this work for the solution polymerization of MMA have been taken from Ekpo (2006). The free radical polymerization mechanism as discussed before in section 2.5 is used to express the simple kinetic model. The standard assumptions of the model for the solution polymerization of MMA are as follows;

a) Quasi-steady state approximation (QSSA) and long chain hypothesis are valid for the system.

b) All reactions steps in the system are irreversible.

c) Chain transfer to solvent is negligible compared to other reaction steps.

d) The gel and glass effects for the polymerization are included.

As with polystyrene, the polymerization process start with the decomposition of initiator to breakdown the initiator molecules, followed by the reaction of the free radicals with the monomer. The initiator and monomer balances can be given by equations:

$$\frac{dC_i}{dt} = -k_d C_i \tag{3.61}$$

$$\frac{dC_m}{dt} = -(k_p + k_{fm})C_m \xi_0 \tag{3.62}$$

where C_i and C_m are the concentrations of initiator and monomer respectively.

The decomposition of initiator molecules to form very active primary radicals are depend on the initiator efficiency, *f*. Not all initiator molecules decomposed to form primary radicals since some of them might either have self-terminate or react with other reactants in the system which make the initiator efficiency less than 100%.

Achilias and Kiparissides (1992) had reported that there are quite a lot of published paper has treated the initiator efficiency, f as a constant value. Ekpo (2006) and Ekpo and Mujtaba (2008) used a constant value of 0.53 for the initiator efficiency. However, it is believed that the initiator efficiency is not constant and will decrease as the viscosity inside the reactor increases. In this work, the initiator efficiency used in the simple model is improved by using the free volume theory.

Dube et al (1997) have used the free volume theory to model the changing of initiator efficiency as below:

$$f = f_0 exp\left(-C_f\left(\frac{1}{V_F} - \frac{1}{V_{F,crit}}\right)\right) \quad (3.63)$$

Formatted: Font: 11 pt

Formatted: Font: (Asian) +Body, Complex Script Font: Times New Roman

Where;

f_0 is the initial initiator efficiency.

C_f is a parameter which modifies the rate of change of the efficiency.

V_F is free volume

$V_{F,crit}$ is critical free volume.

The value of C_f and f_0 are 0.006 and 0.53 respectively (Fan et al., 2003). The free volume (V_F) and critical free volume ($V_{F,crit}$) equations were given by Fan et al. (2003) as below:

$$V_F = 0.025 + 0.001(T - 167)\emptyset_m + 0.00048(T - 387)\emptyset_p + 0.00048(T - 249)\emptyset_s \quad (3.64)$$

Formatted: Font: (Asian) +Body, Complex Script Font: Times New Roman

Formatted: Font: 11 pt

$$V_{Fcrit} = 0.1856 - 2.965x10^{-4}(T - 273) \quad (3.65)$$

where $\emptyset_m, \emptyset_p$ and $\emptyset_s$ are the volume fraction of monomer, polymer and solvent which can be obtained by the equations below:

$$\emptyset_s = C_m MW_m/\rho_m \quad (3.66)$$

$$\emptyset_p = \mu_1 MW_m/\rho_p \quad (3.67)$$

$$\emptyset_s = 1 - \emptyset_m - \emptyset_p \quad (3.68)$$

The first three moments equations of living and dead polymer are presented in equation (3.70) – (3.75).

$$\frac{d\xi_0}{dt} = 2fk_dC_i - k_t\xi_0^2 \quad (3.69)$$

$$\frac{d\xi_1}{dt} = 2fk_dC_i - k_pC_m\xi_0 + \left(k_{fm}C_m + k_{fs}C_s\right)(\xi_0 - \xi_1) - k_t\xi_0\xi_1 \quad (3.70)$$

$$\frac{d\xi_2}{dt} = 2fk_dC_i - (2\xi_0 - \xi_1)k_pC_m + \left(k_{fm}C_m + k_{fs}C_s\right)(\xi_0 - \xi_1) - k_t\xi_0\xi_2 \quad (3.71)$$

$$\frac{d\mu_0}{dt} = \left(k_{fm}C_m + k_{fs}C_s\right)\xi_0 + (0.5k_t)\xi_0^2 \quad (3.72)$$

$$\frac{d\mu_1}{dt} = \left(k_{fm}C_m + k_{fs}C_s + k_t\xi_0\right)\xi_1 \quad (3.73)$$

$$\frac{d\mu_2}{dt} = \left(k_{fm}C_m + k_{fs}C_s\right)\xi_2 + k_t\xi_0\xi_2 + k_t\xi_1^2 \quad (3.74)$$

The monomer conversion at any point, the number and weight average molecular weight are:

$$X_n = \frac{\mu_1}{C_{m,0}} \quad (3.75)$$

Formatted: Font: 11 pt
Formatted: Font: (Asian) +Body, Complex Script Font: Times New Roman
Formatted: Font: (Asian) +Body, 11 pt, Font color: Auto, Complex Script Font: Not Bold
Formatted: Font: 11 pt
Formatted: Font: (Asian) +Body, Complex Script Font: Times New Roman
Formatted: Font: 11 pt
Formatted: Font: 11 pt
Formatted: Font: (Asian) +Body, Complex Script Font: Times New Roman
Formatted: Font: (Asian) +Body, 11 pt, Font color: Auto, Complex Script Font: Not Bold
Formatted: Font: 11 pt
Formatted: Font: (Asian) +Body, Complex Script Font: Times New Roman
Formatted: Font: (Asian) +Body, 11 pt, Font color: Auto, Complex Script Font: Not Bold

$$M_n = \frac{\mu_1 + \xi_1}{\mu_0 + \xi_0} MW_m \tag{3.76}$$

$$M_w = \frac{\mu_2 + \xi_2}{\mu_1 + \xi_1} MW_m \tag{3.77}$$

Where MW_m is the molecular weight of the MMA monomer. Then the polydispersity index can be written:

$$PD = \frac{M_w}{M_n} \tag{3.78}$$

The gel effect is very pronounced in MMA polymerization. This is an auto acceleration effects that occurs when the increasing viscosity of the reacting mixture slows down the termination rate because of diffusional limitations. Autoacceleration modifies the rate constant as the polymer fraction increases. The equations given below express the temperature dependent rate constant used in the simple kinetic model for the solution polymerization of MMA.

$$k_d = 1.58\ x\ 10^{15} exp\left(-1.2874\ x\ 10^5 / R_g T\right) \tag{3.79}$$

$$k_{p0} = 7.0\ x\ 10^6 exp\left(-2.6334\ x\ 10^4 / R_g T\right) \tag{3.80}$$

$$k_{t0} = 1.76\ x\ 10^9 exp\left(-1.1704\ x\ 10^4 / R_g T\right) \tag{3.81}$$

$$k_{fm} = 4.661\ x\ 10^9 exp\left(-7.4479\ x\ 10^4 / R_g T\right) \tag{3.82}$$

$$k_{fs} = 1.49\ x\ 10^9 exp\left(-6.6197\ x\ 10^4 / R_g T\right) \tag{3.83}$$

$$k_{\theta p} = 3.0233\ x\ 10^{13} exp\left(-1.1700\ x\ 10^5 / R_g T\right) \tag{3.84}$$

$$k_{\theta t} = 1.4540\ x\ 10^{20}\ C_{i0}\ exp\left(-1.4584\ x\ 10^5 / R_g T\right) \tag{3.85}$$

$$k_p = k_{p0} / \left(1 + k_{p0} / D k_{\theta p}\right) \tag{3.86}$$

$$k_t = k_{t0} / (1 + k_{t0} / D k_{\theta t}) \tag{3.87}$$

$$D = exp\left[\frac{2.303(1-\emptyset_p)}{0.168 - 8.21\ x\ 10^{-6}(T-387)^2 + 0.03(T-\emptyset_p)}\right] \quad (3.88)$$

3.4.2 Energy Balance Model

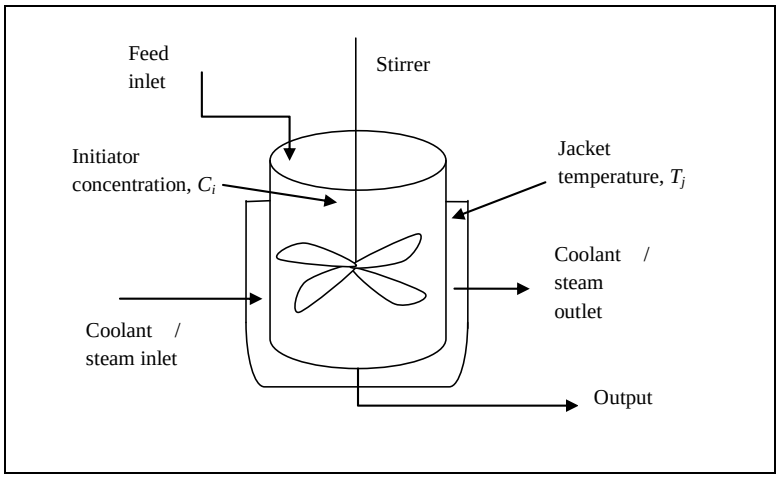

Figure 3.1: Schematic diagram of batch reactor system

As shown previously for polystyrene process, an energy balance model is developed by adding energy balance equations to the simple model. The reactor is assumed to be well mixed. The dynamics of the reactor wall are assumed to be negligible with respect to the reacting mixture. Based on these assumptions, the energy balance for the reactor temperature and jacket temperature can be expressed as:

$$\frac{dT}{dt} = \frac{(-\Delta H_r)R_p}{C_p \rho_{mix}} - \frac{UA(T - T_J)}{C_p V \rho_{mix}} \tag{3.89}$$

$$\frac{dT_J}{dt} = \frac{(T_{Jsp} - T_J)}{\tau_J} - \frac{UA(T - T_J)}{C_{pJ} V_J \rho_J} \tag{3.90}$$

T_{Jsp} is the jacket temperature set point and is used as the control variable in place of reaction temperature in the energy balance model. This model is similar to Type 2 (page 70) model presented for styrene polymerization and was used by Ekpo and Mujtaba (2008). However, online implementation of the optimal control paths obtained in this work is not done within this research and will be put as the suggestion for future work in chapter 7. τ_J is the jacket time constant while R_p is the rates of polymerization.

The specific heat capacity and the density of the the reacting mixture are given below

$$C_p = \frac{\mu_1 C_{p,p} + C_m C_{p,m} + C_s C_{p,s}}{\mu_1 + C_m + C_s} \tag{3.91}$$

$$\rho_{mix} = (\mu_1 + C_m) MW_m + C_s MW_s + C_i MW_i \tag{3.92}$$

The specific heat is calculated from the mole average value of the various components in the reacting mixture namely polymer, monomer and solvent.

3.5 Modelling Free Radical Emulsion Copolymerization of Styrene and MMA

The mathematical model for emulsion copolymerization of Styrene and MMA using zero-one kinetics system in this work adopted from Alhamad (2005). The emulsion copolymerization process of two monomers (styrene and MMA) begins with the decomposition of the initiator to become free radical initiators in the water phase, with coefficient of k_d (s^{-1}). These initiator radicals are needed to initiate the polymerization process where they react with the monomers A and B to generate oligomeric radicals in the water phase as describe below:

$$I - I \xrightarrow{k_d} 2I^{\bullet} \tag{3.93}$$

$$I^{\bullet} + M \xrightarrow{k_{p1}} IM_1^{\bullet} \tag{3.94}$$

Since this copolymerization process involves two types of monomer, the primary radical will undergo propagation process by propagated with monomer A (styrene) or B (MMA), with coefficient of $k_{p,A}$ or $k_{p,B}$ and can be described by,

$$I^{\bullet} + M_A \xrightarrow{k_{p,A}} IM_A^{\bullet} \tag{3.95}$$

$$I^{\bullet} + M_B \xrightarrow{k_{p,B}} IM_B^{\bullet} \tag{3.96}$$

Then these oligomeric radicals undergo a sequence of reactions as shown below:

$$IM_1^{\bullet} + M \xrightarrow{k_{p,aq}^{i}} IM_{i+1}^{\bullet} \tag{3.97}$$

These oligomeric radicals will continue the propagation process with monomer A or monomer B with coefficient of k_{pAA}, k_{pAB}, k_{pBB} *or* k_{pBA}.

$$IM_A^{\bullet} + M_A \xrightarrow{k_{p,AA}} IM_{AA}^{\bullet} \quad (3.98)$$

$$IM_A^{\bullet} + M_B \xrightarrow{k_{p,AB}} IM_{AB}^{\bullet} \quad (3.99)$$

$$IM_B^{\bullet} + M_A \xrightarrow{k_{p,BA}} IM_{BA}^{\bullet} \quad (3.100)$$

$$IM_B^{\bullet} + M_B \xrightarrow{k_{p,BB}} IM_{BB}^{\bullet} \quad (3.101)$$

There are three fates of these oligomeric radicals; they can undergo termination with another radical, enter into a latex particle or a micelle, or further propagate and form a new particle by homogeneous nucleation when it achieve its critical size for homogeneous nucleation, j_{crit}.

$$IM_i^{\bullet} + T^{\bullet} \xrightarrow{k_{t,aq}} inert\ product, i < z\ ; \quad (3.102)$$

$$IM_i^{\bullet} + latex\ particle \xrightarrow{k_e^i} entry, i = z, \dots, j_{crit} - 1\ ; \quad (3.103)$$

$$IM_i^{\bullet} + micelle \xrightarrow{k_{e,micelle}^i} new\ particle, i = z, \dots, j_{crit} - 1\ ; \quad (3.104)$$

$$IM_{j_{crit}}^{\bullet} \rightarrow new\ particle \quad (3.105)$$

The dissociation of the initiator can be described with:

$$\frac{d[I]}{dt} = -2k_d f[I] + \frac{F_I}{V_w} \quad (3.106)$$

$$f = \left(\frac{\left(k_d[I]k_{t,aq}\right)^{0.5}}{k_{p,aq}C_w} + 1 \right)^{1-z} \quad (3.107)$$

$$k_d = 8\ x\ 10^{15} e^{135\ 000/RT_r} \quad (3.108)$$

Where f is the initiator efficiency and k_d is the dissociation coefficient (l/mol.s). There are four types of radical species that need to be addressed and balanced in the aqueous phase. They are the oligomeric radicals of degree 1; oligomeric radicals for

degree greater than 1 and less than *z*; oligomeric radicals degree greater than or equal to *z* and less than j_{crit} -1; and oligomeric when it achieved the j_{crit}. The balance equation for the four types of oligomeric mentioned above can be represented by the set equations below:

$$IM_1 = \frac{2k_d[I]}{k_{p,aq}^1 C_w + k_{t,aq} T} \tag{3.109}$$

$$IM_i = \frac{k_{p,aq}^{i-1}\, IM_{i-1}\, C_w}{k_{p,aq}^i C_w + k_{t,aq} T} \qquad \text{for } i = 2 \text{ to } (z-1); \tag{3.110}$$

$$IM_i = \frac{k_{p,aq}^{i-1}\, IM_{i-1}\, C_w}{k_{p,aq}^i\, C_w + \sum(k_e^i n)\Delta r + k_{e,micelle}^i\, C_{micelle} + k_{t,aq}\, T} \tag{3.111}$$

for i = z to (j_{crit}-1);

$$IM_{jcrit} = \frac{k_{p,aq}^{jcrit-1}\, IM_{jcrit-1}\, C_w}{k_{t,aq} T} \tag{3.112}$$

Where;

C_w is the monomer concentration in water phase

T is total concentration of the radicals in the aqueous phase

The monomeric radicals formed by radical transfer to the monomer, $M^{\bullet}$, either the terminal monomer could be styrene or MMA, $M^{\bullet}_A$ or $M^{\bullet}_B$ may desorb from the particle with such "excited radicals". This adsorption- desorption process is reversible.

The decomposition coefficient, k_d of the persulfate is given by,

$$k_d = 8\,x\,10^{15}\exp(-135000/RT_r) \quad (3.113)$$

The entry processes to the particle and to the micelles are assumed to be diffusion controlled. The entry coefficient of monomer A and B to a micelle or pre-existing particle can be calculated as follows;

$$k^i_{e,micelle,A}\,(\mathrm{V}) = 4\pi r_{micelle}\ Na\frac{Dw,A}{i} \quad , \qquad \text{for i} \geq \text{z;} \quad (3.114)$$

$$k^i_{e,micelle,A}(V) = 0 \quad , \qquad \text{for i} < \text{z;} \quad (3.115)$$

$$k^i_{e,micelle,B}\,(V) = 4\pi r_{micelle}\ Na\frac{Dw,B}{i} \quad , \qquad \text{for } i \geq \text{z;} \quad (3.116)$$

$$k^i_{e,micelle,A}\,(V) = 0 \quad , \qquad \text{for i} < \text{z;} \quad (3.117)$$

The average entry of the monomer to the micelle is given by,

$$k^i_{e,micelle} = k^i_{e,micelle,A}.f_A.\emptyset_A + k^i_{e,micelle,B}.f_B.\emptyset_B \quad (3.118)$$

While the entry rate coefficient of monomer A and B to the particles are given by,

$$k^{i,j}_{e.A} = 4\pi r^j_s Na\ \frac{D_{w,A}}{i}, \ \text{for i} \geq \text{z;} \qquad k^i_e\,(\mathrm{V}) = 0, \ \text{i<z} \quad (3.119)$$

$$k^{i,j}_{e.B} = 4\pi r^j_s Na\ \frac{D_{w,B}}{i}, \ \text{for i} \geq \text{z;} \qquad k^i_e\,(\mathrm{V}) = 0, \ \text{i<z} \quad (3.120)$$

The average entry of the monomer to the particle is given by,

$$k^{i,j}_e = f_A.\emptyset_A.k^{i,j}_{e,A} + f_B.\emptyset_B.k^{i,j}_{e,B} \quad (3.121)$$

Where f_A is a fraction of monomer A and f_B is the fraction of monomer B which can be calculated by,

$$f_A = \frac{N_{m,A}^{fed}}{N_{m,A}^{fed} + N_{m,B}^{fed}} \quad (3.122)$$

$$f_B = 1 - f_A \quad (3.123)$$

Where;

Na is Avogadro's number

$N_{m,A}^{fed}$ is the number of moles fed for A

$N_{m,B}^{fed}$ is the number of moles fed for B

$\emptyset_A$ is the probability of the reaction of radicals A in the water phase

$\emptyset_B$ is the probability of the reaction of radicals B in the water phase

The propagation constant for monomer A and monomer B at low conversion are given as follows;

$$k_{po,A} = 10^{7.63} e^{-32\,500/RTr} \quad (3.124)$$

$$k_{po,B} = 10^{6.4} e^{-22\,200/RTr} \quad (3.125)$$

These propagation coefficients are diffusion controlled at high conversion and are given by,

$$\frac{1}{k_{p,A}} = \frac{1}{k_{po,A}} + \frac{1}{k_{diff,A}} \quad (3.126)$$

$$\frac{1}{k_{p,B}} = \frac{1}{k_{po,B}} + \frac{1}{k_{diff,B}} \quad (3.127)$$

Where $k_{diff,A}$ and $k_{diff,B}$ are the diffusion controlled rate coefficient defined as:

$$k_{diff,A} = 4\pi\sigma N_A (D_{mon,A} + D_{rd,A}) \quad (3.128)$$

$$k_{diff,B} = 4\pi\sigma N_A (D_{mon,B} + D_{rd,B}) \quad (3.129)$$

The average propagation coefficient in aqueous phase is given by,

$$k^i_{p,aq} = k^i_{p,aq,A}.f_A.\emptyset_A + k^i_{p,aq,B}.f_B.\emptyset_B \quad (3.130)$$

The average propagation coefficient in the particle phase is calculated by,

$$k_p = k_{pAA}.P_A^2 + k_{pAB}.P_A.P_B + k_{pBA}.P_B.P_A + k_{pBB}.P_B^2 \quad (3.131)$$

Transfer to monomeric radicals takes place within the particle phase. No transfer to polymeric radicals is assumed since no transfer agents are involved in the reaction. The transfer coefficient for styrene and MMA as given by,

$$k_{tr,A} = k_{p,A}\, x\, 10^{-0.658} e^{-23\,400/RT_r} \quad (3.132)$$

$$k_{tr,B} = 4\, x\, 10^{5.3} e^{-45\,900/RT_r} \quad (3.133)$$

The average transfer coefficient is given by,

$$k_{tr} = k_{tr,AA}P_A^2 + k_{tr,BB}P_B^2 + k_{tr,AB}P_AP_B + k_{tr,BA}P_BP_A \quad (3.134)$$

The particles with a radical could undergo termination reactions. However, they may further be activated and propagate again, and then terminate and so on. The termination coefficient at high conversions is subjected to the gel effect and is given by,

$$k_{t,aq,A} = 1.703\, x\, 10^9 e^{-2263*4.182/RT_r} \quad (3.135)$$

$$k_{t,aq,B} = 9.8\, x\, 10^7 e^{-701*4.182/RT_r} \quad (3.136)$$

$$k_{to} = k_{t,aq,A}f_A + k_{t,aq,B}f_B \quad (3.137)$$

$$g^2 = (g_A^2 g_B^2)^{1/2} \quad (3.138)$$

$$g_A^2 = \left[\frac{1}{1-X_n} \exp\left(-6.59X_n - 1.896X_n^2\right)\right]^2 \quad (3.139)$$

$$g_B^2 = [\exp\left(-0.94X_n - 3.87X_n^2 + 0.49X_n^3\right)]^2 \quad (3.140)$$

$$k_t = k_{t,AA} P_A^2 + 2k_{t,AB} P_A P_B + k_{t,BB} P_B^2 \quad (3.141)$$

Where k_t is the average termination coefficient in the particle phase and X_n is overall conversion.

The conversion of monomer A (x_A) and monomer B (x_B) to a copolymer is given by,

$$x_A = 1 - \frac{N_{m,A}}{N_{m,A}^{fed}} \quad (3.142)$$

$$x_B = 1 - \frac{N_{m,B}}{N_{m,B}^{fed}} \quad (3.143)$$

$$X_n = \frac{x_A M_{w,A} + x_B M_{w,B}}{M_{w,A} + M_{w,B}} \quad (3.144)$$

For a semi-batch process, the rate of monomer accumulates in the reaction vessel can be obtained from the equation below:

$$\frac{dN_{m,A}}{dt} = F_{mA} - R_{pAP} V_p - R_{pAw} V_w \quad (3.145)$$

$$\frac{dN_{m,B}}{dt} = F_{mB} - R_{pBP} V_p - R_{pBw} V_w \quad (3.146)$$

$$\frac{dN_{m,A}^{fed}}{dt} = F_{mA} \quad (3.147)$$

$$\frac{dN_{m,B}^{fed}}{dt} = F_{mB} \quad (3.148)$$

The surfactant added into the reactor can be calculated by,

$$\frac{dN_s}{dt} = F_S \quad (3.149)$$

The area and average diameter of the particle is given as:

$$A_p = (36\pi\ x\ N_{tot})^{1/3}\ x\ V_p^{2/3} \tag{3.150}$$

$$D_{mm} = \left(\frac{A_p}{\pi N_{tot}}\right)^{1/2} \tag{3.151}$$

A detailed model of emulsion copolymerization of styrene and MMA can be found in Alhamad (2005) and Alhamad et al. (2005a).

3.6 Conclusions

This chapter presents three process models of the polymerization systems used in this work. They are bulk polymerization of styrene, solution polymerization of MMA and emulsion copolymerization of styrene and MMA. The simple kinetic models and energy balance model are shown for the first two models which were adopted from the work of Ekpo (2006) while for the latter process the model was adopted from Alhamad (2005).

The process model for the bulk polymerization of styrene was improved by including the gel and glass effect which was absent in the earlier work of Ekpo (2006). The equations used to calculate the gel and glass effects in polystyrene polymerisation for this work are the same as in Ekpo and Mujtaba (2008); Fan, Gretton-Watson et al. (2003) and Baillagou and Soong (1985b) which was used for MMA polymerization. However some parameters have been changed in order to fit the process of bulk free radical polystyrene process. The value for $k_{\theta p}$ and $k_{\theta t}$ are taken from Baillagou and Soong (1985b) with some amendment of the value of activation energy in calculation

of $k_{\theta t}$. This value have been chosen based on the theory that the termination kinetic rate will decrease due to severe diffusion limitations. The result shows that the trend of k_p and k_t agreed with the theory of the diffusion limitation.

The process model for the solution polymerization of MMA was improved by including the free volume theory to calculate the initiator efficiency,*f*. In the earlier work of Ekpo (2006), the value of f was set at a constant value in order to avoid introducing more complexity to the models. However, the initiator efficiency is not constant and will decrease as the viscosity inside the reactor increases.

The process model for emulsion copolymerization of styrene and MMA was adopted from Alhamad (2005). The details of the process model can be found in the referenced text.

The final forms of the model equations are used within gPROMS environment to carry out the dynamic optimizations which are presented in Chapter 4, 5 and 6 for dynamic optimization of bulk polymerization process of styrene, solution polymerization process of MMA and emulsion copolymerization process of styrene and MMA respectively.

Chapter Four

Dynamic Optimization of Bulk Polymerization Process of Styrene in Batch Reactor

4.1 Introduction

Typical problems in chemical engineering process design or plant operation can be represented by some equations. These equations have many and possibly an infinite number of solutions. An optimization is concerned with selecting the best among the entire set by efficient quantitative methods with its aim to find the values of the variables in the process that yield the best value of the performance criterion.

In plant operations, optimization can be applied to improve plant performance which includes the improved yields of valuable products, reduced energy consumption and higher processing rates among many others. Besides that, optimization can also lead to reduced maintenance costs, less equipment used and for a better staff utilization. It is extremely helpful yet very useful to a process plant to systematically identify the objective, constraints and also degrees of freedom which can lead to such benefits as improved quality of design, faster and more reliable troubleshooting, and faster decision making.

This chapter discusses the dynamic optimization for free radical bulk polymerization process of styrene in batch reactor. The mathematical models for the process is presented in chapter three. The initiator used to initiate the polymerization process for this work is 2, 2 azobisisobutyronitrile catalyst (AIBN). A dynamic optimization method using the Control Vector Paramerisation (CVP) technique is used to find the optimal temperature profile that will yield a desired level of monomer conversion (m) and number average molecular weight (M_n) in minimum batch time by taking into account the gel and glass effects. The batch time is divided into a finite number of intervals and piecewise constant temperature is used in each interval. The same model and method have been used by Ekpo (2004; 2006) in his bulk polymerization of styrene but without taking into account the gel and glass effect. In this work, the gel and glass effect is considered for the same process.

4.2 Formulation for Optimization of Styrene Batch Polymerization Reactor

For batch reactors there are three broad optimization problems known as minimum time problem, maximum conversion problem and maximum profit problem. This work only considers minimum time problem and will be discussed here.

4.2.1 Minimum Time problem

The optimization problem can be described as:

Given	*Fixed volume of reactor, Fixed monomer conversion, Number average molecular weight*
Optimize	*Values for control variables such as F_j, T_{j0}, T, Initial initiator concentration (I_0), Controller switching times*
So as to minimize	*Final batch time for polymerization (t_f)*
Subject to	*Process constraints: Model equations, Constraints on initiator conversion, Polydispersity values (PD), Linear bounds on the coolant flow rate (Fj), Inlet cooling / jacket temperature (T_{j0}), Reactor temperature (T)*

The free radical bulk polymerization of styrene only incorporates 2,2'-azo-bis-isobutyronitrile (AIBN) as the initiator and styrene monomer which are fed into the tank reactor where the process of polymerization are occur. After the cycle batch time the product of polystyrene can be taken out from batch reactor which the chain termination is predominantly by combination.

4.3 Case Study 1 – Optimal temperature profile in minimum batch time

Case study 1 solves the minimum time problem for simple kinetic model of bulk styrene polymerization in order to find optimal reactor temperature profiles. Measured constant values for the kinetic model for Styrene are the same as in Ekpo

(2006) are given in Table 4.1 below. According to Raja (1995), the same constant values have been used by Duerksen et al. 1967, Ponnuswamy et al. 1987 and Chen and Huang 1981.

Table 4.1: Kinetic model constant values for styrene polymerization

$A_d = 1.58 \times 10^{15}$ sec^{-1}	E_d = 30800 cal/gmol
$A_p = 1.1050 \times 10^{7}$ l/gmol-sec	E_p = 7060 cal/gmol
$A_t = 1.255 \times 10^{9}$ l/gmol-sec	E_t = 1680 cal/gmol
R = 1.987 cal/gmol.K	

The results obtained from this case study are compared with the previous study by Ekpo (2006) who disregards the gel and glass effects.

Monomer conversion (m) for the optimization of free radical polymerization of styrene is fixed (m^*) at 0.3, 0.4, 0.5, 0.6 and 0.7 while the number average molecular weight, M_n is fixed (M_n^*) at 500 g/mol, 1000 g/mol and 1500 g/mol for several different runs. Initiator conversion (c) is fixed to be between 95% and 100% at the end of the batch. This is necessary to ensure that very little traces of initiator are left over at the end of the batch, so that there is no defect of the finished polymer. The value for the polydispersity (PD) of the final product is specified to be between 1.5 and 2.0 at the end of the batch cycle time which is same as in the previous research that are used here for the comparison.

Mathematically, the optimization problem for the simple model of the free radical styrene polymerization in batch reactor can be represented as:

$$\min_{T,\, I_0} \; t_f$$

$$\text{s.t.} \quad f\left(t, x'(t), x(t), u(t), v\right) = 0, \quad [t_0, t_f] \qquad \text{model equations}$$

$$m = m^*$$

$$M_n = M_n^*$$

$$0.95 < c < 1.0 \;\; \text{(lower and upper bound on } c\text{)}$$

$$320\text{K} < T < 375\text{K} \;\; \text{(lower and upper bound on } T\text{)}$$

$$1.5 < PD < 2.0 \;\; \text{(lower and upper bound on } PD\text{)}$$

$$0.0003 < I_0 < 0.03 \;\; \text{(lower and upper bound on } I_0\text{)}$$

f represents the DAE model equations (see Chapter 3) for the polymerization process in compact form (as explained in section 2.9.1).

Results for case study 1 using three control intervals are presented in Table 4.2~~Table 4.2~~Table 4.2 and Table 4.3~~Table 4.3~~Table 4.3. The results of Ekpo (2006) for the same system but without gel and glass effect are also shown in Table 4.2~~Table 4.2~~Table 4.2. When compared with Ekpo (2006) the results show the reduction in cycle batch is very pronounced with the gel effects while the initial initiator concentration are a bit higher.

The trend of the results shows that when lower monomer conversions and lower number average molecular weight are specified, batch time is lower than for higher conversions and higher molecular weight which is obvious. The initial initiator concentration required decreases with increasing molecular weight. For example for 30% conversion of styrene monomer, the initial initiator concentration required decreases from 0.9143 x10^{-2} to 0.4564 x10^{-2} to 0.3038 x10^{-2} for number average

molecular weight (M_n) 500 g/mol, 1000 g/mol and 15000 g/mol respectively. This is due to less primary radical needed from the decomposition of the AIBN initiator for further propagation and termination process until attain the higher molecular weight desired. Lower initial initiator concentration (I_0) produces less primary free radical at the beginning of the process. This will contribute to higher M_n since the propagation will occur with less initiator radical and leads to increased the chain length, meaning higher number average molecular weight (M_n).

Table 4.2 Result summary for case study 1

Run	m*	M_n*	Mw	PD	I_0 (x10^{-2})		t_f	
					This work	Ekpo (2006)	This work	Ekpo (2006)
1	0.3	500	804	1.61	0.9143	0.8880	2298.9	3046.3
2	0.4	500	805	1.61	1.2196	1.1167	3338.5	5823.3
3	0.5	500	811	1.62	1.5249	1.4520	4068.0	10816.7
4	0.6	500	825	1.65	1.8302	1.7409	4503.2	20250.9
5	0.7	500	825	1.65	2.1355	2.0300	4858.3	38845.0
6	0.3	1000	1635	1.63	0.4564	0.4355	3588.4	8870.9
7	0.4	1000	1659	1.66	0.6090	0.5800	4418.3	18290.8
8	0.5	1000	1786	1.79	0.7617	0.7255	4966.0	34502.2
9	0.6	1000	1864	1.85	0.9143	0.8700	5329.3	65788.8
10	0.7	1000	1838	1.84	1.0670	1.0100	5589.2	126183.0
11	0.3	1500	2462	1.64	0.3038	0.2895	4147.7	17603.8
12	0.4	1500	2521	1.68	0.4055	0.3858	4898.4	35768.8
13	0.5	1500	2612	1.74	0.5073	0.4827	5395.7	68622.8
14	0.6	1500	2728	1.82	0.6090	0.5790	5742.4	127138.0
15	0.7	1500	2843	1.90	0.7108	0.6760	5989.4	248977.0

Table 4.3 shows the optimal temperature profiles obtained for nine runs which are selected from Table 4.2 above. These results are piecewise constant temperature profile with 3 intervals. In practice, piecewise constant temperature profiles are

easier to implement by any simple controller compared to the continuously time varying profiles which will require more sophisticated and robust controller to follow. The optimal temperature profiles for all runs followed an upward trend which are similar to that obtained by Ekpo (2006) although the actual numerical values of temperature are different.

Table 4.3: Optimal temperature profile for case study 1 (9 runs)

Run	1	Temp.(K)	367.77	370.53	375	
		Time (secs.)	0	717.5	1234.5	2298.8
Run	3	Temp.(K)	339.73	362.21	374.83	
		Time (secs.)	0	50	3050	4067.9
Run	5	Temp.(K)	358.86	367.11	375	
		Time (secs.)	0	3340.0	3921.8	4858.3
Run	6	Temp.(K)	362.68	363.47	375	
		Time (secs.)	0	682.4	2567.6	3588.4
Run	8	Temp.(K)	360.82	359.16	375	
		Time (secs.)	0	939.1	3939.1	4965.9
Run	10	Temp.(K)	358.62	365.51	375	
		Time (secs.)	0	4199.3	4699.3	5589.2
Run	11	Temp.(K)	360.7	367.29	375	
		Time (secs.)	0	2622.2	3204.8	4147.7
Run	13	Temp.(K)	358.08	365.58	375	
		Time (secs.)	0	3848.1	4453.3	5395.7
Run	15					

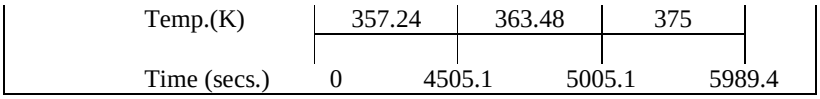
Temp.(K)
357.24
363.48
375
Time (secs.)
0
4505.1
5005.1
5989.4

Table 4.3 shows that the temperature is lower at the first interval to achieve higher desired M_n, since less initiator radical are produced at lower temperature. For example the temperature in the first interval is decreased from 367.77K (Run 1) to 362.68K (Run 6) to 360.7K (Run 11) as shown in Table 4.3 for higher desired M_n from 500 g/mol to 1000 g/mol to 1500 g/mol at 30% conversion.

The time taken to reach the desired monomer conversion (m) and number average molecular weight (M_n) is significantly less than Ekpo (2006) when considered the gel effect. This is because entanglement of the chain diffusion hindered the termination process but increases the propagation process. On top of that, more concentrated initial initiator in this work (Table 4.2) also contributes to faster polymerization process. The results really show that the gel and glass effect occurs in styrene polymerization reactions in a bulk process. As consequences, the equation related to this gel effect cannot be neglected.

Monomer conversion (m) and initiator conversion (c) for cases with and without the gel and effect is presented in Figure 4.1. It clearly shows that by taking into account the gel effect, the time taken for the system to achieve 30% monomer conversion is shorter by 24.53%. Initiator continues to add more free radicals to the system which initiated the polymerization process. The rates of initiation and propagation come out of balance. Chains grow without termination, so the conversion is rapid and the molecular weight will increase dramatically in a very short time (Cassagnau et al., 2006).

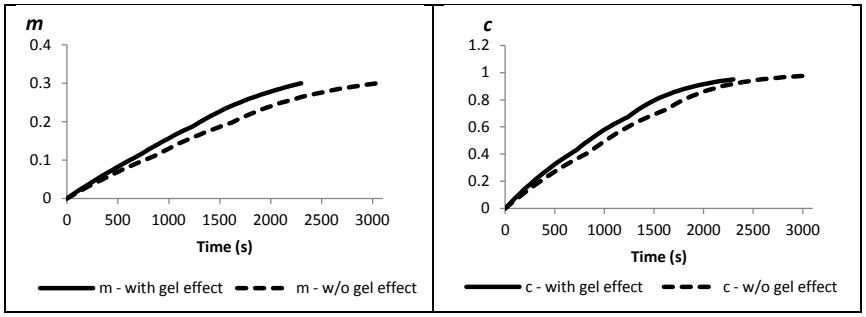

Figure 4.1: Monomer conversion and initiator conversion for run 1 with and without gel effect.

The result for number average molecular weight (M_n) and weight average molecular weight (M_w) for run 1 is given in Figure 4.2 below. These results clearly show that when considered the gel effect equation in the system, the time taken to achieve the desired molecular weight is shorter. The time taken to achieve X_n 500 is 24.53% shorter with the gel effect compared to that without gel effect since the termination rate constant was reduced and the propagation rate constant was increased as mentioned before.

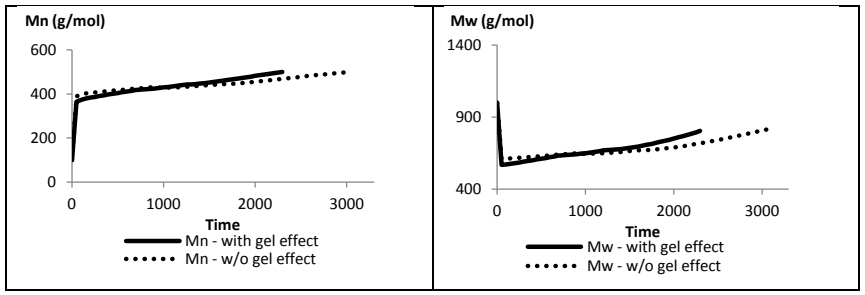

Figure 4.2: Number average molecular weight and weight average molecular weight for run 1 with and without gel effect.

As discussed earlier in Chapter 2, during the early stage of the polymerizations, the initiation kinetic rate constant is equal to the initial kinetic rate constant for termination. As time proceeds the concentration of polymer in the tank reactor will

increase. When the viscosity of the polymer is increased, terminations are difficult to occur because this high viscosity hinders the diffusion of chains because of entanglements, so the rate of termination slows considerably (Achilias and Kiparissides, 1992). However, the diffusion of small molecular monomers is hardly affected by viscosity, so propagation proceeds as before.

The described phenomenon can be seen in Figure 4.3 below where the rate of termination is going down and affected by the gel effect while the rate of propagation proceeds as before.

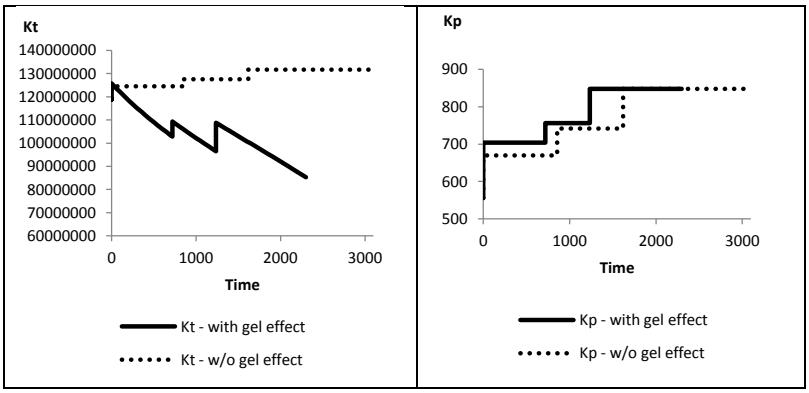

Figure 4.3: Kinetic rate for termination, k_t and kinetic rate for propagation, k_p for run 1 with and without gel effect.

Final batch times for each run are presented here in Figure 4.4. From this bar chart, the trend of time taken for each run can be seen clearly where it is increased with increasing the monomer conversion and number average molecular weight. This result is as expected that higher monomer conversion and higher molecular weight need longer batch time for the polymer reaction compared to that needed for the lower monomer conversion and lower molecular weight.

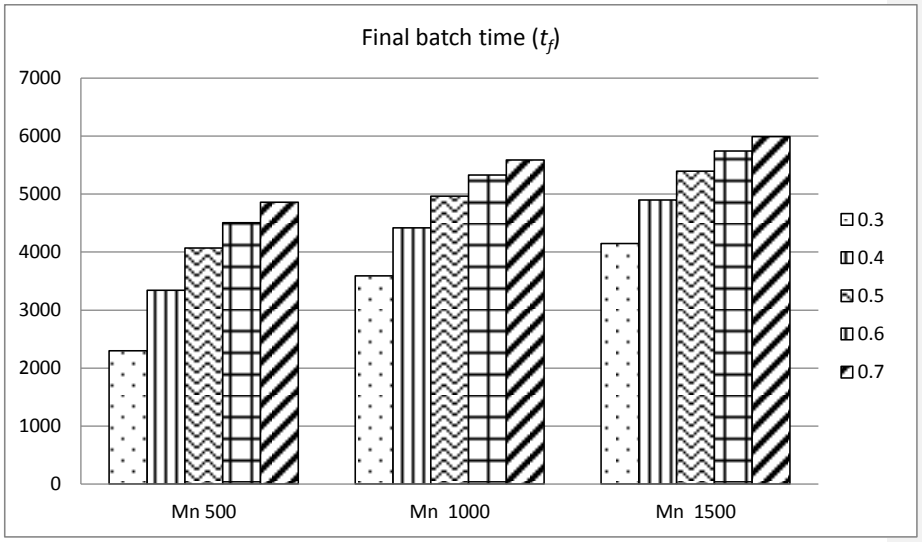

Figure 4.4: Final batch time for case study 1

4.4 Case Study 2 – Effects of number of intervals

The effect for using different number of control interval for case study 1 was investigated here.

The results with three control intervals have been presented in case study 1. Here, the outcome of having 1 interval and 6 intervals are considered. Table 4.4 shows the effect of control intervals on the final batch time for the same kinetic model of styrene polymerization with the gel effects. The batch time is reduced as the number of intervals increases and increases with the increased value of monomer conversion and number average molecular weight as clearly shown in Figure 4.5 below. However, the increase of the number of intervals might not be so significant when

consider all the economic and optimization cost for the multiple intervals when the difference of the final batch time (t_f) is very small.

Table 4.4: Effect of control intervals on the final batch time

Run	m*	M_n*	t_f (s) (1 intervals)	t_f (s) (3 intervals)	t_f (s) (6 intervals)
1	0.3	500	2460.3	2298.85	2297.96
8	0.5	1000	5437.05	4965.99	4954.41
15	0.7	1500	6593.02	5989.42	5974.54

The results in Table 4.4 really show the decrease of the final batch time when 3 intervals and 6 intervals are applied. For example, the desired M_n 1500 g/mol at 70% conversion (Run 15), the reduction of 9.16% (3 intervals) and 9.38% (6 intervals) of total batch time can be achieved compared to 1 interval (Table 4.4). There are reduction of 6.56% (Run1) and 8.66% (Run 8) can be achieved for three intervals compared to one interval. However, very small reduction from three intervals to six intervals shows that the increase of interval might not be so significant since the batch time reduction is very small.

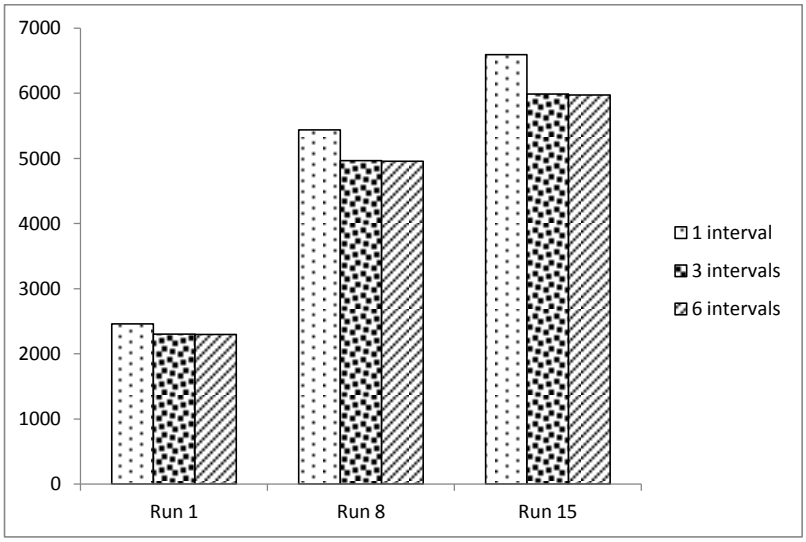

Figure 4.5: Effect of control intervals on the final batch time

4.5 Case Study 3 – Effect of coolant flow on reactor temperature

In this case study, the coolant flow (F_j) at constant feed coolant temperature is optimized using detailed model (Type 1, page 69) with energy balance (presented in Chapter 3). The reactor temperature (T) is calculated within a lower and upper bounds. Constant values from the energy balance model are given in Table 4.5 below.

Table 4.5: Constant and values from the energy balance model

A	= 5.25 m^2	T_{J0}	= 298 K	$-\Delta H_r$	= 16700 cal/gmol
M_0	= 8.7006 gmol/l	V	= 1230 litres	ρ	= 9.06 x 105 g/l
C_p	= 0.54 cal/gK	V_J	= 500 litres	ρ_J	= 9.97 x 105 g/l
C_{pJ}	= 1.003 cal/g K				

The optimization problem formulation for the detailed model of the free radical styrene polymerization in batch reactor can be mathematically represented as:

Min t_f

F_j

s.t. $f\left(t, x^{'}(t), x(t), u(t), v\right) = 0, \quad [t_0, t_f]$ model equations

$Mn = Mn^*$

$m = m^*$

$0.95 < c < 1.0$

$320K < T < 375K$

$0.001 < I_0 < 0.03$

$1.5 < PD < 2.0$

$0.0\ m^3/s < F_j < 1.0\ m^3/s$

Monomer conversion (m) for the optimization of free radical polymerization of styrene for the detailed model is fixed at 0.3, 0.5, and 0.7 and the number average molecular weight, M_n is fixed at 500 g/mol, 1000 g/mol and 1500 g/mol which correspond to run 1, run 8 and run 15 of case study 1(simple kinetic model). These have been chosen to present a general picture of the trends at the top, middle and bottom section from the kinetic model study presented in Table 4.2. Results for case study 3 are presented here in Table 4.6 and Table 4.7.

Table 4.6 shows the results for 1 interval while Table 4.7 for three intervals. The results show that the batch time for three intervals is shorter than 1 interval and is expected. The optimal profile for coolant flow rate (F_j) is increased from 5.57 x 10^{-2}

m^3/s (Run 1) to 27.61 x 10^{-2} m^3/s (Run 2) to 32.36 x 10-2 m^3/s (Run 3) for the increased of monomer conversion (m) and number average molecular weight (M_n) as shown in Table 4.6 for longer final batch time (t_f).

The reduction of 2.6% (Run 1a), 1.75% (Run 2a) and 0.32% (Run 3a) for the final batch time (t_f) can be achieved when using three intervals (Table 4.7) instead of one interval (Table 4.6). This is due to the flexibility of the coolant flow rate (F_j) for the process in order to achieve the desired properties in minimum time.

Table 4.6: Result for energy balance model with control coolant flow rate F_j for 1 interval.

Run	m*	M_n*	M_w	PD	F_j (m^3/s)	t_f (s)
1	0.3	500.0	998.0	1.99	0.0557	2486.8
2	0.5	1000.0	1907.0	1.91	0.2761	3803.2
3	0.7	1500.0	3227.0	2.15	0.3236	4153.7

Table 4.7: Result for energy balance model with control coolant flow rate F_j for 3 intervals.

Run	m*	M_n*	M_w	PD	I_0 (x10^{-2})	t_f
1a	0.3	500.0	1000.0	2.0	0.808	2422.3
2a	0.5	1000.0	1949.4	1.99	0.754	3737.8
3a	0.7	1500.0	3000.0	2.00	0.544	4140.4

The results obtained for using three control intervals (Table 4.7) show that the initial initiator concentration (I_0) is decreased with the increased desired monomer conversion (m) and number average molecular weight (M_n). As discussed before, this is due to the longer batch time (t_f) is needed to achieve higher m and M_n.

The profiles of coolant flow (F_j) and reactor temperature (T) together with the jacket temperature profile (T_j) for Run 1, Run 2 and Run 3 is shown in Figure 4.6 below.

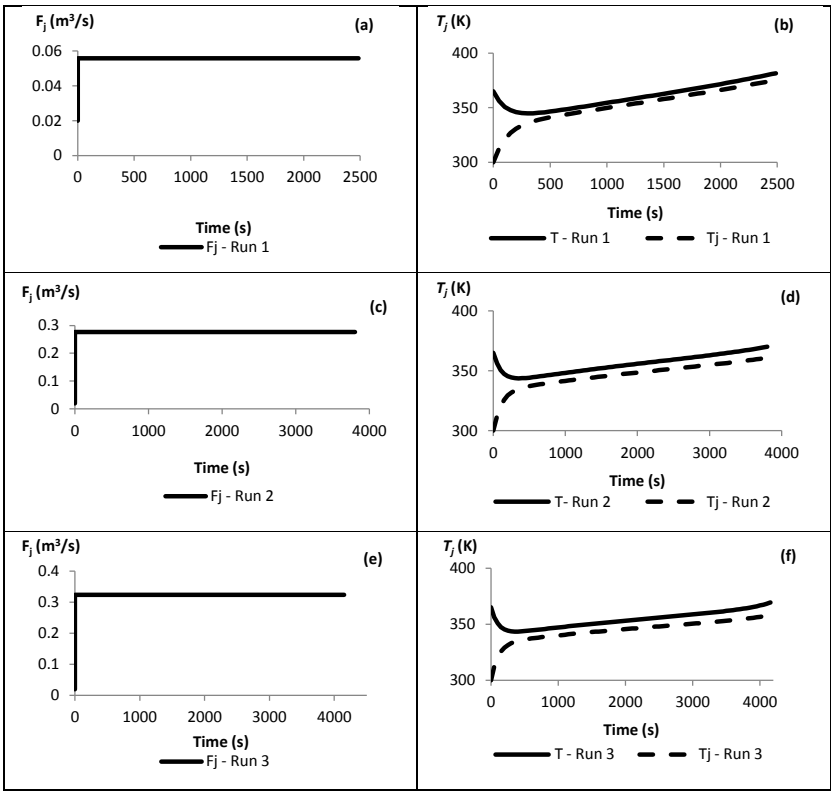

Figure 4.6: Optimal coolant flow profile (F_j), reactor temperature (T) and jacket temperature (T_j) for Run 1, 2 and 3

As mentioned before, the optimal coolant flow rate (F_j) is increased for the increased of monomer conversion (m) and number average molecular weight (M_n) (Figure 4.6a, c and e). The profiles of optimal coolant flow, jacket temperature and reactor temperature for three intervals (Run 1a, Run 2a and Run 3a) are shown in Figure 4.7. The flexibility of using three control intervals for the coolant flow rate (F_j) resulted reduction of the final batch time (t_f) for the same desired characteristics can clearly be seen in Figure 4.7.

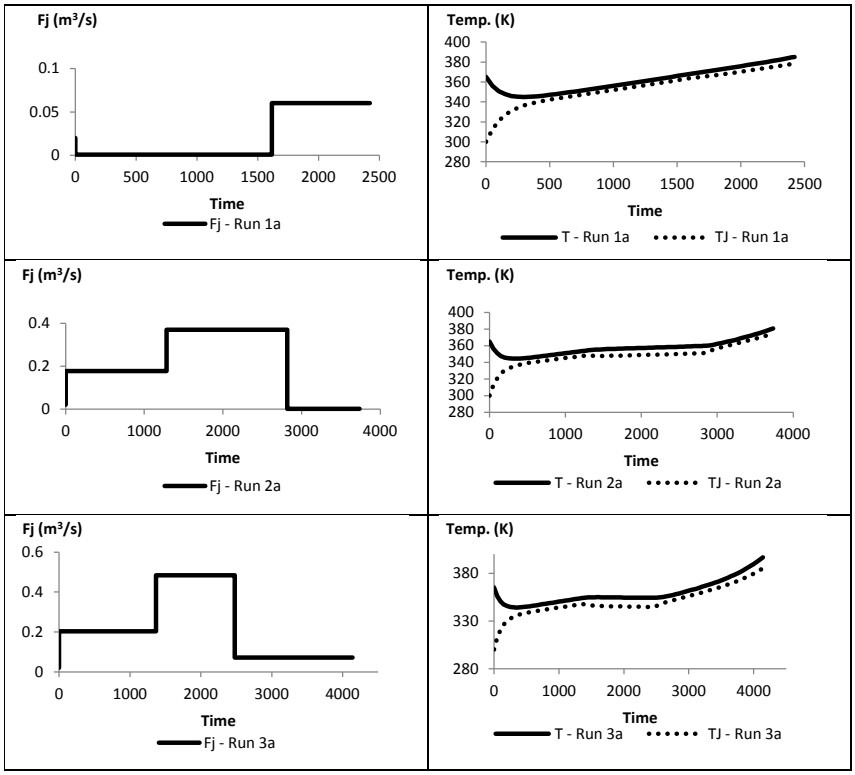

Figure 4.7: Optimal coolant flow profile (F_j), reactor temperature (T) and jacket temperature (T_j) for Run 1a, 2a and 3a

4.6 Case Study 4 – Effect of reactor temperature on coolant flow rate

In this case study, the minimum time optimization problem is solved to study the effect of optimal reactor temperature on the coolant flow trajectories for the polymerization of styrene using detailed model with energy balance (Type 1, page 69). Monomer conversion (m) for the detailed model in this case study is fixed at 0.3 and 0.5 for the number average molecular weight, M_n is fixed at 500 g/mol and 1000 g/mol.

The optimization problem formulation for the detailed model of the free radical styrene polymerization in batch reactor can be mathematically represented as:

Min t_f

T, I_0

s.t. $f\left(t, x'(t), x(t), u(t), v\right) = 0, \quad [t_0, t_f]$ model equations

$Mn = Mn^*$

$m = m^*$

$0.95 < c < 1.0$

$320K < T < 375K$

$0.001 < I_0 < 0.03$

$0.0\ m^3/s < F_j < 1.0\ m^3/s$ (lower and upper bounds on F_j)

As in case study 1, reactor temperature T and initial initiator concentration I_0 are optimized. The coolant flow F_j which will be required to manipulate to achieve the optimized reactor temperature is added as constraint with lower and upper bounds.

Table 4.8 shows the result for one interval while Table 4.9 shows the result for the same optimization process for three intervals. As the previous case study, the time taken for final batch time for three intervals are shorter than one interval as it gives more flexibility to the process variables to achieve the desired m and M_n.

Table 4.8: Result for energy balance model with control reactor temperature T and initial initiator concentration I_0 for 1 interval.

Run	m*	M_n*	M_w	PD	I_0 (x10^{-2})	T	t_f
4	0.3	500	1090	2.18	0.7633	371.8	2434.0
5	0.5	1000	4788	4.79	0.6106	366.8	4284.4

Table 4.9: Result for energy balance model with control reactor temperature T and initial initiator concentration I_0 for 3 intervals.

Run	m*	M_n*	M_w	PD	c	I_0 (x10^{-2})	t_f
4a	0.3	500	977	1.95	95.00	0.7633	2273.1
5a	0.5	1000	3510	3.51	95.00	0.6106	3824.3

Same initial initiator concentration was required for both one and three intervals.

However, a higher polydispersity (PD) is obtained for higher monomer conversion (m) and number average molecular weight (M_n). As shown in Table 4.8, the PD is increased from 2.18 to 4.79 for the increase of m and M_n. It shows that broader molecular weight distribution (MWD) of the polymer can be obtained by optimizing the T_r and I_0 as PD measures the width of a molecular weight distribution. The temperature and coolant flow rate profiles are shown in Figure 4.8 (1 interval) and Figure 4.9 (3 intervals).

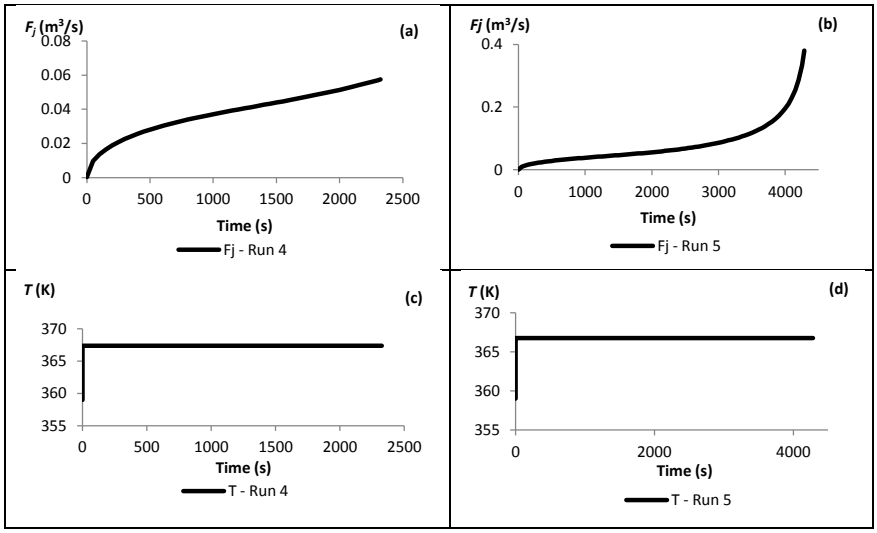

Figure 4.8: Coolant flow rate and reactor temperature for run 4 and run 5

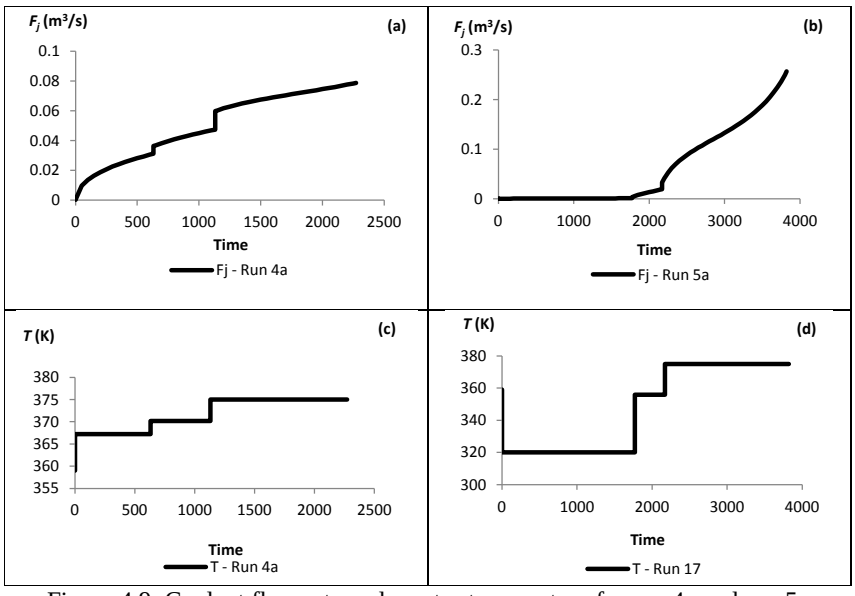

Figure 4.9: Coolant flow rate and reactor temperature for run 4a and run 5a

The coolant flow rate profiles show that more coolant flow is needed to maintain the higher temperature for the reactor (Figure 4.9). This is necessary to prevent reactor runaway and to obtain the preset characteristics of the desired polymer product.

However, by using only 1 interval, the coolant flow rate cannot maintain the increase of temperature in the reactor. Note, when the coolant flow rate is used as control variables (case study 3), it is much easier to maintain the required coolant flow rate practically as shown in Figure 4.7 compared to maintaining the continuously changing coolant flow rate as shown in Figure 4.9.

4.7 Conclusions

The dynamic optimization for free radical polymerization process of styrene in batch reactor was carried out in this chapter by using Control Vector Paramerisation (CVP) technique. The batch time was divided into a finite number of intervals and piecewise constant temperature is used in each interval where the temperature and the length of the interval are optimised. Case studies are presented by taking into account the gel and glass effects. The first two cases are using simple kinetic model while the last two cases are using the energy balance model.

Minimum time optimization problem was carried out and solved for the pre-specified monomer conversion, number average molecular weight and also polydispersity. The kinetic model considered within the optimization framework is sufficient to determine the optimal temperature profile. Optimal temperature profile is the main control parameter affecting the quality of final product. Besides that, the initial initiator concentration I_0 was also optimized for case study 1.

The results obtained from this work were compared with the previous study by other researcher which disregarded the gel and glass effect in their study. This study shows that the batch operation time is significantly reduced while the amount of the initial initiator concentration required is increased. In study case 2, the effect different number of the time intervals was investigated (1, 3 and 6 intervals). The result shows that there was time reduction with the increasing number of intervals.

The third and fourth case studies were with energy balance model (which was the extension of the kinetic model by including the energy balance equations). Two different controllers have been used, they are control coolant flow rate (case study 3) and reactor temperature (case study 4).

The results obtained in case study three and four show that the initial initiator concentration (I_0) is decreased with the increased desired monomer conversion (m) and number average molecular weight (M_n) due to the longer batch time (t_f) is needed to achieve higher m and M_n. Besides that, the results also show that the batch time for three intervals is shorter than 1 interval for the same desired monomer conversion and number average molecular weight for both case studies. The same observations have been made for kinetic model.

In order to achieve the desired m and M_n in minimum time by using detailed model, it is much easier to maintain the required coolant flow rate practically when the coolant flow rate is used as control variables (Case study 3), compared to maintaining the continuously changing coolant flow rate (Case Study 4).

The results obtained in this work show that the gel and glass effect occuring in styrene polymerization reactions in a bulk process cannot be ignored. As consequences, the equation related to this gel effect cannot be neglected.

Chapter Five

Dynamic Optimization of Solution Polymerization Process of Methyl Methacrylate in Batch Reactor

5.1 Introduction

This chapter discusses the dynamic optimization for solution polymerization of Methyl Methacrylate (MMA) in batch reactor. The initiator used to initiate the polymerization process for this work is 2, 2 azobisisobutyronitrile catalyst (AIBN). The mathematical model presented in chapter three are used here for the optimization. Two different models are used in this work, Simple Kinetic Model and Energy Balance Model respectively which was employed from Ekpo and Mujtaba (2004; 2006; 2008).

Two dynamic optimizations were carried out in this work namely minimum time problem (by simple kinetic model) and maximum conversion problem (by energy balance model). The effect of different approach for initiator efficiency, f used in dynamic optimization was investigated for constant value and time-varying value. A

constant value of f (0.53) was employed by of Ekpo (2006) in his previous work. This work is carried out to improve the model by taking into account the varying f with time by using free volume theory.

A dynamic optimization method using the Control Vector Paramerization (CVP) technique is used to find the optimal temperature profile that will yield a desired level of monomer conversion and number average molecular weight in minimum time and maximum conversion at fixed batch time. The batch time is divided into a finite number of intervals and piecewise constant temperature is used in each interval. In each interval, the temperature and the length of the interval are optimized.

5.2 Formulation for Optimization Problem

For batch reactors there are three broad optimization problems known as minimum time problem, maximum conversion problem and maximum profit problem as mentioned in chapter 4. This work will consider minimum time problem with simple kinetic model and maximum conversion problems with detailed energy model.

5.2.1 Minimum time problem

The optimization problem can be described as:

Given	*Fixed volume of reactor* *Fixed monomer conversion* *Average number molecular weight or weight average molecular weight*
Optimize	*Values for control variables such as T* *Initial initiator concentration (C_{i0})* *Controller switching times*
So as to minimize	*Final batch time for polymerization (t_f)*
Subject to	*Process constraint:* *Model equation, Initiator conversion, Polydispersity values (PD), Linear bounds on reactor temperature (T)*

Mathematically the optimization problem for minimum time problem can be described as:

$$\min_{T(t),\, C_{i0}} \quad t_f$$

s.t. $f(t, x'(t), x(t), u(t), v) = 0, \quad [t_0, t_f]$ model equations

$$Mn = Mn^*$$

$$X_n = X_n^*$$

$$c^l < c < c^u$$

$$T^l < T < T^u$$

$$PD^l < PD < PD^u$$

$$C_{i0}{}^l < C_{i0} < C_{i0}{}^u$$

5.2.2 Maximum conversion problem

The optimization problem can be described as:

Given	*Fixed volume of reactor*
	Fixed batch time (t_f)
	Number average molecular weight (M_n)
Optimize	*Values for control variables such as T_{jsp}*
	Initial initiator concentration (C_{i0})
	Controller switching times
So as to maximize	*Monomer conversion (Xn)*
Subject to	*Process constraints:*
	Model equations, Initiator conversion, Polydispersity values (PD), Linear bounds on the jacket temperature set point (T_{jsp}), Linear bounds on reactor temperature (T)

Mathematically the optimization problem for maximum conversion problem can be described as:

Max X_n

$T_{jsp}(t)$, C_{i0}

s.t. $f(t, x'(t), x(t), u(t), v) = 0, \quad [t_0, t_f]$ model equations

$$M_n = M_n^*$$

$$t_f = t_f^*$$

$$c^l < c < c^u$$

$$T_{jsp}{}^l < T_{jsp} < T_{jsp}{}^u$$

$$PD^l < PD < PD^u$$

$$C_{i0}{}^l < C_{i0} < C_{i0}{}^u$$

Subscript *l* and *u* referred to lower and upper bounds.

Unlike bulk polymerization of styrene case studies presented in chapter 4, in this work T_{jsp} is optimized instead of F_j. The use of such optimization is also noticed in Aziz (2001).

5.3 Case Study 1 – Effect of initiator efficiency using Simple Model

The model equations are presented in chapter 3. The constants values used in the model are given in the Table 5.1~~Table 5.1~~~~Table 5.1~~.

Formatted: Font: Not Bold

Formatted: Font: Not Bold

Table 5.1: Constant values used for simple model of solution polymerization of MMA

R_g = 8.314 kJ/kmol.K	MW_m = 100.12 kg/kmol
C_s = 5.0 kmol/m^3	ρ_m = 915.1 kg/m^3
$C_{m,0}$ = 3.76 kmol/m^3	ρ_m = 1200 kg/m^3

The decomposition of initiator molecules at the beginning of the process to form very active primary radicals depends on the initiator efficiency, *f*. As mentioned in chapter three, not all initiator molecules decompose to form primary radicals since some of them might either have self-terminate or react with other reactants in the system which make the initiator efficiency less than 100% (Kiparissides, 1996).

A number of published papers have used a constant value for the initiator efficiency, *f* (Achilias and Kiparissides, 1992). Ekpo (2006) and Ekpo and Mujtaba (2008) used a constant value of 0.53 for the initiator efficiency for the MMA polymerization process. However, it is believed that the initiator efficiency is not constant and will decrease as the viscosity inside the reactor increases. In this work, the initiator efficiency used in the simple kinetic model is improved by using the free volume theory (Dube et al., 1997; Fan et al., 2003).

5.3.1 Formulation of Optimization Problem

In this case study optimization of solution polymerization of MMA is carried out in order to achieve desired number average molecular weight (M_n* = 150000 kg/kmol) and monomer conversion (X_n* = 0.6 and 0.75) at minimum time by using three

control intervals. The dynamic optimization formulation and constraints are described as:

Min t_f

T, C_{i0}

s.t. $f(t, x'(t), x(t), u(t), v) = 0, \quad [t_0, t_f]$ model equations

$M_n = 150000$ kg/kmol

$Xn = Xn^*$ (0.6 or 0.75)

$0.0001 < C_{i0} < 0.150$

$1.5 < PD < 1.8$

$320 < T < 398$ K

The optimization is carried out using the value 0.53 as f (F1) and the time-varying initiator efficiency (F2) employed by Achilias and Kiparissides (1992); Dube et al. (1997); and Fan et al. (2003).

5.3.2 Results

The effect of two different approaches for the initiator efficiency, f can be observed in the results shown in Table 5.2 below.

Table 5.2: Results for the optimization of MMA simple kinetic model using different initiator efficiency, *f*

Run	*f*	C_{i0}	X_n	M_n	*PD*	t_f (s)
1	F1	1.41E-3	0.60	150014.7	1.8	2969.5
1a	F2	1.45E-3	0.60	149999.0	1.8	3772.7
2	F1	2.13E-3	0.75	150003.7	1.8	6142.5
2a	F2	2.21E-3	0.75	150003.5	1.8	8419.6

The results clearly show that the minimum batch time and initial initiator concentration required for the process had increased for the increased monomer conversion (X_n) at desired number average molecular weight (M_n* = 150000 kg/kmol) for both initiator efficiency used. The same observation was made by Ekpo (2006). However, longer batch time (increased by 21.29% for Run 1 and 27% for Run 2) and higher initial initiator (C_{i0}) was required when using the free volume theory to calculate the initiator efficiency compared to the batch time required for constant *f* at 0.53. This is because the initiator efficiency was decreased when using F2 (Figure 5.1b) resulting in less primary free radical produced inside the reactor.

As the propagation proceeds, the viscosity of the reaction mixture is increased. However, the mixture with variable *f* (F2) is less concentrated than that with constant *f* (F1) since lower primary radical was produced in the reactor to propagate further. The termination rate constant (k_t) is lower for Run 1 (more concentrated mixture) as shown in Figure 5.1e which makes the monomer conversion faster (Figure 5.1c). Longer time was required for the process to achieve the desired monomer conversion for Run 1a since the termination rate constant is higher (Fig. 5.1e) which slows down the monomer conversion. Therefore, higher concentration of initial initiator was

needed to initiate free radicals at the beginning of the process. The optimum temperature profile for this case study is shown in Figure 5.1a.

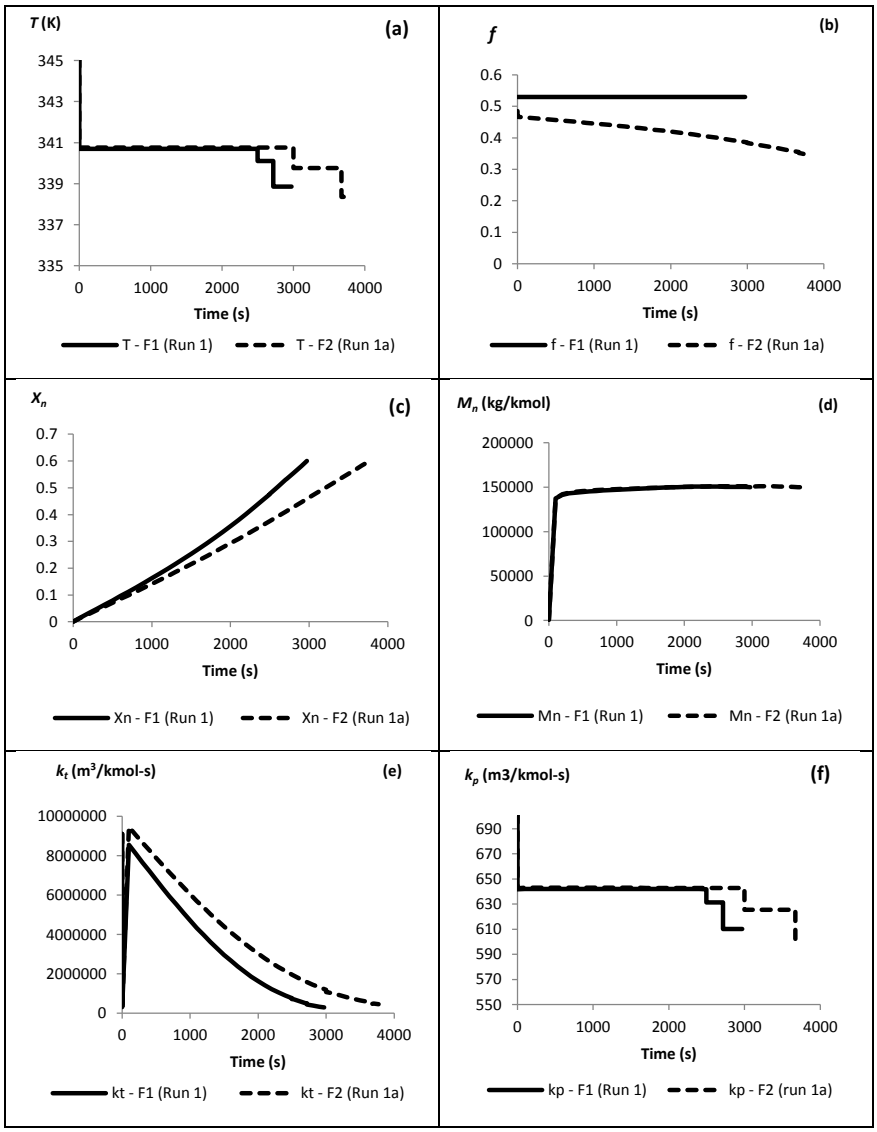

Figure 5.1: Results for case study 1 (a) Temperature profile (T); (b) initiator efficiency (f); (c) monomer conversion (X_n); (d) termination rate constant (k_t); (e) propagation rate constant (k_p)

5.4 Case Study 2 – Effect of solvent concentration on different initiator efficiency using simple model

The same (as in the last case study) minimum time optimization problem is solved for two other solvent concentration values. The concentration of the solvent (Toluene) used for case study 1 was 5.0 kmol/m^3. The two new solvent concentration considered in this case study are 2.5 kmol/m^3 and 0.0 kmol/m^3 (monomer is 100% concentrated without any solvent).

5.4.1 Results

The results are presented together with the base case from case study 1 (Run 1 and 1a) as comparison in Table 5.3.

Table 5.3: Results for different solvent concentrations

Run	C_s (kmol/m^3)	f	C_{i0} (kmol/m^3)	X_n	M_n (kg/kmol)	PD	t_f (s)
1	*5.0*	*F1*	*1.41E-3*	*0.6*	*150014.7*	*1.8*	*2969.5*
1a	*5.0*	*F2*	*1.45E-3*	*0.60*	*149999.0*	*1.8*	*3772.7*
2	2.5	F1	1.23E-3	0.6	149996.8	1.8	1903.5
2a	2.5	F2	1.29E-3	0.6	150000.1	1.8	2490.2
3	0.0	F1	0.80E-3	0.6	150000.4	1.77	828.7
3a	0.0	F2	0.80E-3	0.6	150000.5	1.61	951.1

The results of this case study show that reducing the solvent concentration will decrease the batch time. This is to be expected since the model incorporates the gel and glass effect. A less concentrated reacting mixture inside the reactor will initiate

these effects quicker and reach the specified values in shorter time. For all cases, the results also show that time varying f (F2) needs longer time than using constant f (F1). It seems that solvent is not needed in order to achieve the desired monomer conversion and number average molecular weight in minimum time. However, solvents need to be added to the polymerization reactor to aid an effective heat removal.

The optimum temperature profile are shown in Figure 5.2a for concentrated mixture without addition of the solvent (Run 3 and Run 3a). The temperature for Run 3 (F1) was very high during the first control interval (Figure 5.2a) which leads to increase the propagation rate constant k_p (Figure 5.2f) and termination rate constant k_t (Figure 5.2e). This is because the particles will have more kinetic energy and there would be more productive collisions at higher temperature. This high temperature resulted lower number average molecular weight M_n (Figure 5.2d) at the early stage before it is increased to achieve the desired M_n at 150000 kg/kmol .

As discussed earlier, the batch time for the optimization process to achieve monomer conversion 0.6 using the free volume theory to calculate the initiator efficiency (F2) is longer than constant value of f at 0.53 (F1) as shown in Fig. 5.2c. As mentioned before, less primary radical produced for the time varying initiator efficiency of f (Figure 5.2b), leading to less concentrated mixture.

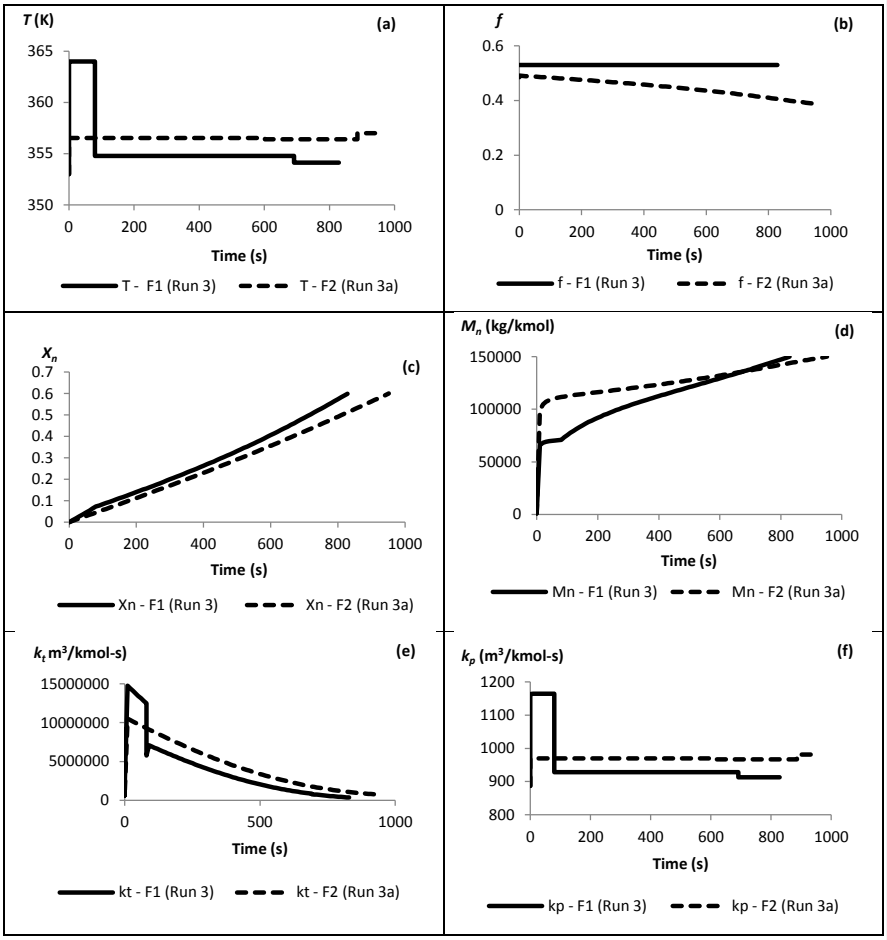

Figure 5.2: Results for case study 2 (Run 3 and Run 3a): (a) optimum temperature profile (T); (b) initiator efficiency (f); (c) monomer conversion (X_n); (d) number average molecular weight (M_n); (e) termination rate constant (k_t); (f) propagation rate constant (k_p)

5.5 Case Study 3 – Maximum monomer conversion for fixed number average molecular weight (M_n) using detailed model

The constants values used for the detailed model (presented in Chapter 3) are same as those used by Ekpo (2006) and is given in Table 5.4.

Table 5.4: Constants and values from the detail model of MMA polymerization

A = 0.0774 m^2	MW_s = 106.17 kg/kmol
$C_{P,J}$ = 4.184 kJ/kg.K	MW_m = 100.12 kg/kmol
$C_{P,m}$ = 1.648 kJ/kg.K	V = 2 L
$C_{P,P}$ = 1.47 kJ/kg.K	V_J = 1.5 L
$C_{P,S}$ = 1.70 kJ/kg.K	$-\Delta Hr$ = 5.78 x 104 kJ/kmol
MW_i = 164.21 kg/kmol	ρ_J = 997 kg/m^3
ρ_m = 915.1 kg/m^3	U = 2.55 kJ/s.m^2.K
ρ_p = 1200 kg/m^3	τ_J = 50s

Maximum conversion problem is solved here for different desired number average molecular weight (M_n) such as 50000 kg/kmol, 100000 kg/kmol and 150000 kg/kmol for different fixed batch time 3000s, 5000s and 10000s using the detailed model.

5.5.1 Formulation of Optimization Problem

Optimization problem for maximum conversion can be represented as:

Max X_n

$T_{jsp}(t)$, C_{i0}

s.t. $f(t, x'(t), x(t), u(t), v) = 0, \quad [t_0, t_f]$ model equations

$$M_n = M_n^*$$

$$t_f = t_f^*$$

$$0.0001 < C_{i0} < 0.150$$

$$1.5 < PD < 1.8$$

$$320 < T_{jsp} < 373\ K$$

$$320\ K < T < 398\ K$$

5.5.2 Results

Results obtained for maximum conversion problem at fixed batch time (3000s, 5000s and 10 000s) are presented in Table 5.5.

Table 5.5: Results for maximum conversion at fixed batch time, t_f*

Run	X_n, %	*Mn*	*Mn**	t_f*(s)	*PD*	C_{i0} (x10^{-3})
1	76.5	50 000	50 000	3000	1.8	2.898
2	72.5	100 000	100 000	3000	1.8	1.729
3	56.1	150 000	150 000	3000	1.8	1.448
4	91.7	50 000	50 000	5000	1.8	3.171
5	81.3	100 000	100 000	5000	1.8	2.378
6	69.3	150 000	150 000	5000	1.8	1.907
7	95.5	50 000	50 000	10 000	1.8	4.646
8	91.6	100 000	100 000	10 000	1.8	3.378
9	81.8	150 000	150 000	10 000	1.8	2.859

As expected, monomer conversion increased with increased final batch time since more time is available for the monomer to react inside the reactor. Initial initiator concentration also increased with increased final batch time to ensure that there are more initiators to initiate the polymer process and for the propagation process to happen at longer batch time. In all cases, polydispersity (*PD*) values hit the upper bound set.

Figure 5.3 show the optimum reactor temperature set point (T_{jsp}) profile and the monomer conversion (X_n) profile of each run in this case study. The optimum T_{jsp} profiles (Figure 5.3a, c, e) really show that the temperature is higher for lower molecular weight. This higher temperature is required to decompose higher concentration of C_{i0}.

Monomer conversion decreased with increased molecular weight (Figure 5.3b, d, f), because to achieve higher molecular weight, low initial initiator are needed at the beginning of the process so the monomer will continue the propagation process rather than initiate a new polymerization process with the initiator. This can be seen where initial initiator concentration (C_{i0}) decreased with increased molecular weight in Table 5.5.

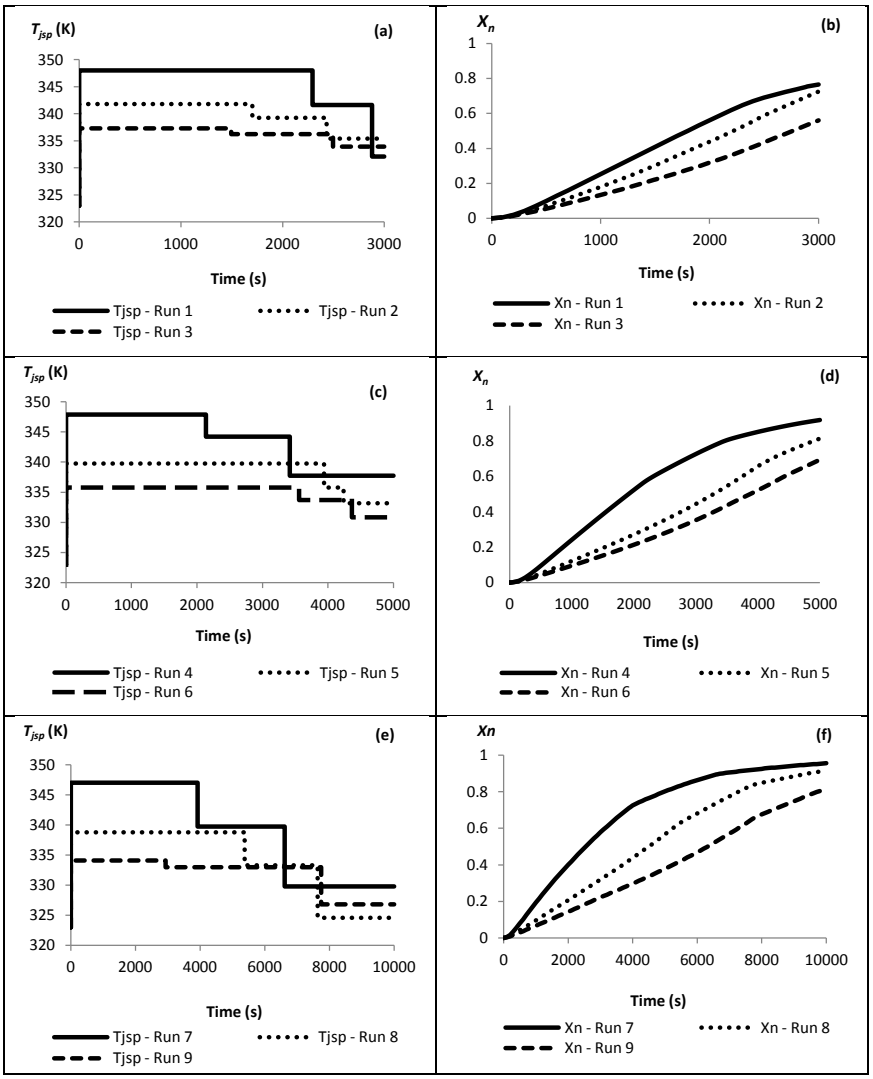

Figure 5.3: Optimum reactor temperature set point profiles (T_{jsp}) and monomer conversion (X_n) profiles for case study 3

5.6 Case Study 4 – Effect of Different f on Maximum Monomer Conversion for fixed Number Average Molecular Weight (Mn) with Detailed Model

In this work, the effect of different initiator efficiency approaches in the optimization process of polymerization of MMA in batch reactor was investigated using detailed model.

5.6.1 Formulation of Optimization Problem

Optimization problem for maximum conversion can be represented as:

Max X_n

$T_{jsp}(t)$, C_{i0}

s.t. $f(t, x'(t), x(t), u(t), v) = 0, \quad [t_0, t_f]$ model equations

$M_n = M_n^*$

$t_f = t_f^*$

$0.0001 < C_{i0} < 0.150$

$1.5 < PD < 2.5$

$320\ K < T_{jsp} < 373\ K$

$320\ K < T < 398\ K$

5.6.2 Results

The optimization problem is solved to achieve number average molecular weight (M_n) 150000 kg/kmol in fixed batch time of 5000s using constant value of f (0.53) (F1) and time varying f (F2). This case is same as that in Run 6 of case study 3 but with wider polydispersity. The results are shown in Table 5.6 and Figure 5.4.

Table 5.6: Results for different initiator efficiency

Run	f	X_n	M_n	M_n*	t_f(s)	PD	C_{i0} (x10^{-3})
1	F1	96.64	149901.5	150000	5000	2.249012	1.00
2	F2	90.18	149989.8	150000	5000	2.048531	1.00

The results, clearly shows the effect of constant and variable f on X_n and PD even though C_{i0} was same. The using of constant f in the model will mislead the expected results as it does not represent the real phenomenon in the process.

The optimum profile for jacket temperature set point (T_{jsp}) for three control intervals is shown in Figure 5.4a. The figure clearly shows that T_{jsp} for time varying f (F2) is higher than for constant f (F1) for each interval. Figure 5.4b shows that f (F2) decreases as the monomer conversion increases (Figure 5.4e).

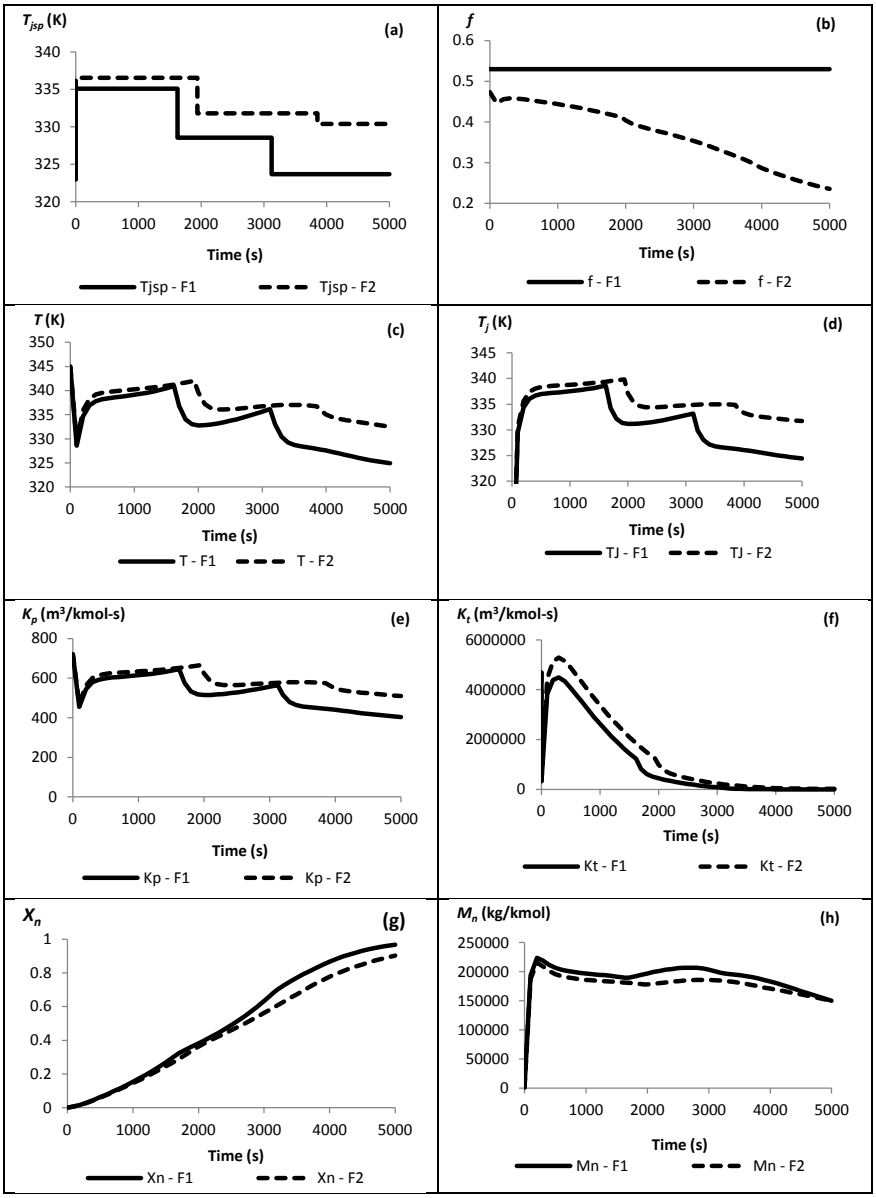

Figure 5.4: Results for case study 4 (Run 1 and Run 2): (a) Optimal profile of jacket temperature set point (T_{jsp}); (b) initiator efficiency (f); (c) reactor temperature T; (d) jacket temperature (T_j); (e) propagation rate constant (k_p); (f) termination rate constant (k_t); (g) monomer conversion (X_n); (h) number average molecular weight (M_n)

As mentioned before (chapter 4, page 94), the concentration of the reaction mixture increases as the time proceeds. However, the concentration of the F2 is lower than F1 since the decrease of the f with time leads to lower the initiator free radical in the process. With the increase of monomer conversion with time, lower initiator concentration reduces the diffusion of primary radicals as observed by Achilias and Kiparissides (1992) in their work. This lower concentration (F2) resulting in higher termination rate constant k_t (Figure 5.4f) and propagation rate constant k_p (Figure 5.4e) compared to F1 as discussed before. This means in F2, the polymer chain does not grow beyond a certain limit and new polymer chain starts to grow making overall M_n at anytime lower compared to F1.

It will be interesting to compare the results of Run 2 (F2 of Table 5.6) with that of Run 6 (Table 5.5) to see the effect of polydispersity. It is clear that conversion can be significantly improved (by almost 20%) for the same M_n by having higher PD value that can be used to measure the width of the molecular distribution. Broader molecular weight distribution will increase the melt temperature.

5.7 Conclusions

For the solution polymerization of Methyl Methacrylate in batch reactor, two models are employed namely simple kinetic model and detailed model. In the later model, energy balance equations were added to the simple model.

Most of the steps and effects that occur in polymerization process was incorporated in simple kinetics model for solution MMA. Optimal control paths for the reactor temperature and initial initiator concentration are obtained by using Control Vector Parameterization (CVP) technique to solve the minimum time optimization problem over three intervals.

The effects of different initiator efficiency, f was examined. The results of these studies show that initiator efficiency, f decreased along the process in the solution polymerization of MMA when the free volume theory was applied (F2). The results were compared between two approaches which confirm that the initial initiator needed at the early stage of the process is higher and longer batch time is required in order to achieve the specified X_n and M_n for F2. The effect of solvent are very pronounced for both approaches where there are large decrease in the reaction time for more concentrated reaction mixture in the reactor. This is to be expected since the model incorporates the gel and glass effect.

A dynamic optimization using a detailed model to maximize the monomer conversion was done for solution polymerization process of MMA. Jacket temperature set point (T_{jsp}) is used as the control variables in the MMA detailed model along with the initial initiator concentration (C_{i0}). Monomer conversion (X_n) increased with the increased of final batch time as expected, since more time allocated will ensure to reduce the unreacted monomer inside the reactor. Initial initiator concentration also increased with the longer final batch time as more initiators will needed to initiate the primary radicals for the polymerization process to occur in the batch reactor. Higher monomer conversion also observed when broader

molecular weight distribution was in the optimization problem. Finally, the effect of different initiator efficiency need to take into account since it follows the theory lied behind. These really show the significance of using the free volume theory for the initiator efficiency rather than a constant value.

Chapter Six

Dynamic Optimization of Emulsion Copolymerization of Styrene and Methyl Methacrylate in Batch and Semi-batch Reactor

6.1 Introduction

This chapter discusses the dynamic optimization of emulsion copolymerization of Styrene and Methyl Methacrylate (MMA) in batch and semi batch reactor. The initiator used to initiate the polymerization process for this work is Persulfate $K_2S_2O_8$ and the surfactant is Sodium Dedocyl Sulfate (SDS). The model adopted from Alhamad (2006) was used to optimize the emulsion copolymerization process in order to maximize the number average molecular weight (M_n) and also overall monomer conversion (X_n). Five variables were used as optimization variables namely Styrene monomer feed rate (F_{mA}), MMA monomer feed rate (F_{mB}), initiator feed rate (F_I), surfactant feed rate (F_S) and also reaction jacket temperature (T_{J0}). Alhamad (2005) and Alhamad et al. (2005) maximized the M_n at fixed pre-batch time of 1500s for different optimization formulation. The same model as Alhamad (2005) is employed in this work, however, the effect of different pre-batch time is investigated.

6.2 Optimization Problem Formulation of Emulsion Copolymerization Process

6.2.1 Maximum number average molecular weight problem

The optimization problem can be described as:

Given	*Fixed diameter of particle (D_{mm}), Fixed total amount of monomer ($N_{m,T}$), Fixed overall conversion (X_n), Fixed pre-batch time (t_{bp}), Fixed number of intervals (Int), Fixed final batch time*
Optimize	*Styrene feed rate (F_{mA}), MMA feed rate (F_{mB}), Surfactant feed rate (F_S), Initiator feed rate (F_I), Jacket temperature (T_{j0}), Controller switching times*
So as to maximize	*Number Average Molecular weight (M_n)*
Subject to constraint	*Model equations, Linear bounds on:* *Initial Initiator concentration (C_{I0}), Initial Surfactant concentration (S_0), Initial styrene concentration ($F_{mA,0}$), Initial MMA concentration ($F_{mB,0}$), Reactor temperature (T_r), Copolymer composition*

Mathematically the optimization problem can be described as:

Max Mn

$F_{mA}(t)$; $F_{mB}(t)$; $F_S(t)$; $F_I(t)$; T_{j0}

s.t. $f(t, x'(t), x(t), u(t), v) = 0, \quad [t_0, t_f]$ model equations

$$t_f = t_f^*$$

$$X_n^{\,l} < X_n < X_n^{\,u}$$

$$F_{mA}^{\,l} < F_{mA} < F_{mA}^{\,u}$$

$$F_{mB}^{\,l} < F_{mB} < F_{mB}^{\,u}$$

$$F_S^{\,l} < F_S < F_S^{\,u}$$

$$F_I^{\,l} < F_I < F_I^{\,u}$$

$$T_r^{\,l} < T_r < T_r^{\,u}$$

$$D_{mm}^{\,l} < D_{mm} < D_{mm}^{\,u}$$

$$N_{m,T} = 8\ mol$$

6.2.2 Maximum conversion problem

The optimization problem can be described as:

Given *Fixed diameter of particle (D_{mm}), Fixed total amount of monomer ($N_{m,T}$), Fixed molecular weight (M_n), Fixed pre-batch time (t_{pb}), Fixed number of intervals, Fixed batch time*

Optimize *Styrene feed rate (F_{mA}), MMA feed rate (F_{mB}), Surfactant feed rate (F_S), Initiator feed rate (F_I), Jacket temperature (T_{j0}), Controller switching times*

So as to maximize *Overall conversion (X_n)*

Subject to constraint *Model equations, Linear bounds on:*

Initial Initiator concentration (C_{I0}), Initial Surfactant concentration (S_0), Initial styrene concentration ($F_{mA,0}$), Initial MMA concentration ($F_{mB,0}$), Reactor temperature (T_r), Copolymer composition

Mathematically the optimization problem for minimum time problem can be described as;

$$\text{Max} \quad X_n$$

$$F_{mA}(t)\ ;\ F_{mB}(t)\ ;\ F_S(t)\ ;\ F_I(t)\ ;\ T_{j0}$$

s.t. $f(t, x'(t), x(t), u(t), v) = 0, \quad [t_0, t_f]$ model equations

$$M_n = M_n^*$$

$$F_{mA}{}^l < F_{mA} < F_{mA}{}^u$$

$$F_{mB}{}^l < F_{mB} < F_{mB}{}^u$$

$$F_S{}^l < F_S < F_S{}^u$$

$$F_I{}^l < F_I < F_I{}^u$$

$$T_r^{\,l} < T_r < T_r^{\,u}$$

$$D_{mm}{}^{l} < D_{mm} < D_{mm}{}^{u}$$

$$N_{m,T} = 8\ mol$$

Where subscript *l* and *u* referred to lower and upper bounds.

When batch time is fixed, $t_f = t_f^*$ is also added as constraint to the optimization problem. When the batch time is free, t_f is optimized with all other parameters.

6.3 Description of Case Studies

This section looks at the dynamic optimization of a batch and semi-batch emulsion copolymerization process of styrene and MMA. There are nine case studies presented in this work and was classified into three groups namely semi-batch process (with pre-batch time); batch process; and semi-batch process (without pre-batch time) respectively. These nine study cases have been carried out and grouped as shown below:

6.3.1 Semi-batch process (with pre-batch time)

- Case study 1 - Maximize the number average molecular weight (M_n) for different pre-batch time at fixed total batch time (5 intervals)

- Case study 2 - Maximize the number average molecular weight (M_n) for different pre-batch time at fixed total batch time (3 intervals)

- Case study 3 - Maximize overall conversion (X_n) for specified number average molecular weight (M_n) with free final batch time

- Case study 4 - Maximize overall conversion (X_n) for specified number average molecular weight (M_n) at fixed total batch time

- Case study 5 – Maximize number average molecular weight (M_n) for different initial initiator concentration (pre-batch time 1500s)

6.3.2 Batch process

- Case study 6 – Maximize overall conversion (X_n) for batch process

- Case Study 7 – Maximize number average molecular weight (M_n) for batch process

6.3.3 Semi-batch process (without pre-batch time)

- Case study 8 – Maximize number average molecular weight (M_n) for different number of intervals

- Case study 9 – Maximize number average molecular weight (Mn) for 5 intervals with control the monomer flow of 5th interval.

The objective functions are maximized by optimizing five variables namely styrene feed rate (F_{mA}), MMA feed rate (F_{mB}), initiator feed rate (F_I), surfactant feed rate (F_S) and also jacket reactor temperature (T_{j0}). The initiator used in this work is Persulfate $K_2S_2O_8$ and the surfactant is Sodium Dodecyl Sulfate (SDS) which has been widely used in conventional emulsion polymerization of Styrene (Luo et al., 2011). Data and procedure for emulsion copolymerization of styrene and MMA is given in Table 6.1 below. In semi-batch process, ~~17.1%~~53.45 g of ~~ total~~ monomer was added at the beginning of the process for seed formation. Then the rest of the monomer was added continuously along the process. The ratio of the copolymer composition for the styrene/MMA feed inside the reactor is 50/50 with the constraint of total amount of monomer added inside the reactor is 8 mols.

Table 6.1: Data from emulsion copolymerization process

Styrene monomer (g)	410.40
MMA monomer (g)	410.40
Water (g)	2.50
Initiator-persulfate $K_2S_2O_8$ (g)	1.875
Surfactant-SDS (g)	5.39
Monomer feed: 8~~2~~6.96% semibatch charge 13.04~~7.1~~% initial charge (seeding process)	

Formatted: Space After: 0 pt, Don't keep with next

6.4 Case study 1 - Maximize the number average molecular weight (M_n) for different pre-batch time at fixed total batch time (5 intervals)

6.4.1 Optimization Problem Formulation and Constraints

The number average molecular weight for different pre-batch time in 5 intervals was maximized in this case study. Previous study by Alhamad (2005) and Alhamad et al. (2005a) have maximized the molecular weight of emulsion copolymerization of styrene and MMA with 5 intervals and 1500s pre-batch time without fixing the total batch time (t_f). In this work, the pre-batch time (t_{pb}) is set at 1800s, 1500s, 1200s, 900s, 600s, 300s and without pre-batch time for the total batch time 5500s. The reason for the pre-batch time is for the seeds formation, which means by reducing the pre-batch time will reduce the time for the seed formation. The dynamic optimization formulation and constraints for this case study can be described as:

Max M_n

$F_{mA}(t)$; $F_{mB}(t)$; $F_S(t)$; $F_I(t)$; T_{j0}

s.t. $f(t, x'(t), x(t), u(t), v) = 0, \quad [t_0, t_f]$ model equations

$t_{pb} = t_{pb}^*$

$t_f = t_f^* = 5500s$

$0.94 < X_n < 1.0$

$0.0\ g/s < F_{mA} < 0.2\ g/s$

$0.0\ g/s < F_{mB} < 0.2\ g/s$

$$0.0\ g/s < F_S < 0.2\ g/s$$

$$0.0\ g/s < F_I < 0.2\ g/s$$

$$343.00\ K < T_r < 358.00\ K$$

$$0.4 \times 10^{-7} m < D_{mm} < 9.0 \times 10^{-7} m$$

$$N_{m,T} = 8\ mol$$

6.4.2 Results and discussions

Results for maximum number average molecular weight for different pre-batch time are summarized in Table 6.2 below. As the pre-batch time decreases, the number average molecular weight (M_n) increases with slight decrease in overall conversions (X_n).

The results in Table 6.2 show that the maximum molecular weight 258654.4 g/mol can be achieved with 300s pre-batch time with an overall conversion of 94.13%. A seed population with a smaller particle and larger size particles are produced during the pre-batch time (Zeaiter et al., 2002). The results clearly show that the pre-batch time for seed formation is needed but can be reduced to maximize the molecular weight (M_n) (although by 3% only in this case) for run 1 and run 6.

Table 6.2: Maximize the molecular weight for different pre-batch time (5 intervals)

Run	M_n (g/mol)	X_n (%)	D_{mm} (nm)	t_{pb} (s)
1	251199.0	94.29	87.7	1800
2	253041.0	94.25	87.7	1500
2a (Alhamad)	*248109.9*	*94.18*	*87.2*	*1500*
3	254816.0	94.20	87.7	1200
4	256371.6	94.18	87.7	900
5	257717.6	94.16	87.7	600
6	258654.4	94.13	87.6	300
7	258077.5	93.56	87.6	0

This optimization process also was carried out to achieve maximum M_n without any pre-batch time (Run 7) in order to compare with the process where the pre-batch time was allocated as shown in Table 6.2. The results show that the M_n for Run 6 is decreased by only 0.22% for the decreased of 300s (compared to Run 7) however the M_n (Run 7) is much higher (2.74%) when compared to the longer pre-batch time (Run 1). The results show that the pre-batch time can be reduced to achieve the higher M_n but without pre-batch time allocated for the seed formation, a small decrease in M_n and X_n is observed.

Figure 6.1 shows the optimization result with the optimal profile of monomer feed rate (Fig. 6.1c) and jacket temperature (Fig. 6.1d) for Run 2. During 1500s pre-batch time (Run 2), no further feed of monomer was added to the reactor. It can be seen that the temperature will remain constant at 358 K until 4200s before it goes down to 343 K when the reaction stop. At high temperature, the radical transfer in the polymerization process will increase (Fig. 6.1d) which will lead to shorter chains of polymer (low M_n) as shown in Figure 6.1a.

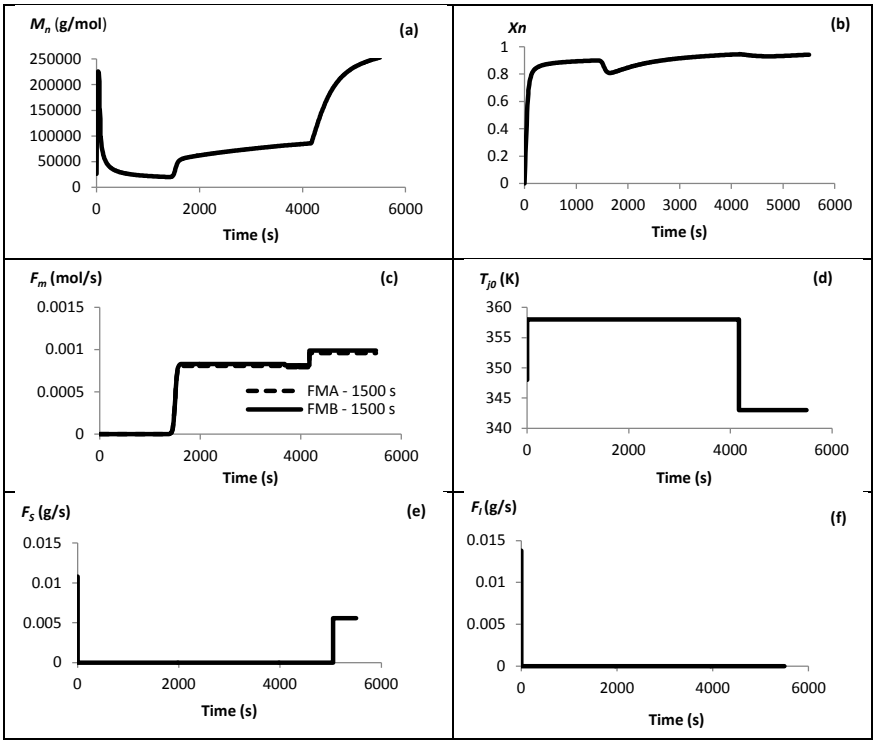

Figure 6.1: Case study 1 (Run 2); Optimization result (a) number average molecular weight (M_n); (b) overall conversion (X_n); (c) optimal profile of monomer flow rate [F_{mA} - styrene; F_{mB} - MMA]; (d) optimal profile of jacket temperature T_{j0}; (e) optimal profile of surfactant flow rate (F_S); (f) optimal profile of initiator flow rate (F_I)

When the temperature is decreased the molecular weight will increase to achieve the maximum molecular weight. On the other hand, increasing the temperature will increase the kinetic transfer coefficient (k_{tr}).When the transfer coefficient is increased, the monomeric radicals are increased resulting in an increase in termination reaction. Besides that, the entry of radicals to the particles also will result in instantaneous termination for zero-one emulsion process. The transfer and termination reaction will stop the increase of molecular weight. The jacket temperature profile (Fig.6.1d) was constant at 358 K until 4200s to ensure that the reactor temperature is high for the radical transfer to happen in the process. Then it was decreased to 343 K to ensure that M_n was increased to its maximum value with

the lower reactor temperature. On the other hand, lowering the reaction temperature, will lead to decrease in the transfer event resulting in longer polymer chains meaning higher molecular weight. Alhamad (2005) made similar observation. However, the maximum M_n in his work for 1500s feed batch time was 235758 g/mol which is lower than that obtained in this work due to lower batch time of 4998s. This is due to decreasing the reaction time also can reduce the molecular weight. The surfactant feed was about 0.0056 mol/s for about 450s towards the end of the process. The addition of surfactant at very slow feed rate is to stabilize the bigger particles formed, without producing any new micelles for micellar nucleation. No initiator added along the process since the addition can reduce the M_n.

Note, Run 2a in Table 6.2 is carried out using X_n = 94.17 (same as Alhamad (2005)), t_{pb} = 1500s (same as Alhamad (2005)) but with t_f = 4998s (same as Alhamad (2005) but fixed in this work). The comparison shows that higher number average molecular weight can be achieved when the final batch time is fixed.

6.5 Case study 2 - Maximize the number average molecular weight (M_n) for different pre-batch time at fixed final batch time (3 intervals)

6.5.1 Optimization Problem Formulation and Constraints

In Case study 2 the number average molecular weight is maximized for different pre-batch time in 3 intervals. The pre-batch time (t_{pb}*) is set at 1500s, 1200s, 900s and 600s for the total batch time 5500s and 5000s. Total amount of monomer ($N_{m,T}$)

added into the reactor is 8 mol. The dynamic optimization formulation and constraints can be described as:

$$Max \qquad M_n$$

$$F_{mA}(t)\ ;\ F_{mB}(t)\ ;\ F_S(t)\ ;\ F_I(t)\ ;\ T_{j0}$$

$$s.t. \qquad f(t, x'(t), x(t), u(t), v) = 0, \quad [t_0, t_f] \qquad \text{model equations}$$

$$t_{pb} = t_{pb}^*$$

$$0.94 < X_n < 1.0$$

$$0.0\ g/s < F_{mA} < 0.2\ g/s$$

$$0.0\ g/s < F_{mB} < 0.2\ g/s$$

$$0.0\ g/s < F_S < 0.2\ g/s$$

$$0.0\ g/s < F_I < 0.2\ g/s$$

$$343.00\ K < T_r < 358.00\ K$$

$$0.4 \times 10^{-7} m < D_{mm} < 9.0 \times 10^{-7} m$$

$$N_{m,T} = 8\ mol$$

6.5.2 Results and discussions

Results for case study 2 are shown in Table 6.3 and Table 6.4 for total batch time 5500s and 5000s respectively. The results show that by decreasing the pre-batch time, the molecular weights were increased while the overall conversion is slightly the same.

For a total batch time 5500s (Table 6.3), the M_n is 0.72% higher for 1200s pre-batch time (Run 3) compared to 1500s pre-batch time (Run 2). However, 1.44% increase of the M_n can be observed for longer difference of the pre-batch time (1200s) from Run 1 and Run 5 (Table 6.3).

For a total batch time 5000s, the M_n is increased 2.56% for the difference of 900s (Run 1 and Run 4) as shown in Table 6.4. A higher increased of M_n can be observed for a smaller decrease of pre-batch time (900s) for shorter total batch time of 5000s compared to 5500s. On top of that, for shorter total batch time (5000s), the decrease of 1.95% of M_n can be seen for the same 1500s pre-batch time (Run 2 in Table 6.3 and Run 1 in Table 6.4). This is because with longer processing time, it gave the opportunity to the monomer added along the process to react and increase the polymer chain inside the particle.

The results in Table 6.3 and Table 6.4 below show good agreement with the results in case study 1 in the sense that decreasing the pre-batch time increases the number average molecular weight (M_n). As mentioned before, this is happened due to the fact that the sooner the monomers added into the reactor, the sooner the propagation occurs in the particle. This will lead to increasing the chain length of the polymer in the particles as time increases.

The results show that the molecular weight of copolymerization of Styrene and MMA with 3 intervals (Table 6.3) is lower compared with 5 intervals (Table 6.2) especially for lower pre-batch time (600s and 900s) for the same total batch time 5500s. However, for the pre-batch time 1200s and above, the results of the M_n are

quite the same. This is because more flexibility for the optimization process was needed when shorter time for seed formation was allocated. Same optimal temperature profile also observed with the last case study in order to maximize the number average molecular weight (Mn).

Table 6.3: Maximize the molecular weight for different pre-batch time (3 intervals) total time 5500s

Run	M_n (g/mol)	X_n (%)	Diameter (nm)	Pre-batch time (s)
1	251198	94.29	87.7	1800
2	253053	94.25	87.7	1500
3	254863	94.22	87.7	1200
4	253621	94.01	87.8	900
5	254881	93.98	87.8	600

Table 6.4: Maximize the molecular weight for different pre-batch time (3 intervals) total time 5000s

Run	M_n (g/mol)	X_n (%)	Diameter (nm)	Pre-batch time (s)
1	248212	94.27	87.2	1500
2	251520	94.28	87.7	1200
3	253250	94.24	87.7	900
4	254741	94.22	87.7	600

The optimal profile of the jacket temperature, monomer flow rates (styrene and MMA) and initiator flow rates case study 2 (Run 2) for the total batch time 5500s is shown in Figure 6.2 below. The rest of the optimal profile shown the same observation and are given in the appendix 2.

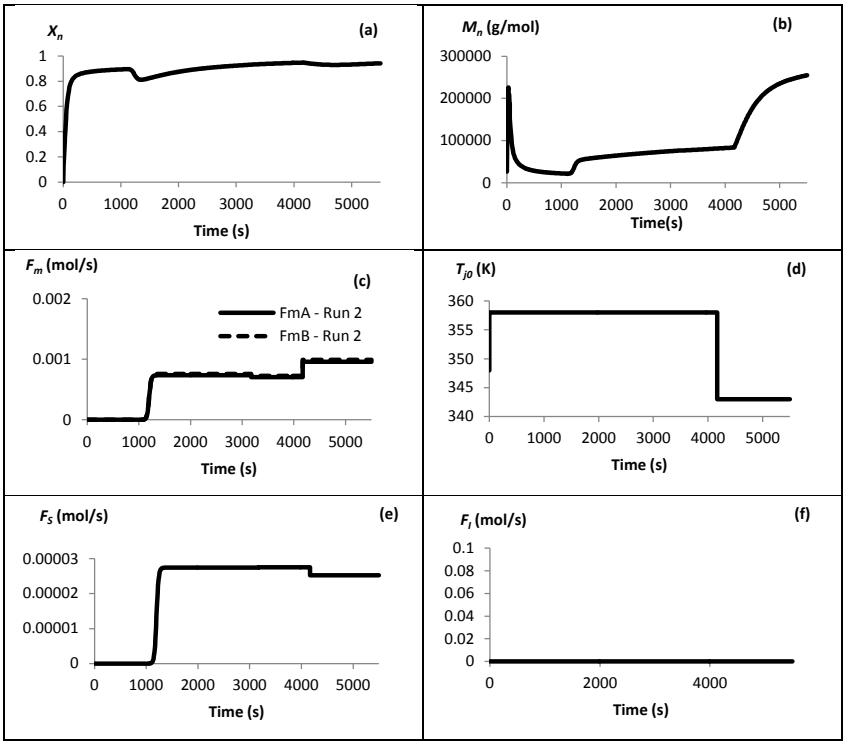

Figure 6.2: Case study 2 (Result Run 2) for total batch time 5500s, (a) overall conversion (X_n); (b) number average molecular weight (M_n); (c) monomer flow rate (F_{mA} and F_{mB}); (d) jacket temperature (T_{j0}) ;(e) optimal profile of surfactant flow rate (F_S); (f) optimal profile of initiator flow rate (F_I).

6.6 Case study 3 - Maximize overall conversion (X_n) for specified molecular weight with free final batch time

6.6.1 Optimization Problem Formulation and Constraints

Case study 3 is for maximization of the overall conversion of the reaction process of emulsion copolymerization of styrene and MMA for specified molecular weight in 5 control intervals. The pre-batch time is set constant at 1200s and 1500s for

comparison and effect of different pre-batch time. The constraint on total monomer added into the reactor is 8 mols. The dynamic optimization formulation and constraints for this case study can be described as:

Max X_n

$F_{mA}(t)$; $F_{mB}(t)$; $F_S(t)$; $F_I(t)$; T_{j0} ; t_f

s.t. $f(t, x'(t), x(t), u(t), v) = 0, \quad [t_0, t_f]$ model equations

$M_n = M_n^*$

$t_{pb} = t_{pb}^*$

$0.0\ g/s < F_{mA} < 0.2\ g/s$

$0.0\ g/s < F_{mB} < 0.2\ g/s$

$0.0\ g/s < F_S < 0.2\ g/s$

$0.0\ g/s < F_I < 0.2\ g/s$

$343.00\ K < T_r < 358.00\ K$

$0.4 \times 10^{-7} m < D_{mm} < 9.0 \times 10^{-7} m$

$N_{m,T} = 8\ mol$

6.6.2 Results and discussions

Maximum conversion is very important to ensure that most of the monomers have reacted in the reactor and the product is at high quality. In this case study the process is optimized to achieve the desired number average molecular weight (M_n) in 1200s and 1500s pre-batch time using 5 control intervals. The desired number average molecular weight is set at 100000 g/mol, 150000 g/mol and 200000 g/mol. Results

are shown in Table 6.5. The maximum overall conversion for specified molecular weight of 100000 g/mol, 150000 g/mol and 200000 g/mol is compared with different pre-batch time of 1200s and 1500s.

Table 6.5: Maximize overall conversion for specified molecular weight (pre-batch time 1200s and 1500s)

		1200s pre-batch time			1500s pre-batch time		
Run	M_n* (g/mol)	X_n (%)	M_n (g/mol)	Time (s)	X_n (%)	M_n (g/mol)	Time (s)
1	100000	96.24	100002	4895.48	96.16	100047	5079.93
2	150000	97.10	150004	5170.87	96.96	150039	5214.09
3	200000	95.79	200012	5293.15	95.67	200013	5546.68

The results show that by reducing the pre-batch time, the desired molecular weight can be achieved in shorter time and with higher overall conversion as observed previously. For example, for a given M_n* = 200000 g/mol (Run 3), the total batch time is 4.79% shorter with pre-batch time of 1200s compared to the pre-batch time of 1500s. Very small increases of overall conversion (X_n) for 1200s pre-batch time compared to 1500s pre-batch time in each run as shown in Table 6.5.

Even though the final batch time for 1500s pre-batch time is higher (5079.93s) compared to 1200s pre-batch time (4895.48s) as shown in Table 6.5, less time are required for the propagation process to occur (after pre-batch time) to achieve the desired M_n for longer pre-batch time (1500s). For example, 3579.93s is required after the 1500s pre-batch time (Run 1) while 3695.48s is required after the 1200s pre-batch time (Run 1) to achieve the desired M_n 100000 g/mol. This is due to higher

number of particles being produced during the pre-batch time when longer pre-batch time (1500s) was allocated.

The optimal profile of the jacket temperature, monomer flow rates (styrene and MMA) and initiator flow rates case study 3 (Run 2) for the 1200s pre-batch time is shown in Figure 6.3 below.

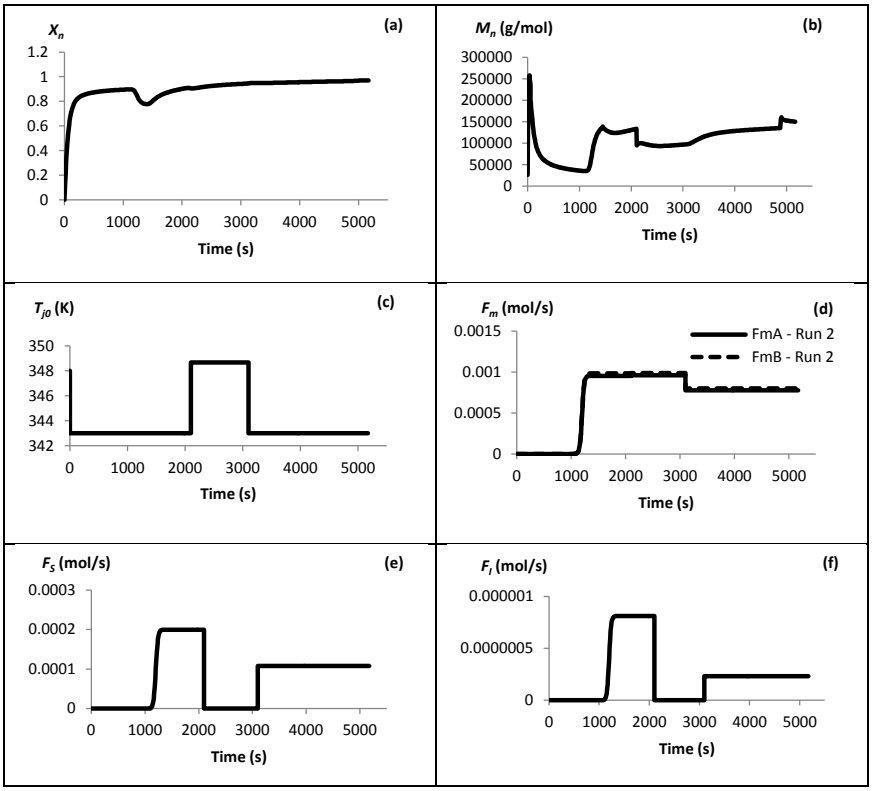

Figure 6.3: Case study 3 (Result Run 2) for 1200s pre-batch time, (a) overall conversion (X_n); (b) number average molecular weight (M_n); (c) jacket temperature (T_{j0}); (d) monomer flow rate (F_{mA} and F_{mB}); (e) optimal profile of surfactant flow rate (F_S); (f) optimal profile of initiator flow rate (F_I).

The results show that the jacket temperature is increased from about 2100s to 3100s to decrease the M_n, which then increase the X_n. As the monomer added after the pre-batch time, the addition of surfactant and initiator can be observed which retarded the increases of the M_n. The rest of the optimal profile shown the same observation and are given in the appendix 3.

6.7 Case study 4 - Maximize overall conversion (X_n) for specified molecular weight at fixed final batch time in a semi-batch process with pre-batch time

6.7.1 Optimization Problem Formulation and Constraints

The objective function of case study 4 is to maximize the overall conversion of the reaction process of emulsion copolymerization of styrene and MMA in 5 intervals with the fixed reaction time 5500s. Constraint for the total monomer added into the reactor is 8 mols. The pre-batch time is set constant at 1200s. The dynamic optimization formulation and constraint for case study 5 can be described as:

Max Xn

$F_{mA}(t)$; $F_{mB}(t)$; $F_S(t)$; $F_I(t)$; T_{j0}

s.t. $f(t, x'(t), x(t), u(t), v) = 0, \quad [t_0, t_f]$ model equations

$M_n = M_n^*$

$t_f = 5500s$

$$t_{pb} = 1200s$$

$$0.0\ g/s < F_{mA} < 0.2\ g/s$$

$$0.0\ g/s < F_{mB} < 0.2\ g/s$$

$$0.0\ g/s < F_S < 0.2\ g/s$$

$$0.0\ g/s < F_I < 0.2\ g/s$$

$$343.00\ K < T_r < 358.00\ K$$

$$0.4 \times 10^{-7} m < D_{mm} < 9.0 \times 10^{-7} m$$

$$N_{m,T} = 8\ mol$$

6.7.2 Results and discussions

In this case study the process is optimized to achieve the desired molecular weight in 1200s pre-batch time and 5 intervals with fixed total batch time 5500s. The styrene feed rate (F_{mA}), MMA feed rate (F_{mB}), initiator feed rate (F_I), surfactant feed rate (F_S) and jacket reactor temperature (T_{j0}) are optimized here. The desired number average molecular weight is set at 100000 g/mol, 150000 g/mol and 200000 g/mol and the results are shown in Table 6.6. The desired molecular weight can be achieved at fixed time 5500s with higher conversion, 99.38%, 97.92% and 95.84% when compare without fixed batch time (Table 6.5) for 100 000 g/mol, 150 000 g/mol and 200 000 g/mol respectively (same pre-batch time 1200s). This is because in previous case study, the maximum overall conversion was achieved at lower batch time.

Table 6.6: Maximize overall conversion for specified molecular weight (pre-batch time 1200s)

Run	M_n* (g/mol)	X_n (%)	M_n (g/mol)	D_{mm} (nm)
1	100000	99.38	100006.7	90.0
2	150000	97.92	149998.7	89.7
3	200000	95.84	200001.8	88.7

Overall conversion (X_n) and particle diameter (D_{mm}) were decreased with the increase of molecular weight. For a given batch time, with the desired low number average molecular weight, formation of new radicals and new polymer chains continue to occur thus leading more conversion of the monomer. On the other hand, for the same batch time, to achieve a polymer with higher number average molecular weight, formation of new polymer chain is restricted and the polymer chains already in propagation continue to grow (no secondary nucleation occur) and this leads to comparatively lower overall conversion (X_n) of the monomers.

Also for the higher molecular weight polymer, lower particle diameter will be obtained. This is because the addition of surfactant and initiator for the secondary nucleation (for lower M_n) produced higher number of polymer particles (N_{tot}). In order to achieve the maximum conversion, the desired number average molecular weight can be achieved with broader particle distribution, thus lower the diameter of the particle.

Figure 6.4 presents the results and optimal profiles (F_{mA}, F_{mB}, F_S, F_I *and* T_{j0}) for Run 3 in case study 4.

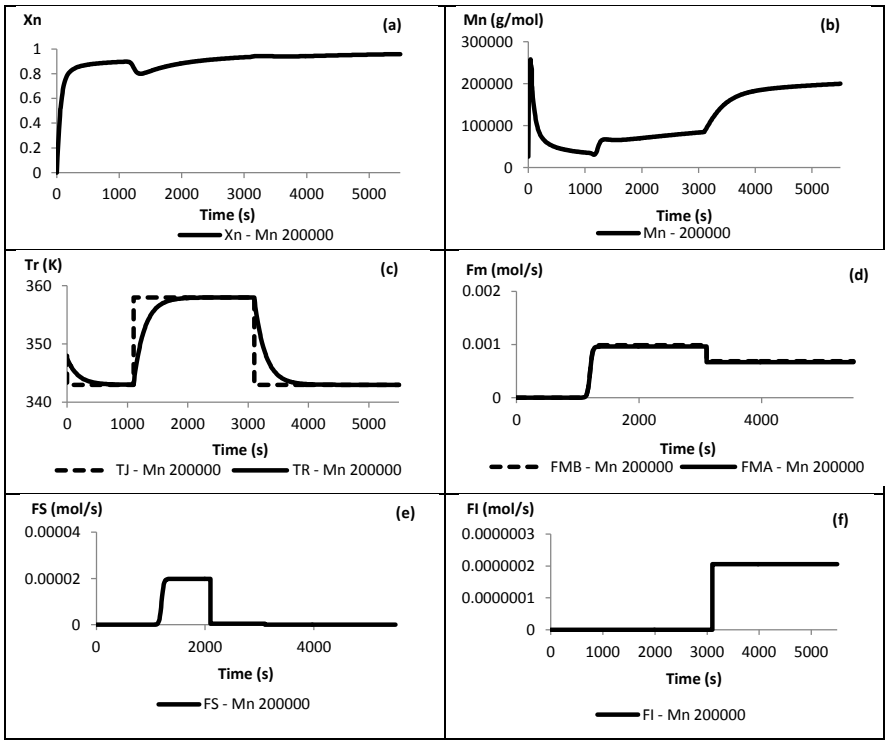

Figure 6.4: Result case study 4 (Run 3); (a) overall conversion (X_n); (b) number average molecular weight (M_n); (c) jacket temperature (T_{j0}) and reaction temperature (T_r); (d) monomer flow rate (F_{mA} and F_{mB}); (e) optimal profile of surfactant flow rate (F_S); (f) optimal profile of initiator flow rate (F_I).

The overall conversion drops (Fig. 6.4a) at 1200s during the addition of monomer to the reactor. This is because most of the monomers had converted to polymer particles, and at the time of addition, the total amount of monomer in the reactor increases. Surfactant also increases (Fig 6.4e) at that time to produce micelles for the particle nucleation. The temperature decreases to 343 K (Fig. 6.4c) with the increase

of initiator flow rate (Fig. 6.4f) to the reactor in order to achieve the desired M_n (Fig. 6.4b). The rest of the optimal profiles for this case study is given in the appendix 4.

6.8 Case study 5 - Maximize number average molecular weight (M_n) for different initial initiator concentration in a semi-batch process with pre-batch time

6.8.1 Optimization Problem Formulation and Constraints

The objective of case study 5 is to maximize the number average molecular weight (M_n) for different concentration of initial initiator purged into the reactor using 5 control intervals. The mass of initial initiator was set at 1.875 g, 1.775 g, 1.575 g, 1.375 g, 1.175 g and 1.075 g at the beginning of the process. The pre-batch time is set constant at 1500s for the fixed final batch time 5500s. The dynamic optimization formulation and constraint for case study 5 can be described as:

Max M_n

$F_{mA}(t)$; $F_{mB}(t)$; $F_S(t)$; $F_I(t)$; T_{j0}

s.t. $f(t, x'(t), x(t), u(t), v) = 0, \quad [t_0, t_f]$ model equations

$C_{i0} = C_{i0}^*$

$t_f = 5500s$

$0.90 < X_n < 1.0$

$$0.0\ g/s < F_{mA} < 0.2\ g/s$$

$$0.0\ g/s < F_{mB} < 0.2\ g/s$$

$$0.0\ g/s < F_S < 0.2\ g/s$$

$$0.0\ g/s < F_I < 0.2\ g/s$$

$$343.00\ K < T_r < 358.00\ K$$

$$0.4 \times 10^{-7} m < dmm < 9.0 \times 10^{-7} m$$

$$N_{m,T} = 8\ mol$$

6.8.2 Results and discussions

The mass of initiator, *I* (g) was decreased in order to decrease the concentration of the initial initiator charged into the reactor at the beginning of the process. The results in Table 6.7 show that the number average molecular weight can be increased by decreasing the initial initiator concentration (C_{i0}). This is because by reducing the concentration of the initiator at the beginning of the process, less oligomeric radical will be produced and this will reduce the polymerization loci leading to lower conversion (Bakshi et al., 2010). These oligomeric radicals then will react with added monomer to increase the chain length. As the added monomer distributed to less oligomeric radicals produced at the early stage of the polymerization process, the increase of chain length are possible to achieve higher molecular weight.

The results in Table 6.7 show that the diameters of the particles were smaller at higher initiator concentration. This is due to the more oligomeric radicals was

produced with higher C_{I0} at the beginning of the process leading to lower the M_n. With the same concentration of monomer, the shorter each polymer chain will become, yielding a lower average molecular weight, resulting smaller average particle size. On the other hand, the overall conversion was slightly decreased with the decreased of the initial initiator concentration.

Table 6.7: Maximize molecular weight for different initial initiator concentration

Run	C_{I0} (mol/L)x10^{-3}	I (g)	M_n (g/mol)	X_n (%)	D_{mm} (nm)
1	2.774	1.875	253041	94.25	87.7
2	2.626	1.775	260167	94.15	87.8
3	2.331	1.575	276684	94.00	88.2
4	2.035	1.375	297740	93.62	88.3
5	1.739	1.175	324562	93.22	89.0
6	1.591	1.075	341013	92.97	89.3

Three graphs were plotted in Figure 6.5 below from the results in Table 6.7. The graphs are number average molecular weight (M_n), overall conversion (X_n) and diameter particle (D_{mm}) versus initial initiator concentration (C_{I0}) respectively.

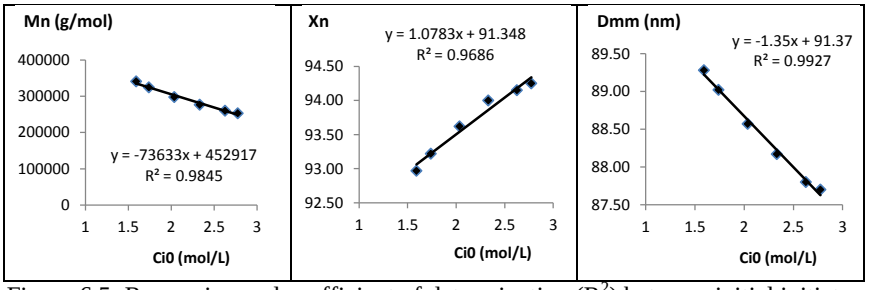

Figure 6.5: Regression and coefficient of determination (R^2) between initial initiator concentration (C_{i0}) and: a) number average molecular weight (M_n) ; b) Overall conversion (X_n) ; c) Particle diameter (D_{mm}).

The linear regression in Figure 6.5 have very strong coefficient of determination (R^2) with the value 0.9845 (Fig. 6.5a); 0.9686 (Fig. 6.5b) and 0.9927 (Fig. 6.5c). It shows that the value of number average molecular weight, overall conversion and particle diameter can be predict by using the related regression above for initial initiator concentration between 1.591 x 10^{-3} mol/L to 2.774 x 10^{-3} mol/L.

The optimal profile of the jacket temperature, monomer flow rates (styrene and MMA), surfactant flow rates and initiator flow rates case study 5 (Run 4) for the different initial initiator concentration is shown in Figure 6.6 below.

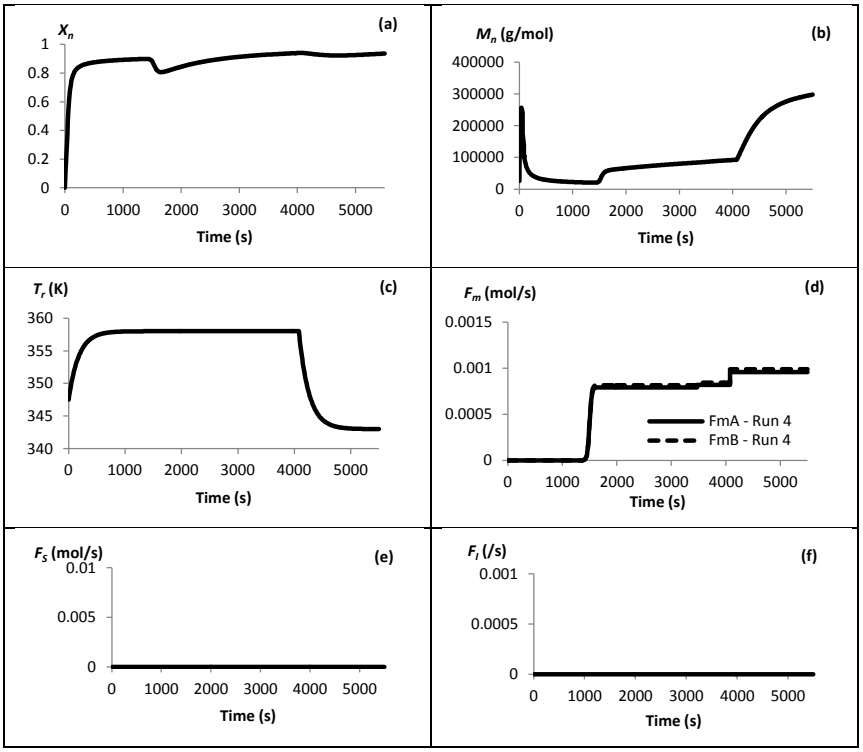

Figure 6.6: Result case study 5 (Run 4); (a) overall conversion (X_n); (b) number average molecular weight (M_n); (c) reaction temperature (T_r); (d) monomer flow rate (F_{mA} and F_{mB}); (e) optimal profile of surfactant flow rate (F_S); (f) optimal profile of initiator flow rate (F_I).

The results show that no surfactant (Figure 6.6e) and initiator (Figure 6.6f) are added along the process in order to avoid the occurrence of the micellar and secondary nucleation which can decrease the M_n. The rest of the optimal profile shown the same observation and are given in the appendix 5.

6.9 Case study 6 – Maximize overall conversion (X_n) in a batch process

6.9.1 Optimization Problem Formulation and Constraints

The objective of case study 6 is to maximize the overall conversion (X_n) for batch process with the fixed number average molecular weight (M_n) using 5 control intervals. The number average molecular weight (M_n) for fixed final batch time (t_f) 5000s was set at 55000 g/mol, 50000 g/mol, 45000 g/mol and 40000 g/mol for each optimization process respectively. Monomer flow rate of styrene and MMA (F_{mA} and F_{mB}) are not optimized for the batch process since all the monomer are feed into the reactor at the beginning of the batch process. The dynamic optimization formulation and constraint for this case study can be described as:

Max X_n

$F_S(t)$; $F_I(t)$; T_{j0}

s.t. $f(t, x'(t), x(t), u(t), v) = 0, \quad [t_0, t_f]$ model equations

$M_n = M_n^*$

$t_f = 5000s$

$$0.0\ g/s < F_S < 0.2\ g/s$$

$$0.0\ g/s < F_I < 0.2\ g/s$$

$$343.00\ K < T_r < 358.00\ K$$

$$0.4 \times 10^{-7} m < D_{mm} < 9.0 \times 10^{-7} m$$

$$N_{m,T} = 8\ mol$$

6.9.2 Results and discussions

Table 6.8 shows the results for maximization of X_n in batch reactor. Jacket temperature (T_{j0}), surfactant flow rates (F_S) and initiator flow rate (F_I) were optimized in order to achieve the maximum overall conversion for the desired molecular weight. The results show that maximum overall conversion for all desired molecular weight can be achieved around 98%. The value of X_n for run 2 is slightly lower than the rest since more initiator was feed at the beginning of the process compared to Run 1, 3 and 4.

Table 6.8: Results for maximization of Xn in batch reactor.

Run	X_n (%)	M_n (g/mol)	M_n*(g/mol)	D_{mm} (nm)
1	98.24	55005.15	55000	93.46
2	97.36	49998.85	50000	96.56
3	98.24	45005.42	45000	93.46
4	98.18	40003.56	40000	93.50

When initiator flow rate is high at the beginning of the process (Fig. 6.7f), the number average molecular weight (M_n) is low (Fig. 6.7a) since more monomer will react with the initiator to initiate the polymerization process rather than continue to

propagate with the oligomeric. This lower molecular weight then makes the X_n for Run 2 faster at the early process where it can achieve 75% at 440s while the rest is about 10 seconds late as shown in Figure 6.7b in small picture and this lead to lower X_n for Run 2. This is due to the fact that monomer conversion is relatively low after the end of particle nucleation.

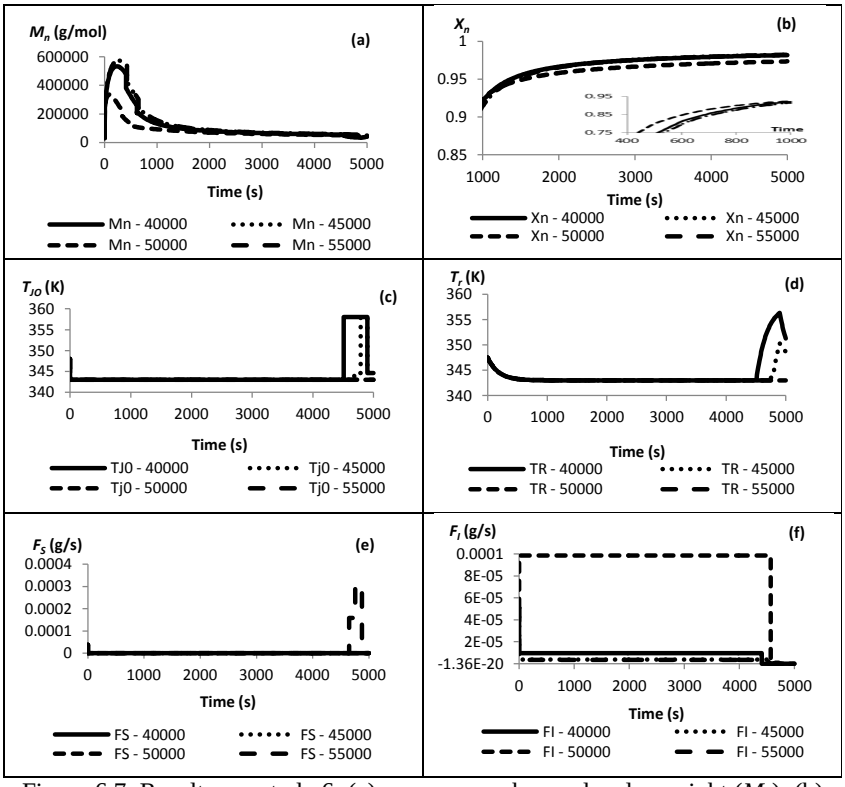

Figure 6.7: Result case study 6: (a) average number molecular weight (M_n); (b) overall conversion (X_n); (c) optimal profile of jacket temperature (T_{j0}); (d) reaction temperature (T_r); (e) optimal profile of surfactant flow rate (F_S); (f) optimal profile of initiator flow rate (F_I).

Temperature was increased for M_n 40000 g/mol and 45000 g/mol at the end of the process (Fig. 6.7c and Fig. 6.7f) to decrease the M_n in the optimization process. This is because by increasing the temperature, the chain length decreases due to the transfer kinetic event (Zeaiter et al., 2002; Alhamad, 2005). The entry of radicals to

the particles would result instantaneous termination. Flow rate of surfactant is increased for M_n 55000 g/mol at the end of the process (Fig. 6.7e) to achieve the desired M_n since the added surfactant will produce new particles by micellar nucleation.

6.10 Case Study 7 – Maximize number average molecular weight (M_n) in a batch process

6.10.1 Optimization Problem Formulation and Constraints

The objective of this case study is to maximize the number average molecular weight (M_n) for batch process using 5 control intervals. Final batch time (t_f*)is fixed at 5000s, 5500s and 6000s. The dynamic optimization formulation and constraints for this case study can be described as:

Max M_n

$F_S(t)$; $F_I(t)$; T_{j0}

s.t. $f(t, x'(t), x(t), u(t), v) = 0, \quad [t_0, t_f]$ model equations

$t_f = t_f$*

$0.90 < X_n < 1.0$

$0.0\ g/s < F_S < 0.2\ g/s$

$0.0\ g/s < F_I < 0.2\ g/s$

$343.00\ K < T_{react} < 358.00\ K$

$$0.4 \times 10^{-7} m < dmm < 9.0 \times 10^{-7} m$$

$$N_{m,T} = 8 \, mol$$

6.10.2 Results and discussions

Table 6.9 shows the results for the maximization of Mn in batch reactor. Jacket temperature, surfactant flow rates and initiator flow rate were optimized in order to achieve the maximum number average molecular weight at fixed time. The results show that molecular weight was decreased with the increased fixed batch time while overall conversion was slightly increased for this study case. Very small increment of the particle diameter also can be observed.

Table 6.9: Results for maximization of M_n in batch reactor

Run	M_n (g/mol)	X_n (%)	D_{mm} (nm)	t_f (s)
1	59371.94	98.18	93.36	5000
2	57080.51	98.28	93.43	5500
3	55585.33	98.34	93.47	6000

The longer the batch time gives more time for monomer radicals to absorb and desorb from one particle to another particle in polymerization loci. This will lead to decrease the number average molecular weight and increased the overall conversion which agreed with the result obtained in Table 6.9.

The results from this case study is compared with case study 2 which was carried out in semi-batch process (1200s pre-batch time) for the same final batch time 5000s (Run 2 from Table 6.4 and Run 1 from Table 6.9) and 5500s (Run 3 from table 6.3

and Run 2 from Table 6.9). It shows that lower number average molecular weight (M_n) and higher overall conversion (X_n) can be achieved in batch process (case study 7) for the same fixed total batch time. M_n is very low in batch process since more monomer will react with the initiator to initiate the polymerization process rather than continue to propagate with oligomeric radicals. Larger volume of particle at the beginning of the process (batch process) leads to produce bigger particle diameter (D_{mm}) compared to semi-batch process. In batch process, all monomer added at the beginning of the process will undergo propagation process without any interfere of monomer addition along the reaction process which leads to increase the X_n.

Figure 6.8 below show the optimal profile for batch process in case study 7 (Run 2). No initiator and surfactant are added along the process, only a very small increment of jacket temperature can be observed (Figure 6.8d) in order to achieve the maximum M_n. The rest of the profile in this study case is presented in appendix 6.

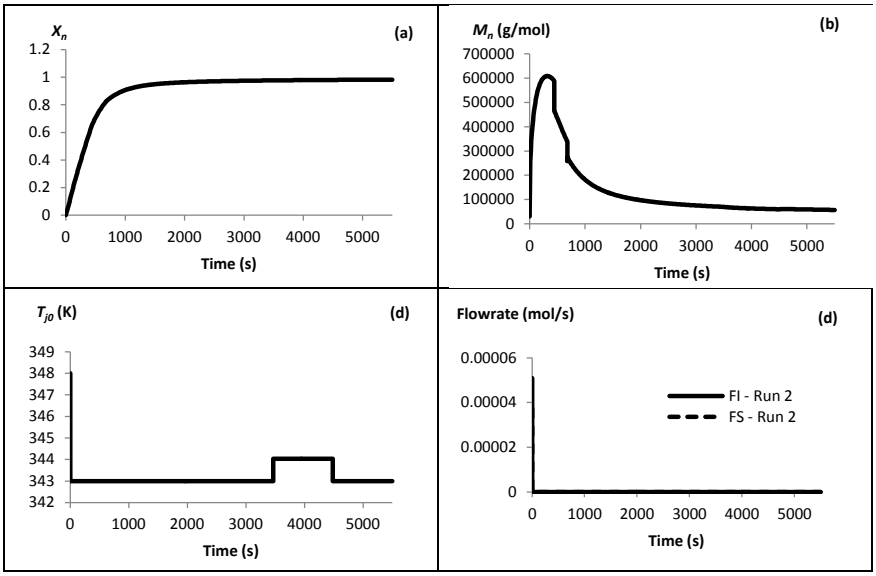

Figure 6.8: Result case study 7 (Run 2); (a) overall conversion (X_n); (b) number average molecular weight (M_n); (c) reaction temperature (T_r); (d) optimal profile of surfactant flow rate (F_S) and optimal profile of initiator flow rate (F_I).

6.11 Case study 8 – maximize number average molecular weight (M_n) for different number of intervals in a semi-batch process without pre-batch time

6.11.1 Optimization Problem Formulation and Constraints

This case study maximizes the molecular weight using different number of control intervals (from one interval to five intervals). No pre-batch time is assigned to the process for the total reaction time 5000s. The dynamic optimization formulation and constraint for this case study can be described as:

Max M_n

$F_{mA}(t)$; $F_{mB}(t)$; $F_S(t)$; $F_I(t)$; $Tj0$

s.t. $f(t, x'(t), x(t), u(t), v) = 0, \quad [t_0, t_f]$ model equations

$0.90 < X_n < 1.0$

$0.0\ g/s < F_{mA} < 0.2\ g/s$

$0.0\ g/s < F_{mB} < 0.2\ g/s$

$0.0\ g/s < F_S < 0.2\ g/s$

$0.0\ g/s < F_I < 0.2\ g/s$

$343.00\ K < T_r < 358.00\ K$

$0.4 \times 10^{-7} m < D_{mm} < 9.0 \times 10^{-7} m$

$N_{m,T} = 8\ mol$

6.11.2 Results and discussions

Different numbers of intervals are used in the dynamic optimization process to control in this study case to see the effect of number of intervals in the optimization process. In each interval, the control value and length of the interval (i.e. switching time) are optimized in order to achieve the maximum value of number average molecular weight.

The results in Table 6.10 show that increasing the number of intervals can increase the molecular weight until certain number of interval where increasing the number of interval does not bring much difference to the process in terms of M_n.

Table 6.10: results for maximize molecular weight for different number of intervals (no pre-batch time)

Run	M_n (g/mol)	X_n (%)	D_{mm} (nm)	Intervals
1	194758.4	95.33	88.64	1
2	251152.0	94.00	87.64	2
3	258991.7	94.00	87.66	3
4	258543.1	93.58	87.65	4
5	258362.6	93.44	87.65	5

However, larger differences in values of M_n for 1 and 2 intervals with the 3 intervals can be observed (32.981% for 1 and 3 intervals and 3.121% for 2 and 3 intervals). This is happened because with the higher number of intervals, it gives more flexibility to the process variables to optimize with certain constraints given to the process. Figure 6.9 below show the results for maximize molecular weight for different number of intervals without any pre-batch time. No initiator was added along the process.

By using only 1 interval, the temperature has to be constant for the whole process, 343 K (Fig. 6.9b). This will lead to higher M_n from the beginning of the process (Fig. 6.9a) since low temperature will increase the transfer rate and termination constant. Flow rate of surfactant increased (Fig. 6.9d) to achieve the maximum M_n since the addition of surfactant produce new particle by micellar nucleation.

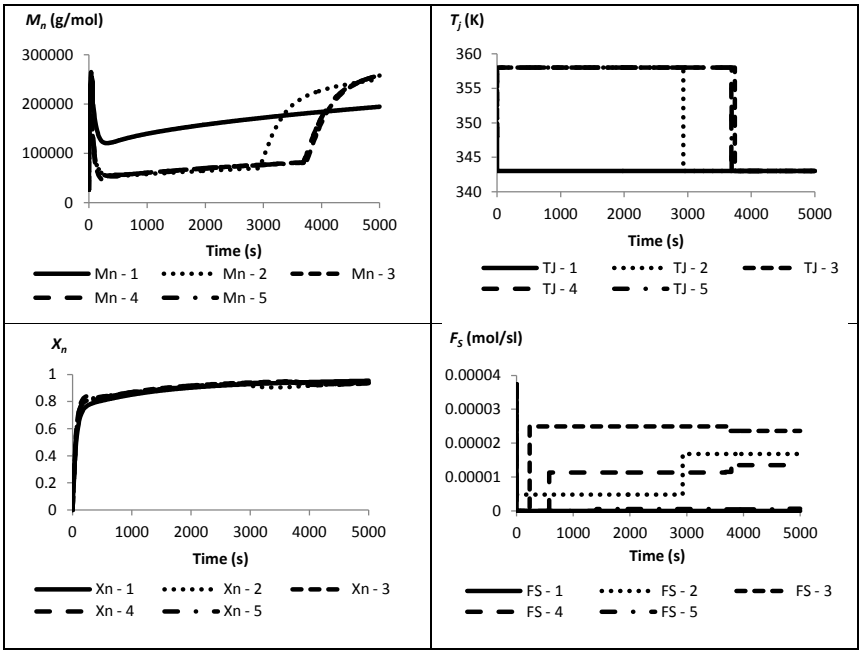

Figure 6.9: Result case study 8: (a) number average molecular weight (M_n); (b) reaction temperature (T_r); (c) overall conversion (X_n); (d) optimal profile of surfactant flow rate (F_S)

6.12 Case Study 9 – maximize number average molecular weight (M_n) for 5 intervals with control the monomer flow of 5th interval.

6.12.1 Optimization Problem Formulation and Constraints

This case study maximizes the number average molecular weight (M_n) with 5 control intervals where the length and flow of the monomer for the fifth interval (t_5*) was varied for the total reaction time 5000s without any pre-batch time. The length of the fifth interval with 0 g/s of monomer flow was set at 600s, 420s, 300s and 180s. The dynamic optimization formulation and constraint for this case study can be described as:

Max M_n

$F_{mA}(t)$; $F_{mB}(t)$; $F_S(t)$; $F_I(t)$; T_{j0}

s.t. $f(t, x'(t), x(t), u(t), v) = 0, \quad [t_0, t_f]$ model equations

$t_f = 5000s$

$0.90 < X_n < 1.0$

$0.0\ g/s < F_{mA} < 0.2\ g/s$

$0.0\ g/s < F_{mB} < 0.2\ g/s$

$0.0\ g/s < F_S < 0.2\ g/s$

$0.0\ g/s < F_I < 0.2\ g/s$

$343.00\ K < T_r < 358.00\ K$

$0.4 \times 10^{-7} m < D_{mm} < 9.0 \times 10^{-7} m$

$N_{m,T} = 8\ mol$

6.12.2 Results and discussions

The length of the fifth interval with no monomer added into the reactor gives a very significant effect to the molecular weight of the polymer in the system. By increasing the length for the fifth interval the maximum value of number average molecular weight can be decreased (Fig. 6.10c and Fig. 6.10d) with increase in the overall conversion of the monomer as shown in Table 6.11.

Table 6.11: Results for maximization of Mn for different length of fifth interval in semi batch process

Run	M_n (g/mol)	X_n	t_5* (s)	D_{mm} (nm)
1	142473.3	99.04	600	90.03
2	164110.3	98.51	420	89.60
3	183351.3	97.63	300	89.21
4	207956.8	96.56	180	88.71

This is happened because no addition of the monomer into the reactor near to the end of the process (Fig. 6.11e and Fig. 6.11f) will help the polymerization process to propagate and terminate with all the monomer already added into the reactor and reduce the unreacted monomer in the reactor. This event can be clearly seen in Figure 6.10a and Figure 6.10b where overall monomer conversion increased drastically when the monomer flow is stop in the fifth interval. Adsorption and desorption of monomer radicals is happened without interference of any added monomer towards the end of the process.

Figure 6.11g and Figure 6.11h show the optimal value of reactor temperature and surfactant flow rate to achieve the maximum M_n. Molecular weight was low (Figure 6.10c) at higher temperature (Figure 6.11g) and was increased when the reaction temperature was reduced. This is due to the increase of the radical transfer rate at high temperature leading to the formation of shorter chains.

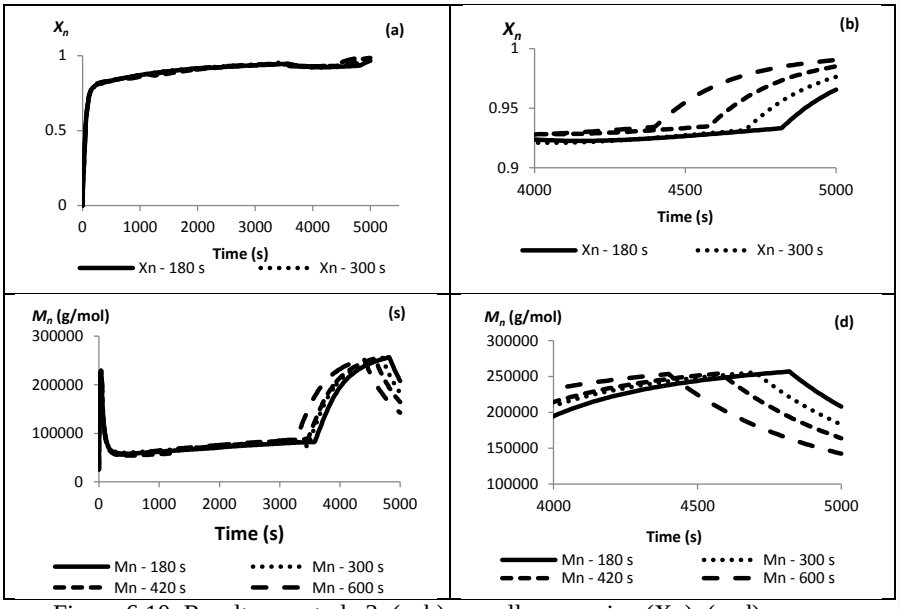

Figure 6.10: Result case study 3: (a, b) overall conversion (Xn); (c, d) average number molecular weight (Mn)

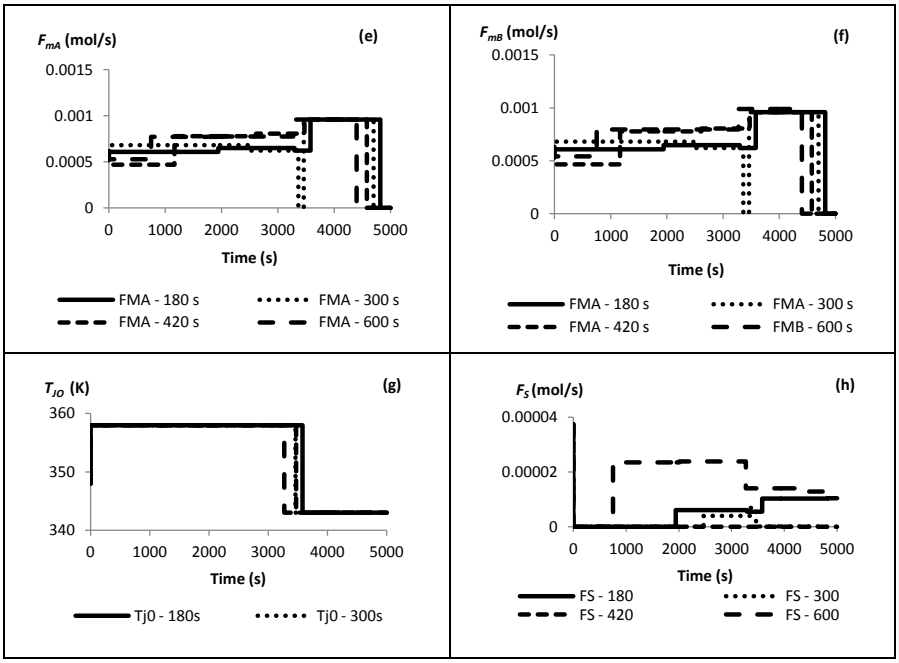

Figure 6.11: Result case study 3: (e) optimal profile of Styrene monomer flow rate (F_{MA}); (f) optimal profile of MMA monomer flow rate (F_{MB}); (g) optimal profile of jacket temperature (T_{j0}); (h) optimal profile of surfactant flow rate (F_S).

6.13 Conclusions

The determination of optimal control trajectories for emulsion copolymerization of Styrene and MMA was carried out in this chapter. The resulting trajectories of F_{mA}, F_{mB}, F_S, F_I and T_{j0} are obtained by formulating and solving different types of dynamic optimization problems with the objective of maximizing number average molecular weight (M_n) and overall conversion (X_n). Several constraints were used with lower and upper bounds to ensure that the process was running towards the desired process. The dynamic optimization technique based on Control Vector Parameterization (CVP) with the Sequential Quadratic Programming (SQP) method is employed for the solution of the optimization problems.

The objectives for case study 1 and 2 were to maximize number average molecular weight (M_n) in different pre-batch time for different number of intervals with fixed final batch time. The results show that by reducing the pre batch time, M_n will be higher but conversion (X_n) will be decreased respectively. In all semi-batch process, 17.1% of total monomer was feed at the beginning of the process for seed formation. Lower pre-batch time for seed formation allows to add the remaining monomer to the reactor earlier. As the monomers enter the micelles at the early stage of the emulsion process, M_n are very high because the monomer will enter into the small amount of particles and increased the molecular chain in the particles. Additional monomers are then fed to the reactor along the process which increases the molecular weight. So the shorter the seed formation time the sooner the molecular weight will increase along the reaction time.

Different pre-batch times are used (1200s and 1500s) in the dynamic optimization process in case study 3 to see the effect of different pre-batch time when overall conversion (X_n) is maximized to achieve desired number average molecular weight (M_n) using free final batch time. The results show that the desired molecular weight can be achieved in shorter time with higher overall conversion for lower pre-batch time. This case study was carried out with free time.

The objectives for case study 4 was to maximize overall conversion (X_n) for desired number average molecular weight (M_n) at 1200s pre-batch time and fixed total batch time 5500s. The results show that higher X_n can be achieved for lower desired M_n since addition of surfactant and initiator formed new micelles and radicals, thus new polymer chains continue to occur. This leads to more conversion of the monomer.

The effect of different initial initiator concentration (C_{i0}) purged inside the reactor at the beginning of the process was study in case study 5. The number average molecular weight (M_n) was maximized for 1500s pre-batch time and fixed final batch time 5500s. The results show that the M_n can be increased by decreasing the C_{i0}. This is due to less oligomeric radicals will be produced (with low C_{i0}) which reduces the polymerization loci for the propagation process to continue with the added monomers thus lowered the overall conversion.

Case studies 6 and 7 were carried out for batch process, to maximize overall conversion and maximize number average molecular weight respectively. The results show that maximum value for overall conversion of both cases can be achieved around 98%. However, maximum value for M_n was decreased as the final batch time

was increased. The results from case study 7 (maximize M_n) was compared with case study 2 which was carried out in semi-batch process (1200s pre-batch time) for the same final batch time 5000s and 5500s. It shows that lower number average molecular weight (M_n) and higher overall conversion (X_n) can be achieved in batch process for the same fixed batch time. M_n is very low in batch process since more monomer will react with the initiator to initiate the polymerization process rather than continue to propagate with oligomeric radicals. Larger volume of particle at the beginning of the process (batch process) leads to produce bigger particle diameter (D_{mm}) compared to semi-batch process. In batch process, all monomer added at the beginning of the process will undergo propagation process without any interfere of monomer addition along the reaction process which leads to increase the X_n.

The effects of number of intervals were investigated in case study 8 where no pre-batch time was allocated for the process. In each interval, the control value and length of the interval (i.e. switching time) are optimized. It shows that increasing the number of intervals can increase the molecular weight until certain number of interval beyond which increasing the number of interval does not give much effect to the process. In this case, three intervals are enough for the flexibility of the control variables to achieve the desired properties. Comparison of the results with 1500s pre-batch time for 3 intervals (Table 6.4 - Run 1) and 5 intervals (Table 6.2 – Run 2) show that higher number average molecular weight (M_n) and lower overall conversion X_n was achieved for the process carried out without any pre-batch time. The chain length of polymer start to increase from the beginning of the process (without pre-batch time), leads to achieve higher number average molecular weight (M_n).

The last study case was carried out to observe the effects of the fifth interval length where the monomer flow in was set at 0 g/s (no monomer added). The longer the fifth interval, the lower the molecular weight achieved. On the other hand, the overall conversion was increased significantly due to more time was given for all the monomer radicals to settle in the particles.

As a conclusion from all case studies carried out in this emulsion copolymerization of styrene and MMA, reduction of pre-batch time can increase the number average molecular weight. However, higher M_n can be achieved for semi-batch process without any pre-batch time when compared to semi-batch process with longer pre-batch time. On the other hand, polymer produced in batch process will have low M_n and a very high overall conversion (X_n) as discussed before. Number average molecular weight (M_n) can be increased by increasing the total batch time. Addition of monomer along the semi-batch process also increased the polymer chain length, means increase of M_n. Besides that, addition of surfactant and initiator along the semi-batch process will form new particles which lower the M_n and increase the X_n respectively. The M_n also decreases with the increase of reaction temperature (T_r) since transfer coefficient is increased at higher T_r leads to increase the monomeric radicals resulting in an increase in termination reaction.

Chapter Seven

Conclusions and Future Work

7.1 Conclusions

This chapter summarizes the work carried out in this work. Three different free radical polymerization processes were considered in this work using Control Vector Parameterization (CVP) techniques. They are bulk polymerization of styrene in batch reactor, solution polymerization of methyl methacrylate (MMA) in batch reactor and emulsion copolymerization of styrene and MMA in batch and semi-batch reactor. Mathematical modelling were presented in chapter three for all the free radical polymerization process.

The process model used for polystyrene polymerization in batch reactors, using 2, 2 azobisisobutyronitrile catalyst (AIBN) as initiator includes the gel and glass effects and this is an improvement over the earlier work of Ekpo and Mujtaba (2004). Four study cases were carried out in this study by taking into account the gel and glass effects. The first two cases were based on simple kinetic model while the last two cases were based on the energy balance model.

Optimal profiles for temperature (T), jacket coolant flow rate (F_j) and jacket temperature set point (T_{jsp}) affecting the quality of final product was obtained. The results obtained from this work were compared with the previous study by other researcher which disregarded the gel and glass effect in their study shows that the batch time operation are significantly reduced while the amount of the initial initiator concentration required is increased. As the concentration of the reaction mixture increases, termination rate constant decreases because entanglement of the polymer chains hindered the termination process (gel effect). However, propagation proceeds as before, so the conversion is rapid and the molecular weight will increase in a very short time.

The process model used for solution polymerization of methyl methacrylate (MMA) in batch reactors, using 2, 2 azobisisobutyronitrile catalyst (AIBN) as the initiator was improved by including the free volume theory to calculate the initiator efficiency which was not considered in the earlier work of Ekpo and Mujtaba (2006). Two types of models were developed in chapter five to investigate the effect of f namely simple model and detailed model.

Optimal temperature profile for solution polymerization of MMA that will yield desired polymerization characteristics in minimum time of the improved process model by using the Control Vector Parameterization (CVP) technique was obtained. The effects of different initiator efficiency, f was examined and compared with previous work of Ekpo and Mujtaba (2006) which used a constant value of f at 0.53. The results of these studies show that initiator efficiency, f decreased along the process with the increased of the monomer conversion in solution polymerization of

MMA when the free volume theory was applied. The results between two approaches confirm that the initial initiator needed at the early stage of the process is higher and longer batch time is required in order to achieve the specified X_n and M_n by using the time-varying initiator efficiency.

The effect of solvent are very pronounced for both approach where there are large decrease in the reaction time for more concentrated reaction mixture in the reactor. This is to be expected since the model incorporates the gel and glass effect. The effect of different initiator efficiency need to take into account since it follows the theory lied behind. These really show the significant of using the free volume theory for the initiator efficiency rather than a constant value and it cannot be ignored.

The determination of optimal control trajectories for emulsion copolymerization of Styrene and MMA was carried out in chapter six. The resulting trajectories of F_{mA}, F_{mB}, F_S, F_I and T_{j0} are obtained by formulating and solving different types of dynamic optimization problems with the objective of maximizing number average molecular weight (M_n) and overall conversion (X_n). These were carried out with different pre-batch time in semi-batch reactor by using the CVP techniques. Three different processes were carried out in chapter six. They are semi-batch process with pre-batch time (case studies 1 – 5), batch process (case study 6 and 7) and semi-batch process without any pre-batch time allocated for the process (case study 8 and 9).

The objectives in the first five case studies were to maximize number average molecular weight (M_n) and overall conversion (X_n) in semi-batch process with different pre-batch time. The results show that by reducing the pre-batch time, M_n

will be higher but conversion (X_n) will be decreased respectively. Addition of monomers fed to the reactor along the process increases the molecular weight. So the shorter the seed formation time the sooner the increase of molecular weight along the reaction time. Besides that effect of different initial initiator concentration (C_{i0}) also studied. The results show that the M_n can be increased by decreasing the C_{i0} due to less oligomeric radicals will be produced with low C_{i0}. This leads to reduce the polymerization loci for the propagation process to continue further with the added monomers thus lowered the overall conversion.

Two study cases (study case 6 and study case 7) were carried out for batch process, to maximize overall conversion and maximize number average molecular weight respectively. The optimal profile of jacket temperature (T_{j0}), surfactant flow rate (F_s) and initiator flow rate (F_I) for emulsion copolymerization of styrene and MMA in batch reactor was obtained. The results show that maximum value for overall conversion of both cases can be achieved around 98%. However, maximum value for M_n was decreased as the final batch time was increased.

The effects of number of intervals were investigated in case study 8 where no pre-batch time was allocated for the semi-batch process. It shows that increasing the number of intervals can increase the molecular weight until certain number of interval where increasing the number of interval does not give much effect to the process in term of M_n. It was observed that three control intervals are enough for the flexibility of the control variables to achieve the desired properties in this case study.

In study case 9, the optimization of the semi-batch process without any pre-batch time was optimized to study the effects of the fifth interval length where the monomer flow in was set at 0 g/s (no monomer added). The results show that the longer the fifth interval, the lower molecular weight will be. Inversely, the overall conversion was increased significantly with longer fifth interval (0 g/s) due to more time was given for all the monomer radicals to settle in the particles.

7.2 Contribution of This Work

Contribution of this work for bulk polymerization of styrene, solution polymerization of Methyl Methacrylate (MMA) and emulsion copolymerization of styrene and MMA are given below:

- The process model used for bulk polymerization of styrene in batch reactor, using 2, 2 azobisisobutyronitrile catalyst (AIBN) as the initiator has been improved by including the gel and glass effect.

- The process model used for solution polymerization of methyl methacrylate (MMA) in batch reactors, using 2,2 azobisisobutyronitrile catalyst (AIBN) as the initiator has been improved by including the free volume theory to calculate the initiator efficiency.

- A set of different pre-batch time for the seed formation is used for optimization process of emulsion copolymerization of styrene and Methyl Methacrylate (MMA).

- Different optimization formulation is used in this work for maximize the number average molecular weight (M_n) in emulsion copolymerization process, where the total batch time is fixed, instead of free time.

- Maximization of overall conversion (X_n) is carried out in batch process and semi-batch process with pre-batch time for emulsion copolymerization process.

- The number average molecular weight (M_n) is maximized in semi-batch process without pre-batch time for emulsion copolymerization of styrene and MMA.

7.3 Future Work

Some suggestions for the future works are outlined below:

1. General batch and semi-batch polymerization was carried out in this work. Optimization can be carried in the future with more specific scenario like

model uncertainty and operating and economic constraints using the CVP techniques.

2. The results obtained in dynamic optimization problems from this work can be used for online control of the each polymerization process in the future work.

3. The results achieved in this thesis should be validated by experimental work. The results from experimental work can be compared with the dynamic optimization obtain in this work.

4. The market prices for finished polymers as well as the cost of manufacturing the polymer at different sites could be added in the future work. So, the maximum profit problems can be solved to establish the feasibility of running a polymerization process at different sites.

5. Copolymerization of bulk and solution process can be carried out using these models which only consider homopolymerization process.

6. The effects of jacket dynamics can be incorporated in future work which are assumed to be negligible in the energy balance models used in this work.

7. It is desirable to study more than one of the effects at the same time to further tune the optimization process and to give closer picture of the real phenomena in the chemical industry.

References

(PSE), P. S. E. L. (2007) gPROMS® ModelBuilder. 3.0.3 ed. London, United Kingdom, Process Systems Enterprise Limited (PSE).

ACHILIAS, D. S. (2007) A review of modeling of diffusion controlled polymerization reactions. *Macromolecular Theory and Simulations,* 16**,** 319-347.

ACHILIAS, D. S. & KIPARISSIDES, C. (1992) Development of a general mathematical framework for modelling diffusion-controlled free-radical polymerization reactions. *Macromolecules,* 25**,** 3739-3750.

ACHILIAS, D. S. & VERROS, G. D. (2010) Modeling of diffusion-controlled reactions in free radical solution and bulk polymerization: Model validation by DSC experiments. Wiley Subscription Services, Inc., A Wiley Company.

ALHAMAD, B. (2005) A Framework For Advanced / Intelligent Operation Of Emulsion Copolymerization Reactors. *Department of Chemical Engineering.* Sydney, The University of Sydney, Australia.

ALHAMAD, B., ROMAGNOLI, J. A. & GOMES, V. G. (2005a) Advanced modelling and optimal operating strategy in emulsion copolymerization: Application to styrene/MMA system. *Chemical Engineering Science,* 60**,** 2795-2813.

ALHAMAD, B., ROMAGNOLI, J. A. & GOMES, V. G. (2005b) On-line multi-variable predictive control of molar mass and particle size distributions in free-radical emulsion copolymerization. *Chemical Engineering Science,* 60**,** 6596-6606.

ANDRZEJEWSKA, E. & BOGACKI, M. B. (1997) Monomolecular and bimolecular termination in the polymerization of di (meth) acrylates. *Macromolecular Chemistry and Physics,* 198**,** 1649-1664.

ARAI, K., YAMAGUCHI, H., SAITO, S., SARASHINA, E. & YAMAMOTO, T. (1986) A Kinetic-Study Of Bulk Thermal Polymerization Of Styrene. *Journal of Chemical Engineering of Japan,* 19**,** 413-419.

ARAI, M., ARAI, K. & SAITO, S. (1979) Polymer particle formation in soapless emulsion polymerization. *Journal of Polymer Science: Polymer Chemistry Edition,* 17**,** 3655-3665.

ARORA, P., JAIN, R., MATHUR, K., SHARMA, A. & GUPTA, A. (2010) Synthesis of polymethyl methacrylate (PMMA) by batch emulsion polymerization. *African Journal of Pure and Applied Chemistry,* 4**,** 152-157.

ASMUSSEN, E. & PEUTZFELDT, A. (2001) Influence of selected components on crosslink density in polymer structures. *European Journal of Oral Sciences,* 109**,** 282-285.

ASTEASUAIN, M., TONELLI, S. M., BRANDOLIN, A., BANDONI, J. A. & SAURO, P. (2000) Modelling and optimisation of polymerisation reactors in gPROMS. *Computer Aided Chemical Engineering.* Elsevier.

ASUA, J. M. (2007) *Polymer reaction engineering,* UK, Blackwell Publishing.

AZIZ, N. (2001) Dynamic optimisation and control of batch reactors. *Department of Chemical Engineering.* Bradford, UK, University of Bradford.

BAILLAGOU, P. E. & SOONG, D. S. (1985a) Major Factors Contributing To The Nonlinear Kinetics Of Free-Radical Polymerization. *Chemical Engineering Science,* 40**,** 75-86.

BAILLAGOU, P. E. & SOONG, D. S. (1985b) Molecular weight distribution of product of free radical non-isothermal polymerization with gel effect - simulation for polymerization of poly(methyl methacrylate). *Chemical Engineering Science,* 40**,** 87-104.

BAKHSHI, H., BOUHENDI, H., ZOHURIAAN-MEHR, M. J. & KABIRI, K. (2010) Semibatch emulsion copolymerization of butyl acrylate and glycidyl methacrylate: Effect of operating variables. Wiley Subscription Services, Inc., A Wiley Company.

BALKE, S. T. & HAMIELEC, A. E. (1973) Bulk polymerization of methyl methacrylate. *Journal of Applied Polymer Science,* 17**,** 905-949.

BALKU, S., YUCEER, M. & BERBER, R. (2009) Control vector parameterization approach in optimization of alternating aerobic–anoxic systems. *Optimal Control Applications and Methods,* 30**,** 573-584.

BEGUM, F. & SIMON, S. L. (2011) Modeling methyl methacrylate free radical polymerization in nanoporous confinement. *Polymer,* 52**,** 1539-1545.

BENYAHIA, B., LATIFI, M. A., FONTEIX, C., PLA, F. & NACEF, S. (2009) Emulsion copolymerization of styrene and butyl acrylate in the presence of a chain transfer agent.: Part 1: Modelling and experimentation of batch and fedbatch processes. *Chemical Engineering Science,* In Press, Corrected Proof.

BONNEFOND, A., PAULIS, M. & LEIZA, J. R. (2011) Kinetics of the emulsion copolymerization of MMA/BA in the presence of sodium montmorillonite. *Applied Clay Science,* 51**,** 110-116.

CAPASSO, V. (2003) *Mathematical modelling for polymer processing: polymerization, crystallization, manufacturing,* Germany, Springer.

CAPEK, I. (2001) On the role of oil-soluble initiators in the radical polymerization of micellar systems. *Advances in Colloid and Interface Science,* 91**,** 295-334.

CASSAGNAU, P., GIMENEZ, J., BOUNOR-LEGARÉ, V. & MICHEL, A. (2006) New rheological developments for reactive processing of poly([epsilon]-caprolactone). *Comptes Rendus Chimie,* 9**,** 1351-1362.

CHEN, C. L. (1988) A class of successive quadratic programming methods for flowsheet optimisation. UK, University of London.

CHEN, K. & WANG, L. (2007) *Trends in neural computation*, Springer.

CHEN, S. & JENG, W. F. (1978) Minimum end time policies for batchwise radical chain polymerization. *Chemical Engineering Science,* 33**,** 735-743.

CHIU, W. Y., CARRATT, G. M. & SOONG, D. S. (1983) A Computer-Model For The Gel Effect In Free-Radical Polymerization. *Macromolecules,* 16**,** 348-357.

CLAY, P. A. & GILBERT, R. G. (1995) Molecular Weight Distributions in Free-Radical Polymerizations. 1. Model Development and Implications for Data Interpretation. *Macromolecules,* 28**,** 552-569.

COEN, E. M., GILBERT, R. G., MORRISON, B. R., LEUBE, H. & PEACH, S. (1998) Modelling particle size distributions and secondary particle formation in emulsion polymerisation. *Polymer,* 39**,** 7099-7112.

COEN, E. M., PEACH, S., MORRISON, B. R. & GILBERT, R. G. (2004) First-principles calculation of particle formation in emulsion polymerization: pseudo-bulk systems. *Polymer,* 45**,** 3595-3608.

CUNNINGHAM, M. F. & MAHABADI, H. K. (1996) Kinetics of High-Conversion Free-Radical Polymerization. 1. Understanding Kinetics through Study of Pseudoinstantaneous Molecular Weight Distributions. *Macromolecules,* 29**,** 835-841.

DAVISSON, L., MACFARLANE, A., KWAKERNAAK, H., MASSEY, J., TSYPKIN, Y., VITERBI, A., KALL, P. & KLÖTZLER, R. (1992) Pontryagin's maximum principle for multiple integrals. *System Modelling and Optimization.* Springer Berlin / Heidelberg.

DUBE, M. A., SOARES, J. B. P., PENLIDIS, A. & HAMIELEC, A. E. (1997) Mathematical Modeling of Multicomponent Chain-Growth Polymerizations in Batch, Semibatch, and Continuous Reactors: A Review. *Industrial & Engineering Chemistry Research,* 36**,** 966-1015.

EDGAR, T. F., HIMMELBLAU, D. M. & LASDON, L. S. (2001) *Optimization of chemical processes*, McGraw-Hill.

EKPO, E. E. (2006) Dynamic optimisation and control of batch polymerisation process. *Department of Engineering, Design and Technology.* Bradford, UK, University of Bradford.

EKPO, E. E. & MUJTABA, I. M. (2004) Dynamic optimisation of styrene polymerisation in batch reactors. *Computer Aided Chemical Engineering,* Volume 18**,** 649-654.

EKPO, E. E. & MUJTABA, I. M. (2008) Evaluation of neural networks-based controllers in batch polymerisation of methyl methacrylate. *Neurocomputing,* 71**,** 1401-1412.

ERDOGAN, S., ALPBAZ, M. & KARAGÖZ, A. R. (2002) The effect of operational conditions on the performance of batch polymerization reactor control. *Chemical Engineering Journal,* 86**,** 259-268.

FAN, S., GRETTON-WATSON, S. P., STEINKE, J. H. G. & ALPAY, E. (2003) Polymerisation of methyl methacrylate in a pilot-scale tubular reactor: modelling and experimental studies. *Chemical Engineering Science,* 58**,** 2479-2490.

FIKAR, M., LATIFI, M., FOURNIER, F. & CREFF, Y. (1998) Control vector parametrisation versus iterative dynamic programming in dynamic optimisation of a distillation column. *Computers & Chemical Engineering,* 22**,** S625-S628.

GARCIA, V., CABASSUD, M., LE LANN, M. V., PIBOULEAU, L. & CASAMATTA, G. (1995) Constrained optimization for fine chemical productions in batch reactors. *The Chemical Engineering Journal and the Biochemical Engineering Journal,* 59**,** 229-241.

GEORGE D. VERROS & DIMITRIS S. ACHILIAS (2009) Modeling gel effect in branched polymer systems: Free-radical solution homopolymerization of vinyl acetate. *Journal of Applied Polymer Science,* 111**,** 2171-2185.

GHOSH, P., GUPTA, S. K. & SARAF, D. N. (1998) An experimental study on bulk and solution polymerization of methyl methacrylate with responses to step changes in temperature. *Chemical Engineering Journal,* 70**,** 25-35.

GILBERT, R. G. (1995) *Emulsion polymerization: A Mechanistic Approach,* London, Academic Press Limited.

GINSBURGER, E., PLA, F., FONTEIX, C., HOPPE, S., MASSEBEUF, S., HOBBES, P. & SWAELS, P. (2003) Modelling and simulation of batch and semi-batch emulsion copolymerization of styrene and butyl acrylate. *Chemical Engineering Science,* 58**,** 4493-4514.

GOMES, V. G., ALTARAWNEH, I. S. & SROUR, M. H. (2009) Advanced Modelling for Investigating the Effects of Reactor Operation on Controlled Living Emulsion Polymerization. *Chemical Product and Process Modeling,* Vol. 4**,** Article 2.

GUPTA, S. K. (2006) *Numerical Methods for Engineers*, New Age International (P) Ltd.

HANGOS, K. M. & CAMERON, I. T. (2001) *Process modelling and model analysis,* London, UK, Academic Press.

HOLMES, R. G., RUEGGEBERG, F. A., CALLAN, R. S., CAUGHMAN, F., CHAN, D. C. N., PASHLEY, D. H. & LOONEY, S. W. (2007) Effect of solvent type and content on monomer conversion of a model resin system as a thin film. *Dental Materials,* 23**,** 1506-1512.

JALEEL VALAPPIL, C. G. (2002) Nonlinear model predictive control of end-use properties in batch reactors. *AIChE Journal,* 48**,** 2006-2021.

KALFAS, G. & RAY, W. H. (1993) Modeling and experimental studies of aqueous suspension polymerization processes. 1. Modeling and simulations. *Industrial & Engineering Chemistry Research,* 32**,** 1822-1830.

KARÁTSON, J. & KOROTOV, S. (2005) Discrete maximum principles for finite element solutions of nonlinear elliptic problems with mixed boundary conditions. *Numerische Mathematik,* 99**,** 669-698.

KIPARISSIDES, C. (1996) Polymerization reactor modeling: A review of recent developments and future directions. *Chemical Engineering Science,* 51**,** 1637-1659.

KURDIKAR, D. L. & PEPPAS, N. A. (1994) Method of determination of initiator efficiency: application to UV polymerizations using 2, 2-dimethoxy-2-phenylacetophenone. *Macromolecules,* 27**,** 733-738.

LOEBLEIN, C., PERKINS, J. D., SRINIVASAN, B. & BONVIN, D. (1997) Performance analysis of on-line batch optimization systems. *Computers & Chemical Engineering,* 21**,** S867-S872.

LORENZINI, P., PONS, M. & VILLERMAUX, J. (1992) Free-radical polymerization engineering--III. Modelling homogeneous polymerization of ethylene: mathematical model and new method for obtaining molecular-weight distribution. *Chemical Engineering Science,* 47**,** 3969-3980.

LUO, Y., WANG, X., LI, B.-G. & ZHU, S. (2011) Toward Well-Controlled ab Initio RAFT Emulsion Polymerization of Styrene Mediated by 2-(((Dodecylsulfanyl)carbonothioyl)sulfanyl)propanoic Acid. *Macromolecules,* 44**,** 221-229.

LYULIN, A. V. & MICHELS, M. A. J. (2002) Molecular Dynamics Simulation of Bulk Atactic Polystyrene in the Vicinity of Tg. *Macromolecules,* 35**,** 1463-1472.

MASCHIO, G., BELLO, T. & SCALI, C. (1992) Optimization of batch polymerization reactors: : Modelling and experimental results for suspension polymerization of MethylMethAcrylate. *Chemical Engineering Science,* 47**,** 2609-2614.

MEAD, R. N. & POEHLEIN, G. W. (1989) Emulsion copolymerization of styrene-methyl acrylate and styrene-acrylonitrile in continuous stirred tank reactors. 2. Aqueous-phase polymerization and radical capture. *Industrial & Engineering Chemistry Research,* 28**,** 51-57.

MEADOWS, E. S., CROWLEY, T. J., IMMANUEL, C. D. & DOYLE, F. J. (2003) Nonisothermal Modeling and Sensitivity Studies for Batch and Semibatch Emulsion Polymerization of Styrene. *Industrial & Engineering Chemistry Research,* 42**,** 555-567.

MEDEIROS, S. F., BARBOZA, J., RÉ, M. I., GIUDICI, R. & SANTOS, A. M. (2010) Solution polymerization of N vinylcaprolactam in 1, 4 dioxane. Kinetic dependence on temperature, monomer, and initiator concentrations. *Journal of Applied Polymer Science,* 118**,** 229-240.

O'NEIL, G. A. & TORKELSON, J. M. (1999) Modeling Insight into the Diffusion-Limited Cause of the Gel Effect in Free Radical Polymerization. *Macromolecules,* 32**,** 411-422.

ODIAN, G. G. (2004) *Principles of polymerization,* New Jersey, Wiley-Interscience.

PENLIDIS, A., PONNUSWAMY, S. R., KIPARISSIDES, C. & O'DRISCOLL, K. F. (1992) Polymer reaction engineering: Modelling considerations for control studies. *The Chemical Engineering Journal,* 50**,** 95-107.

PINTO, J. C. & RAY, W. H. (1996) The dynamic behavior of continuous solution polymerization reactors--IX. Effects of inhibition. *Chemical Engineering Science,* 51**,** 63-79.

PRASAD, V., SCHLEY, M., RUSSO, L. P. & WAYNE BEQUETTE, B. (2002) Product property and production rate control of styrene polymerization. *Journal of Process Control,* 12**,** 353-372.

RAJA, T. M. (1995) Modelling and control of the polymerisation of styrene. *Department of Chemical Engineering.* Bradford, UK, University of Bradford.

RAMTEKE, M. & GUPTA, S. K. (2011) Kinetic Modeling and Reactor Simulation and Optimization of Industrially Important Polymerization Processes: a Perspective. *International Journal Of Chemical Reactor Engineering,* 9**,** 1.

RAY, A. B., SARAF, D. N. & GUPTA, S. K. (1995) Free radical polymerizations associated with the trommsdorff effect under semibatch reactor conditions. I: Modeling. *Polymer Engineering & Science,* 35**,** 1290-1299.

RAY, W. H. (1972) On the mathematical modeling of polymerization reactors. *Polymer Reviews,* 8**,** 1-56.

RUDIN, A. (1999) *The elements of polymer science and engineering: an introductory text and reference for engineers and chemists,* United States of America, Academic Press.

RUSSELL, G. T., NAPPER, D. H. & GILBERT, R. G. (1988) Initiator efficiencies in high-conversion bulk polymerizations. *Macromolecules,* 21**,** 2141-2148.

SALDIVAR, E. (1996) Modeling and Control of Emulsion Copolymerization Reactors. Madison, WI, University of Wisconsin.

SALDIVAR, E. & RAY, W. H. (1997) Mathematical Modeling of Emulsion Copolymerization Reactors: Experimental Validation and Application to Complex Systems. *Industrial & Engineering Chemistry Research,* 36**,** 1322-1336.

SOOTS, C. & STANFORD, T. (1991) Modeling the polymerization process-the gel-effect function. *System Theory, 1991. Proceedings., Twenty-Third Southeastern Symposium.* Columbia, SC, USA.

SOWGATH, T. M. & MUJTABA I. M. (2007) Optimization of MSF desalination process for fixed water demand using gPROMS. *Computer Aided Chemical Engineering*, 24, 763-768.

STEVENS, M. P. (1999) *Polymer chemistry: an introduction*, Oxford University Press.

TIJL, P. (2005) Assessment of the Parameter Estimation Capabilities of gPROMS and Aspen Custom Modeler, using the Sec-butyl-Alcohol Stripper Kinetics Case Study, *Graduation Report,* Eindhoven Technical university, Amsterdam.

TULIG, T. J. & TIRRELL, M. (1981) Molecular theory of the Trommsdorff effect. *Macromolecules,* 14**,** 1501-1511.

VERROS, G. D., LATSOS, T. & ACHILIAS, D. S. (2005) Development of a unified framework for calculating molecular weight distribution in diffusion controlled free radical bulk homo-polymerization. *Polymer,* 46**,** 539-552.

WANG, J. S. & MATYJASZEWSKI, K. (1995) " Living"/Controlled Radical Polymerization. Transition-Metal-Catalyzed Atom Transfer Radical Polymerization in the Presence of a Conventional Radical Initiator. *Macromolecules,* 28**,** 7572-7573.

WINKEL, M. L., ZULLO, L. C., VERHEIJEN, P. J. T. & PANTELIDES, C.C. (1995) Modelling AND Simulation of the Operation of an industrial batch plant using gPROMS. *Computer & Chemical Engineering*, 19, 571-576.

WOLFF, E. H. P. & BOS, A. N. R. (1997) Modeling of polymer molecular weight distributions in free-radical polymerization reactions. Application to the case of polystyrene. *Industrial & Engineering Chemistry Research,* 36**,** 1163-1170.

XIA, J. & MATYJASZEWSKI, K. (1997) Controlled/"living" radical polymerization. Homogeneous reverse atom transfer radical polymerization using AIBN as the initiator. *Macromolecules,* 30**,** 7692-7696.

XUEMEI, Z., RUCHENG, L. & SHUQING, W. (2006) Implementation of Parameter Estimation in Mechanistic Models by Dynamic Optimization. *Intelligent Control and Automation, 2006. WCICA 2006. The Sixth World Congress on.*

ZEAITER, J., A. ROMAGNOLI, J., W. BARTON, G., G. GOMES, V., S. HAWKETT, B. & G. GILBERT, R. (2002) Operation of semi-batch emulsion polymerisation reactors: Modelling, validation and effect of operating conditions. *Chemical Engineering Science,* 57**,** 2955-2969.

ZHOU, X.-G. & YUAN, W.-K. (2004) Control Vector Parameterization with Karhunen-Loeve Expansion. *Industrial & Engineering Chemistry Research,* 43**,** 127-135.

APPENDICES

APPENDIX 1

Optimal profile for case study 1

Case study 1A: Run 1

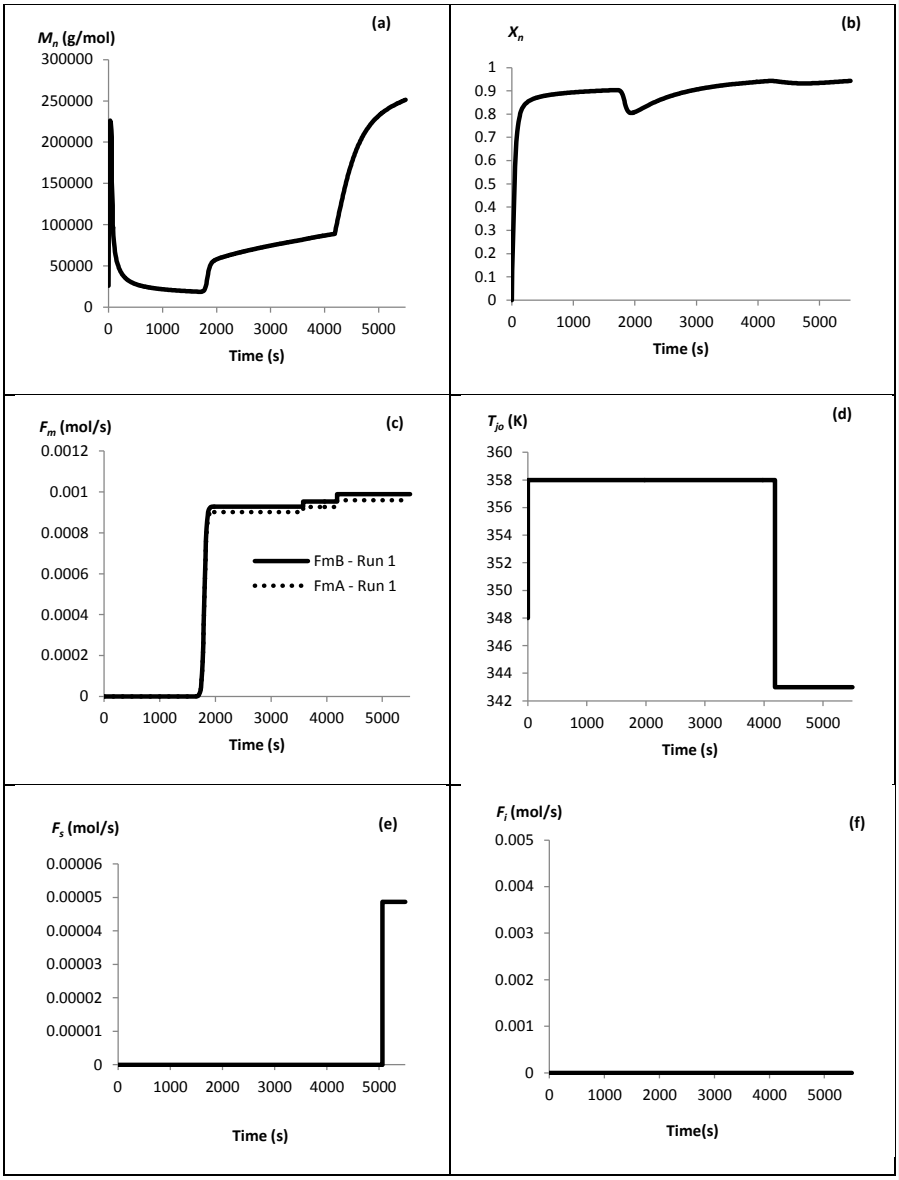

Figure 12: Case study 1 (Run 1); Optimization result (a) number average molecular weight (M_n); (b) overall conversion (X_n); (c) optimal profile of monomer flow rate [F_{mA} - styrene; F_{mB} - MMA]; (d) optimal profile of jacket temperature T_{j0}; (e) optimal profile of surfactant flow rate (F_S); (f) optimal profile of initiator flow rate (F_I)

Case study 1: Run 2

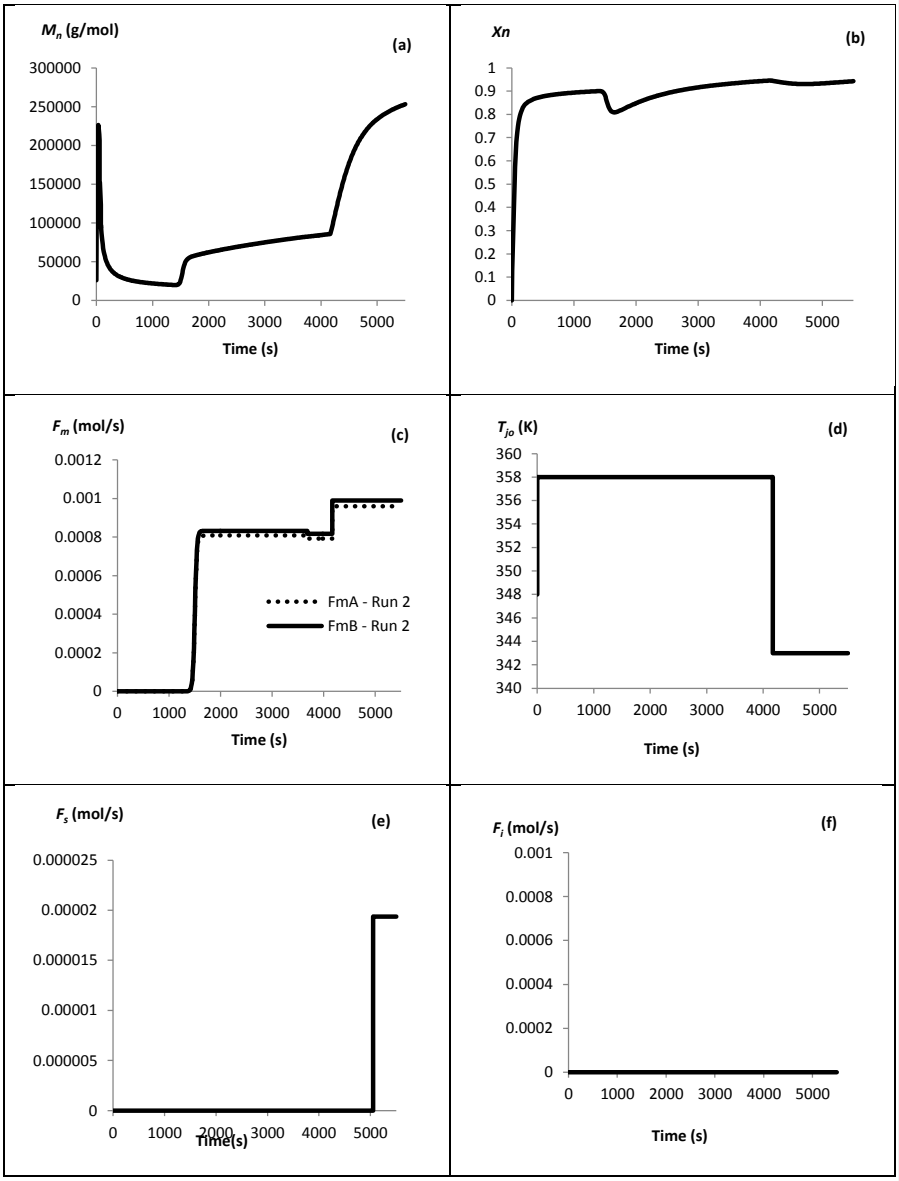

Figure 2: Case study 1 (Run 2); Optimization result (a) number average molecular weight (M_n); (b) overall conversion (X_n); (c) optimal profile of monomer flow rate [F_{mA} - styrene; F_{mB} - MMA]; (d) optimal profile of jacket temperature T_{j0}; (e) optimal profile of surfactant flow rate (F_S); (f) optimal profile of initiator flow rate (F_I)

Case study 1: run 3

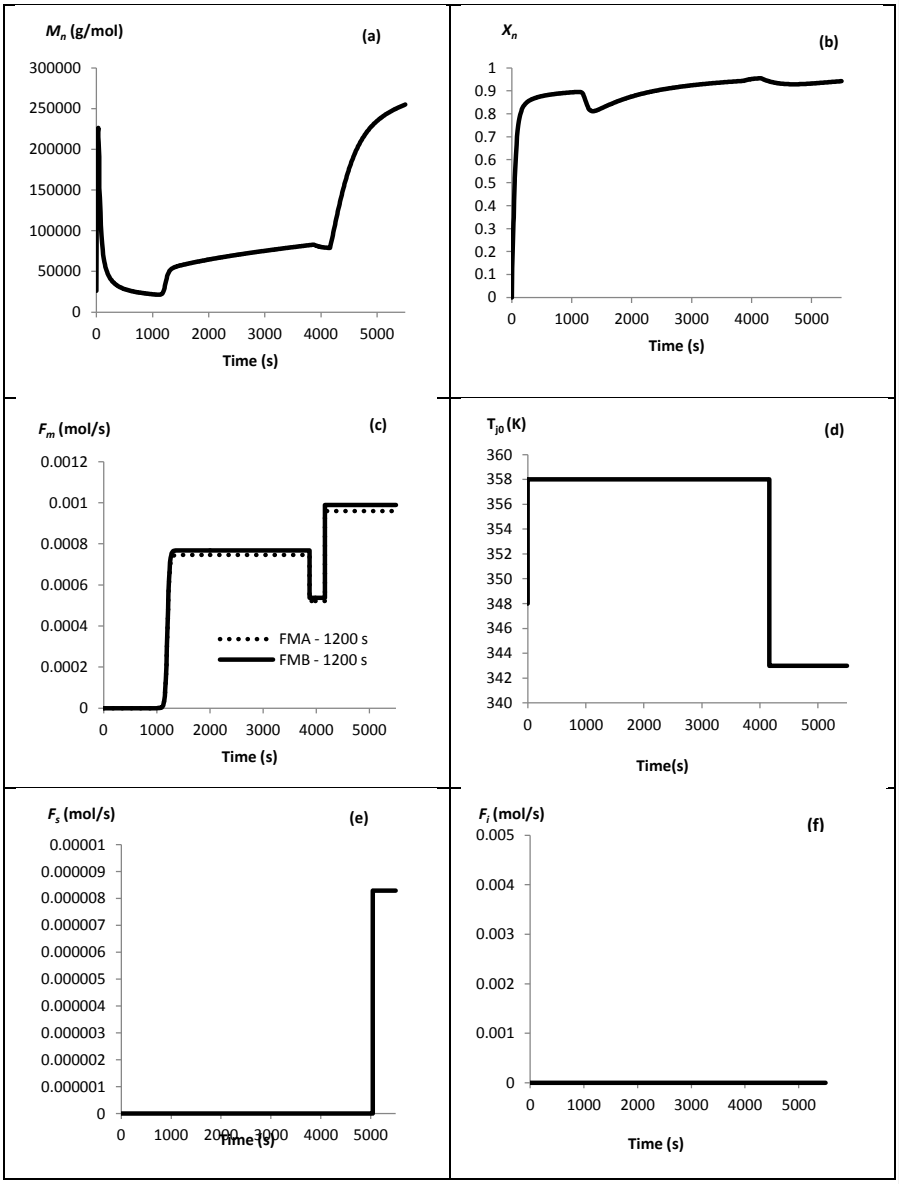

Figure 3: Case study 1 (Run 3); Optimization result (a) number average molecular weight (M_n); (b) overall conversion (X_n); (c) optimal profile of monomer flow rate [F_{mA} - styrene; F_{mB} - MMA]; (d) optimal profile of jacket temperature T_{j0}; (e) optimal profile of surfactant flow rate (F_S); (f) optimal profile of initiator flow rate (F_I)

Case study 1: run 4

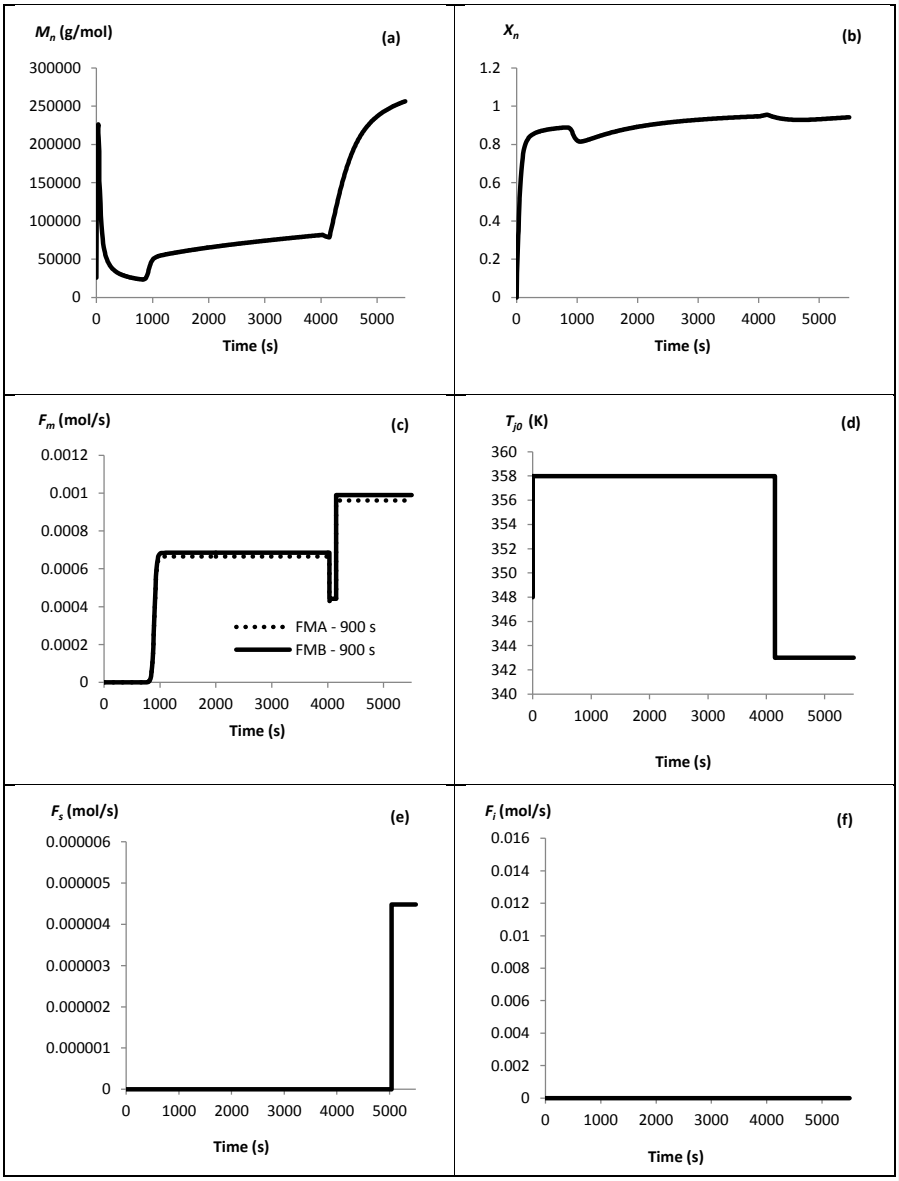

Figure 4: Case study 1 (Run 4); Optimization result (a) number average molecular weight (M_n); (b) overall conversion (X_n); (c) optimal profile of monomer flow rate [F_{mA} - styrene; F_{mB} - MMA]; (d) optimal profile of jacket temperature T_{j0}; (e) optimal profile of surfactant flow rate (F_S); (f) optimal profile of initiator flow rate (F_I)

Case study 1: run 5

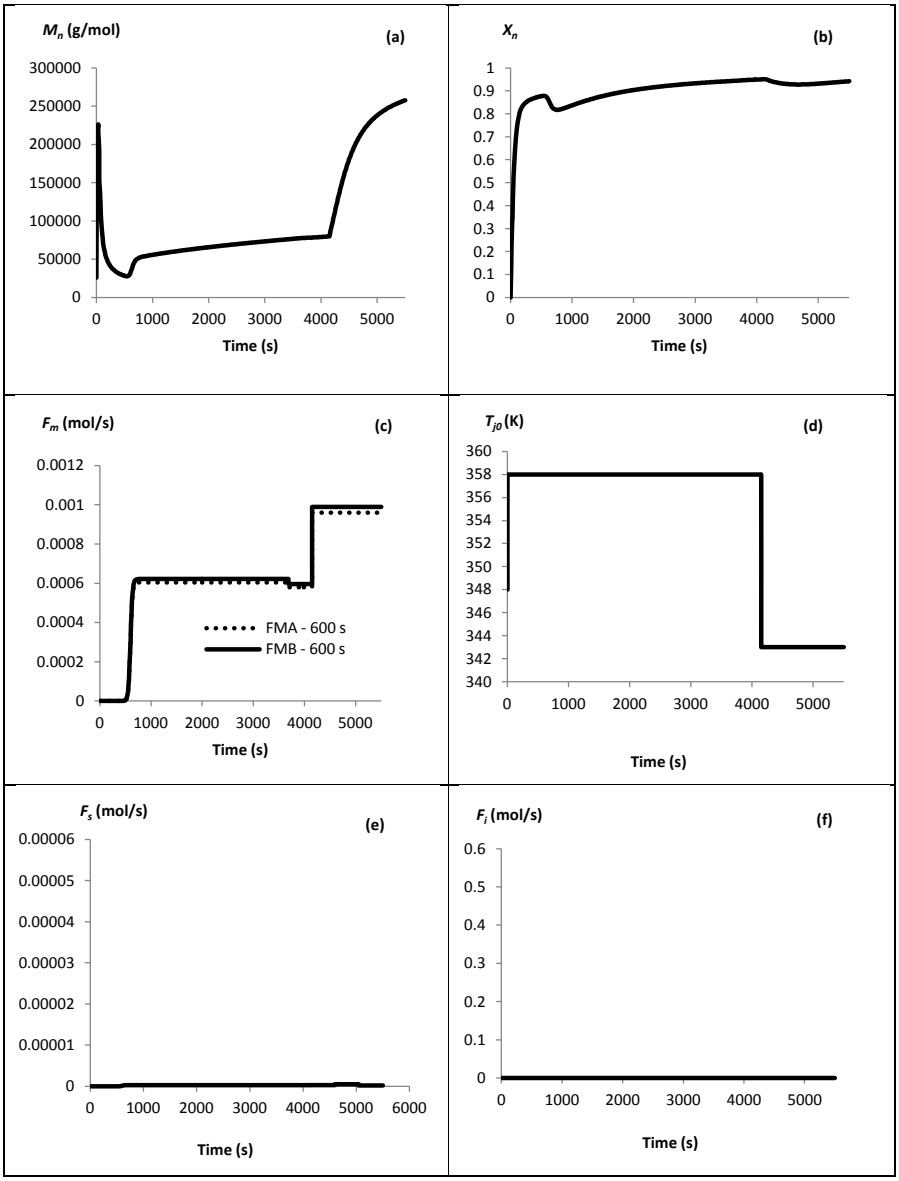

Figure 5: Case study 1 (Run 5); Optimization result (a) number average molecular weight (M_n); (b) overall conversion (X_n); (c) optimal profile of monomer flow rate [F_{mA} - styrene; F_{mB} - MMA]; (d) optimal profile of jacket temperature T_{j0}; (e) optimal profile of surfactant flow rate (F_S); (f) optimal profile of initiator flow rate (F_I)

Case study 1 : run 6

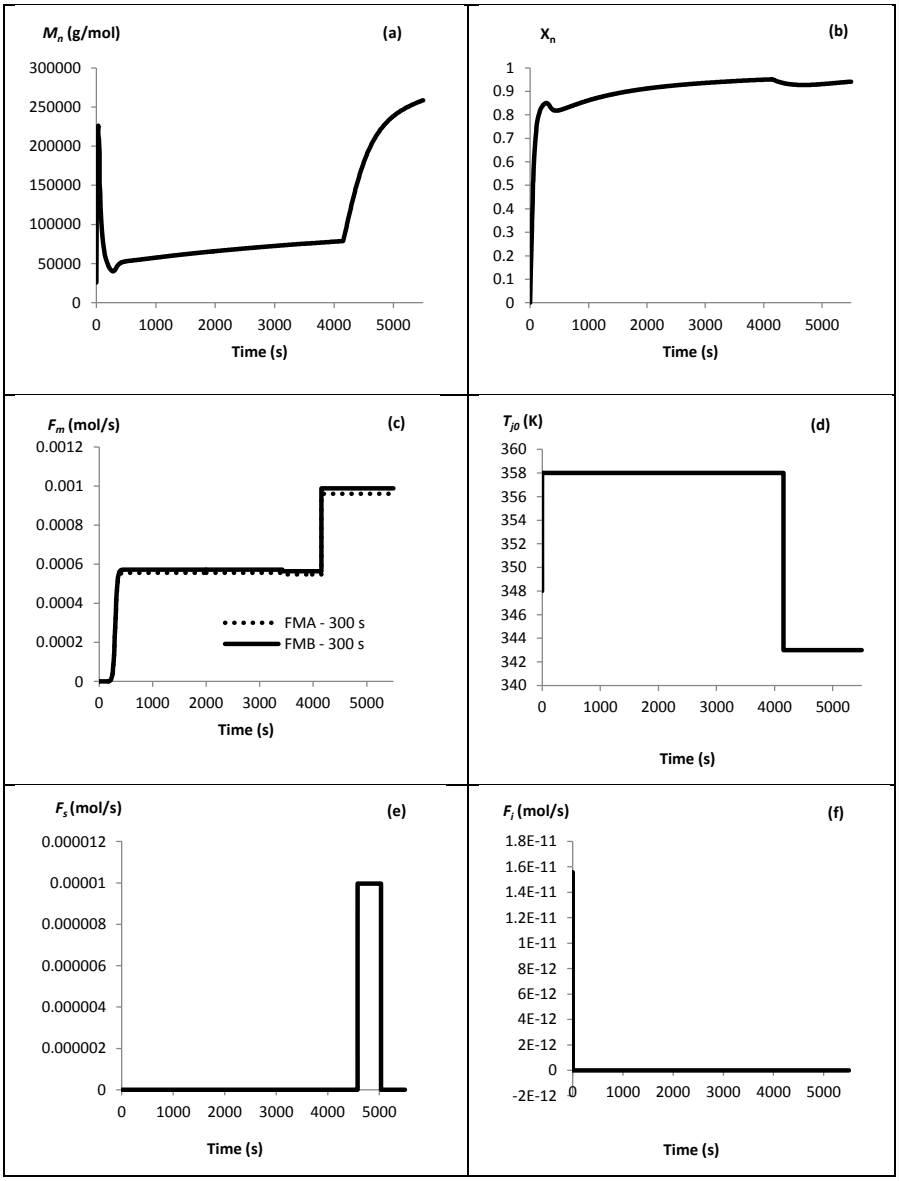

Figure 6: Case study 1 (Run 6); Optimization result (a) number average molecular weight (M_n); (b) overall conversion (X_n); (c) optimal profile of monomer flow rate [F_{mA} - styrene; F_{mB} - MMA]; (d) optimal profile of jacket temperature T_{j0}; (e) optimal profile of surfactant flow rate (F_S); (f) optimal profile of initiator flow rate (F_I)

Case study 1: run 7

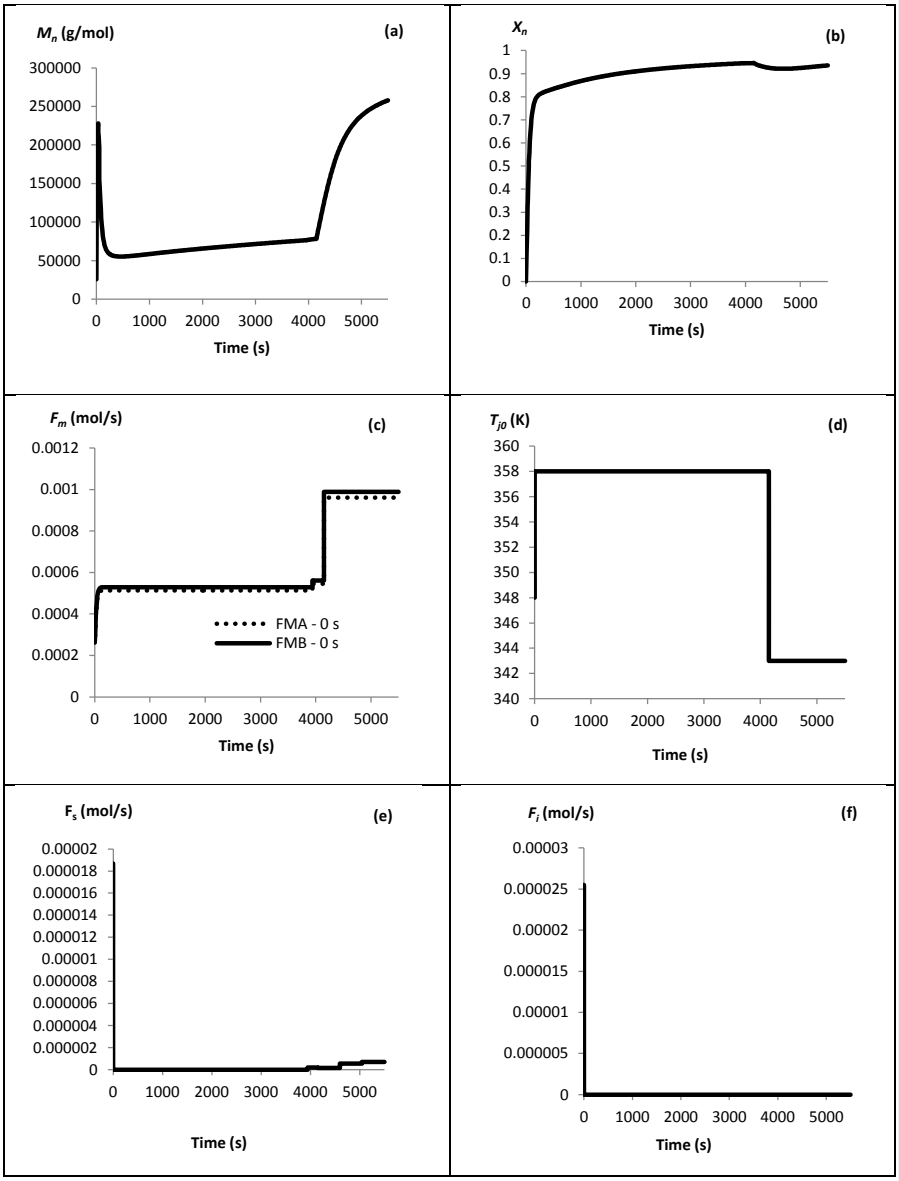

Figure 7: Case study 1 (Run 7); Optimization result (a) number average molecular weight (M_n); (b) overall conversion (X_n); (c) optimal profile of monomer flow rate [F_{mA} - styrene; F_{mB} - MMA]; (d) optimal profile of jacket temperature T_{j0}; (e) optimal profile of surfactant flow rate (F_S); (f) optimal profile of initiator flow rate (F_I)

APPENDIX 2

Optimal profile for case study 2

Case study 2: run 1

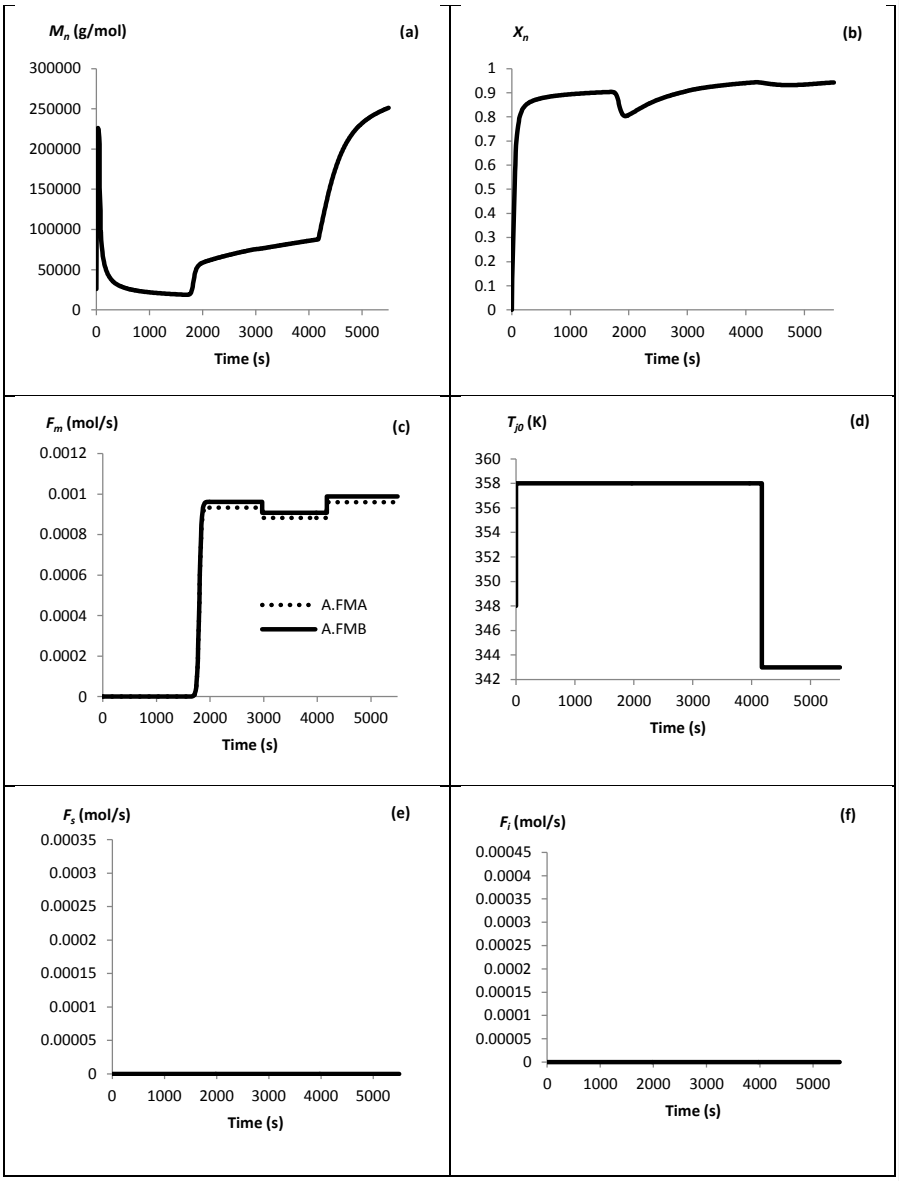

Figure 8: Case study 2 (Run 1); Optimization result (a) number average molecular weight (M_n); (b) overall conversion (X_n); (c) optimal profile of monomer flow rate [F_{mA} - styrene; F_{mB} - MMA]; (d) optimal profile of jacket temperature T_{j0}; (e) optimal profile of surfactant flow rate (F_S); (f) optimal profile of initiator flow rate (F_I)

Case study 2: run 2

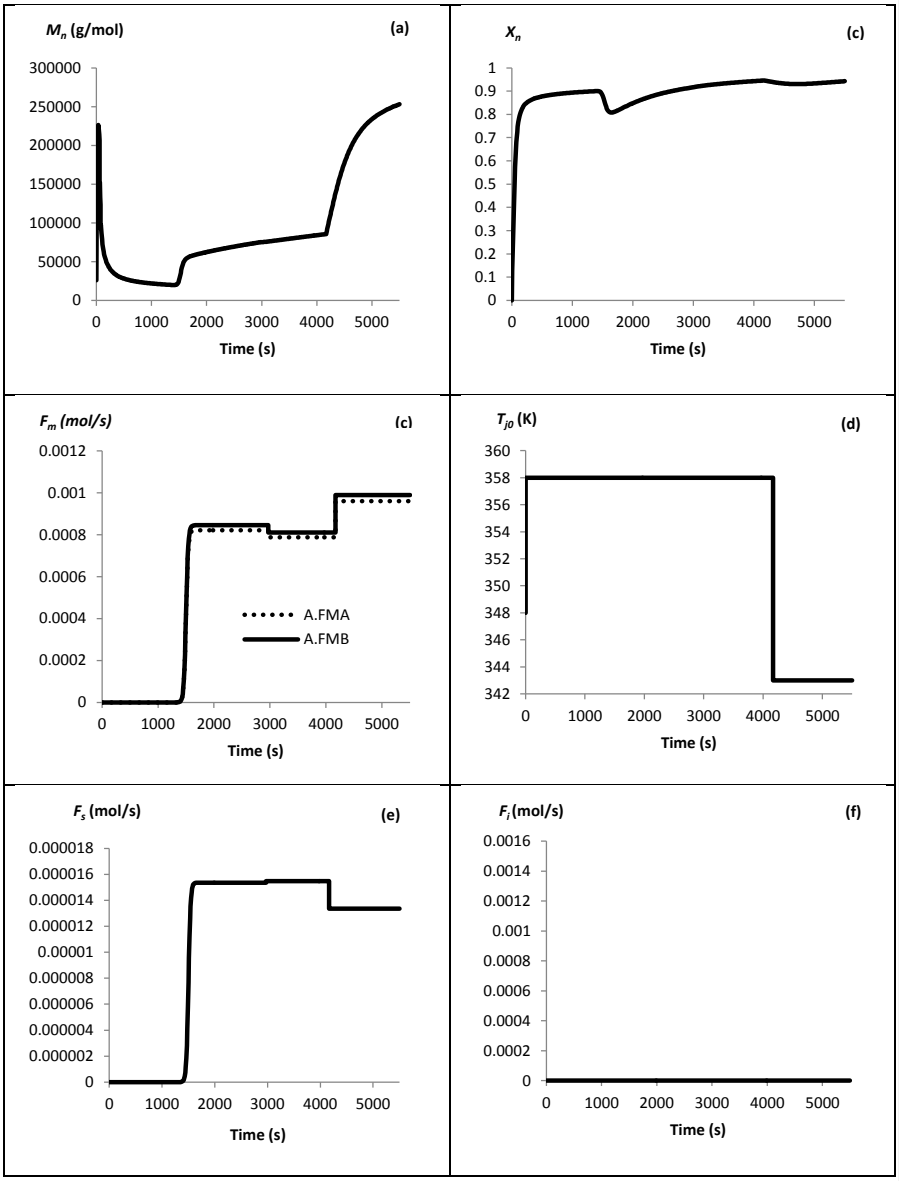

Figure 9: Case study 2 (Run 2); Optimization result (a) number average molecular weight (M_n); (b) overall conversion (X_n); (c) optimal profile of monomer flow rate [F_{mA} - styrene; F_{mB} - MMA]; (d) optimal profile of jacket temperature T_{j0}; (e) optimal profile of surfactant flow rate (F_S); (f) optimal profile of initiator flow rate (F_I)

Case study 2: run 3

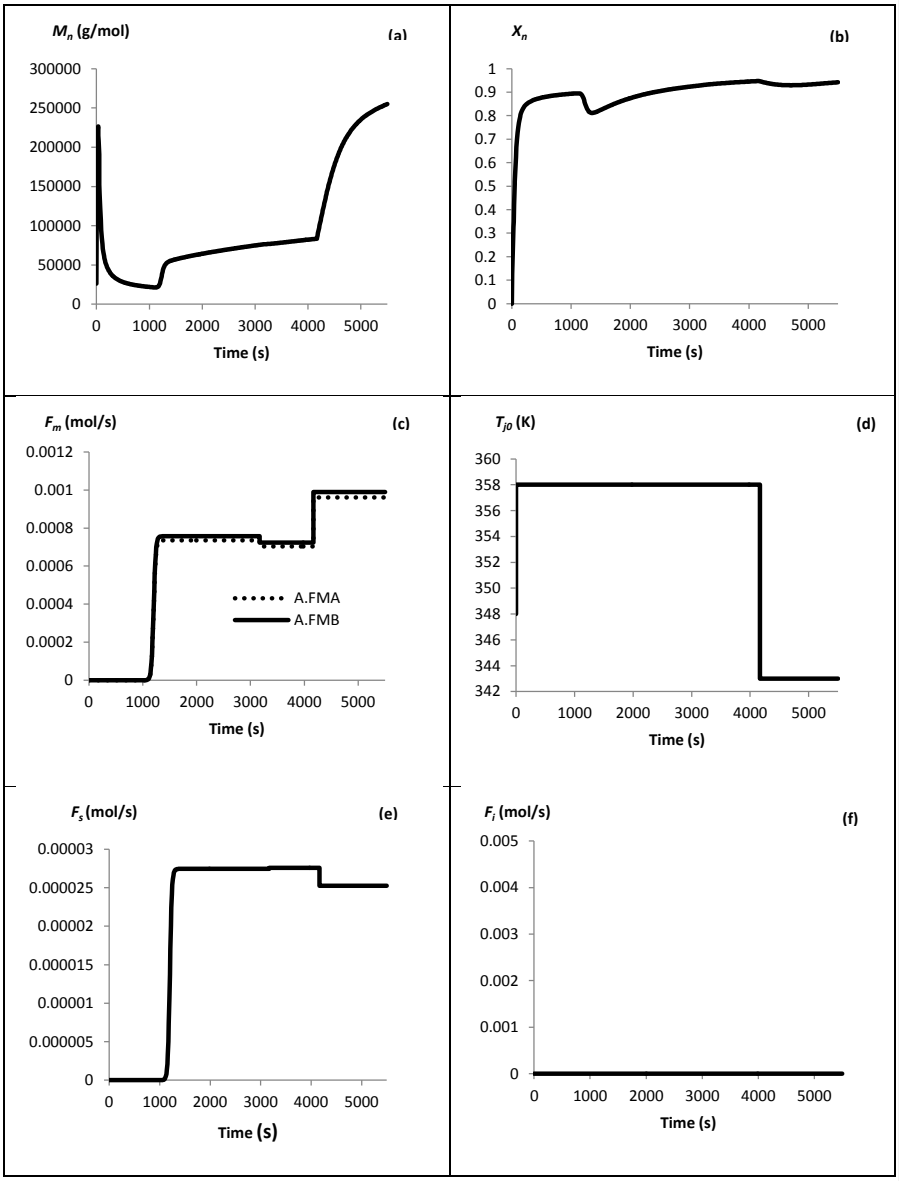

Figure 130: Case study 2 (Run 3); Optimization result (a) number average molecular weight (M_n); (b) overall conversion (X_n); (c) optimal profile of monomer flow rate [F_{mA} - styrene; F_{mB} - MMA]; (d) optimal profile of jacket temperature T_{j0}; (e) optimal profile of surfactant flow rate (F_S); (f) optimal profile of initiator flow rate (F_I)

Case study 2: run 4

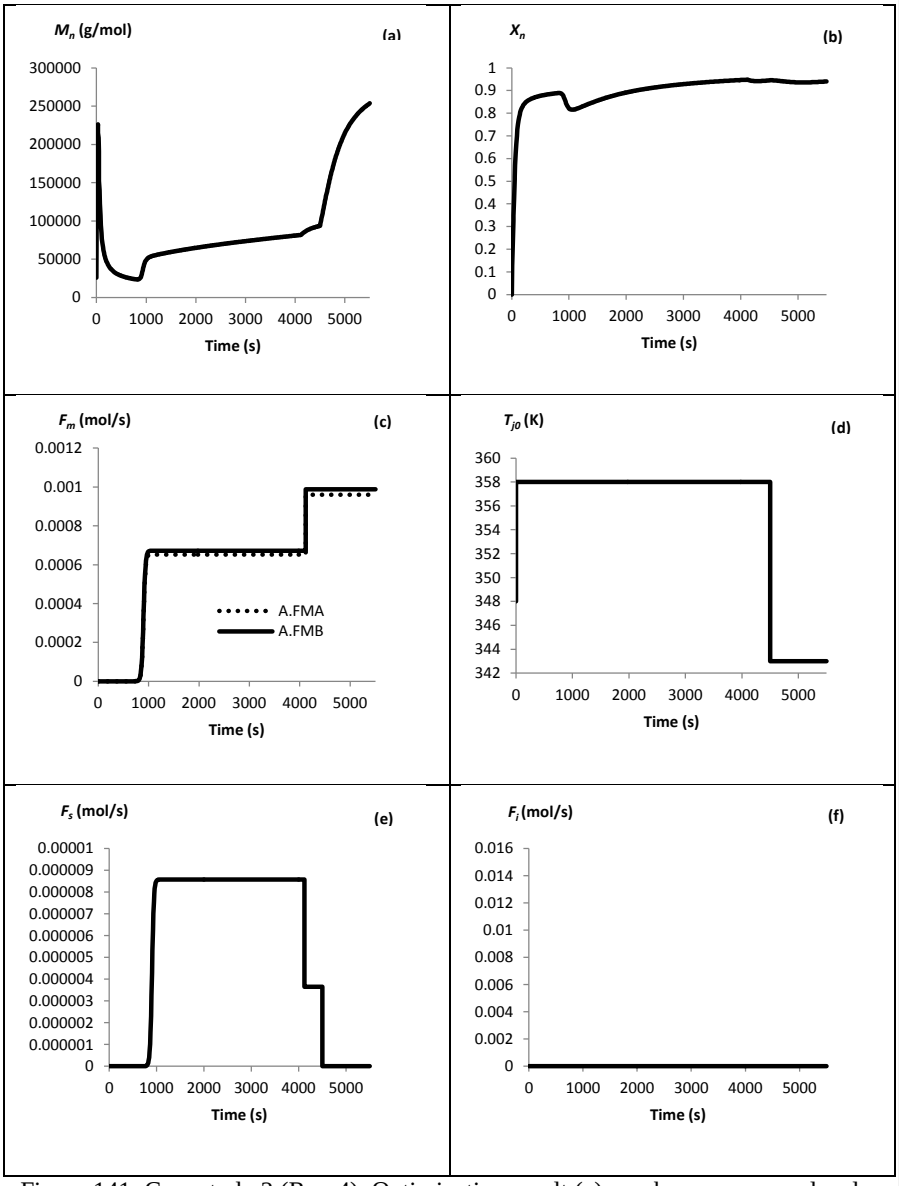

Figure 141: Case study 2 (Run 4); Optimization result (a) number average molecular weight (M_n); (b) overall conversion (X_n); (c) optimal profile of monomer flow rate [F_{mA} - styrene; F_{mB} - MMA]; (d) optimal profile of jacket temperature T_{j0}; (e) optimal profile of surfactant flow rate (F_S); (f) optimal profile of initiator flow rate (F_I)

Case study 2: run 5

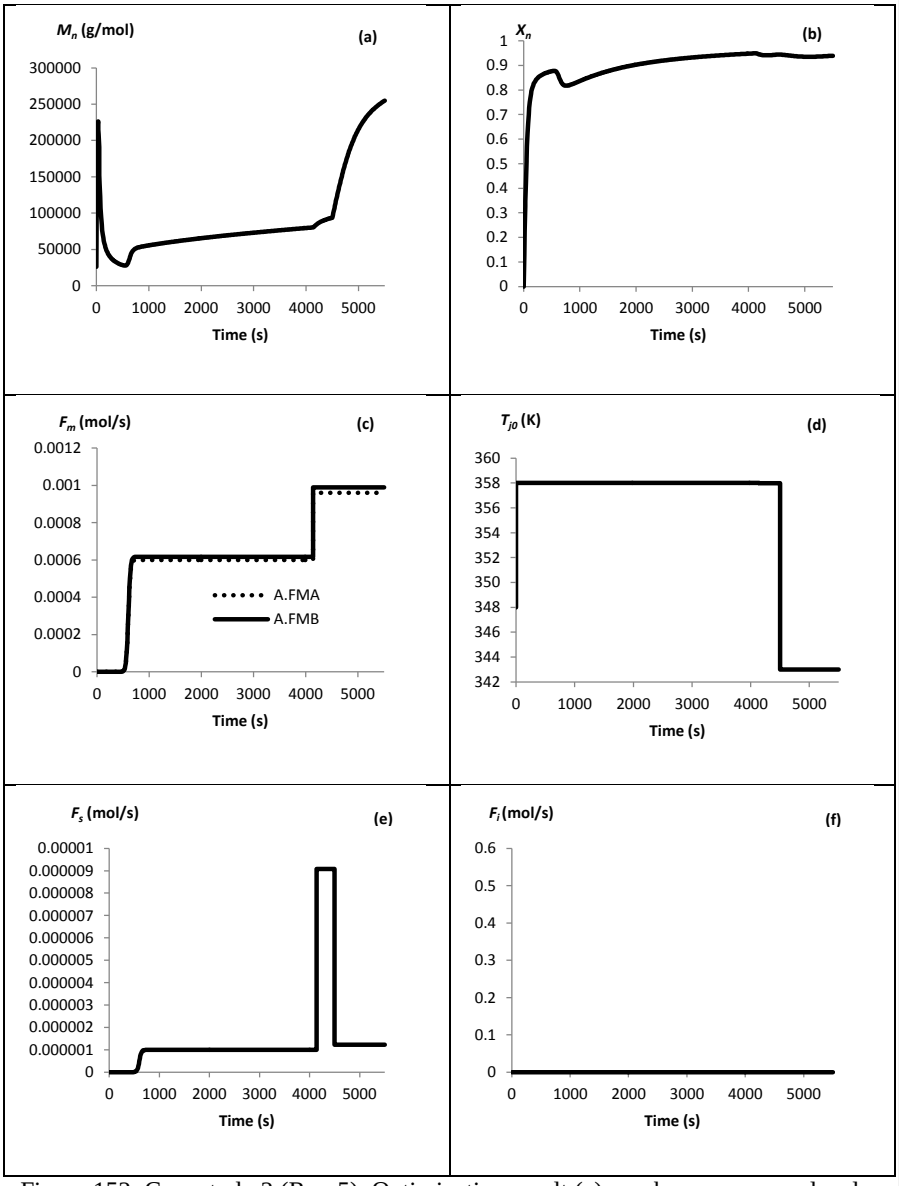

Figure 152: Case study 2 (Run 5); Optimization result (a) number average molecular weight (M_n); (b) overall conversion (X_n); (c) optimal profile of monomer flow rate [F_{mA} - styrene; F_{mB} - MMA]; (d) optimal profile of jacket temperature T_{j0}; (e) optimal profile of surfactant flow rate (F_S); (f) optimal profile of initiator flow rate (F_I)

APPENDIX 3

Optimal profile for case study 3

Case study 3: run 1

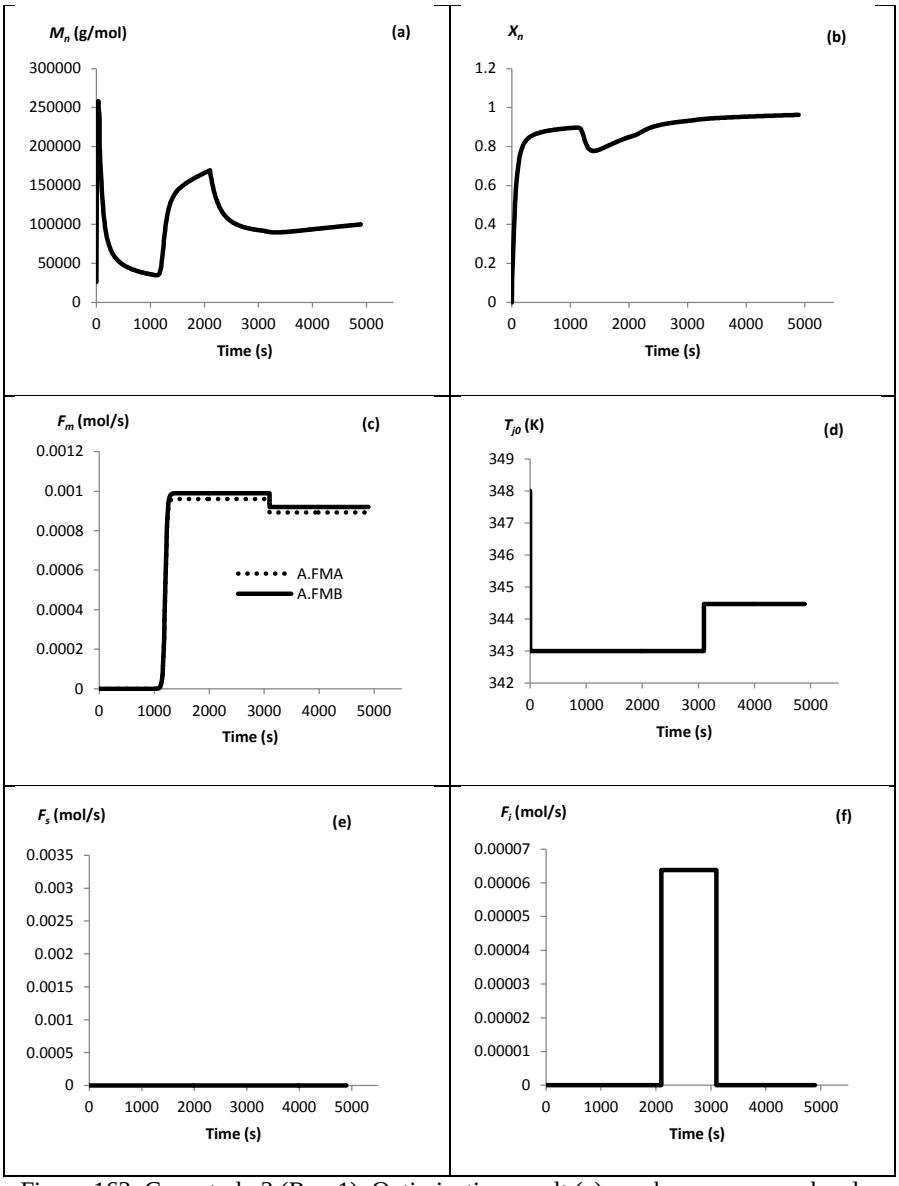

Figure 163: Case study 3 (Run 1); Optimization result (a) number average molecular weight (M_n); (b) overall conversion (X_n); (c) optimal profile of monomer flow rate [F_{mA} - styrene; F_{mB} - MMA]; (d) optimal profile of jacket temperature T_{j0}; (e) optimal profile of surfactant flow rate (F_S); (f) optimal profile of initiator flow rate (F_I)

Case study 3: run 2

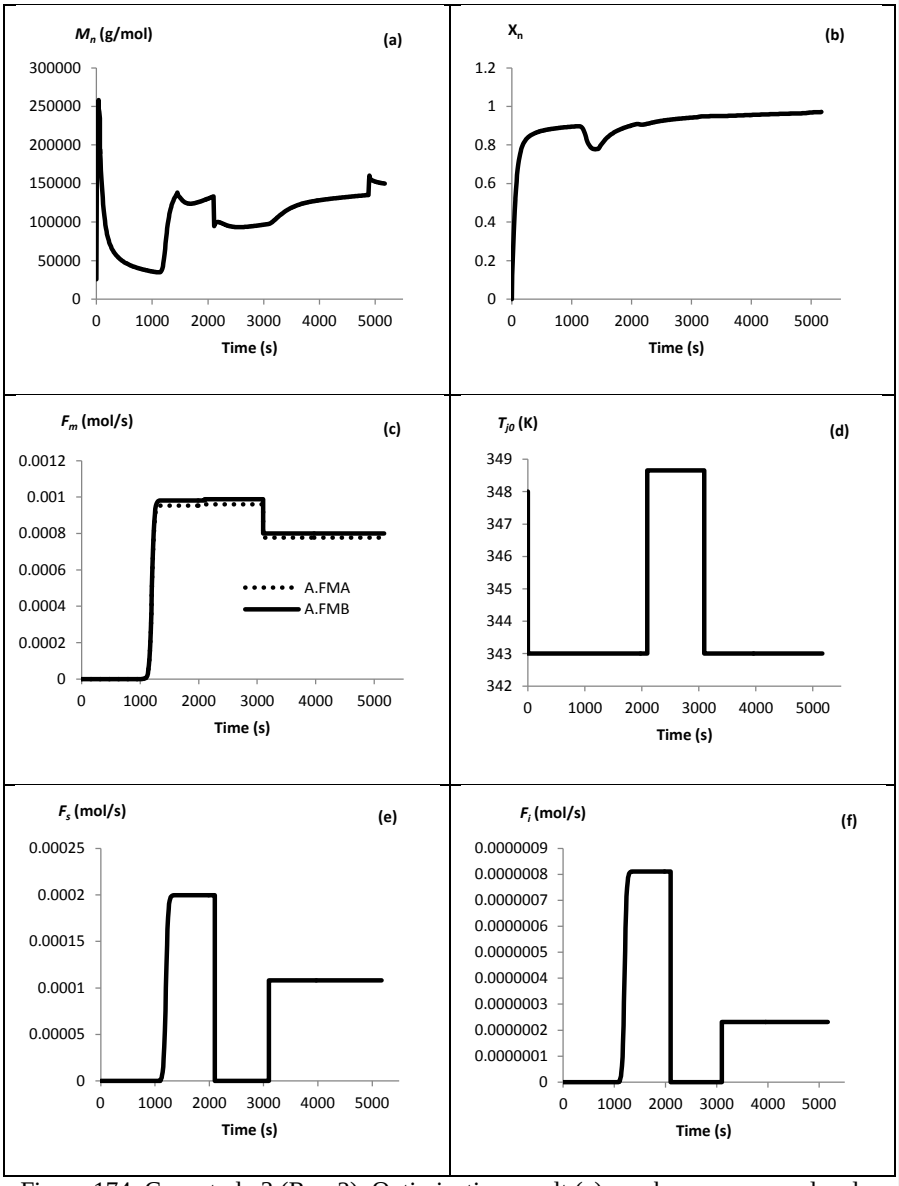

Figure 174: Case study 3 (Run 2); Optimization result (a) number average molecular weight (M_n); (b) overall conversion (X_n); (c) optimal profile of monomer flow rate [F_{mA} - styrene; F_{mB} - MMA]; (d) optimal profile of jacket temperature T_{j0}; (e) optimal profile of surfactant flow rate (F_S); (f) optimal profile of initiator flow rate (F_I)

Case study 3: run 3

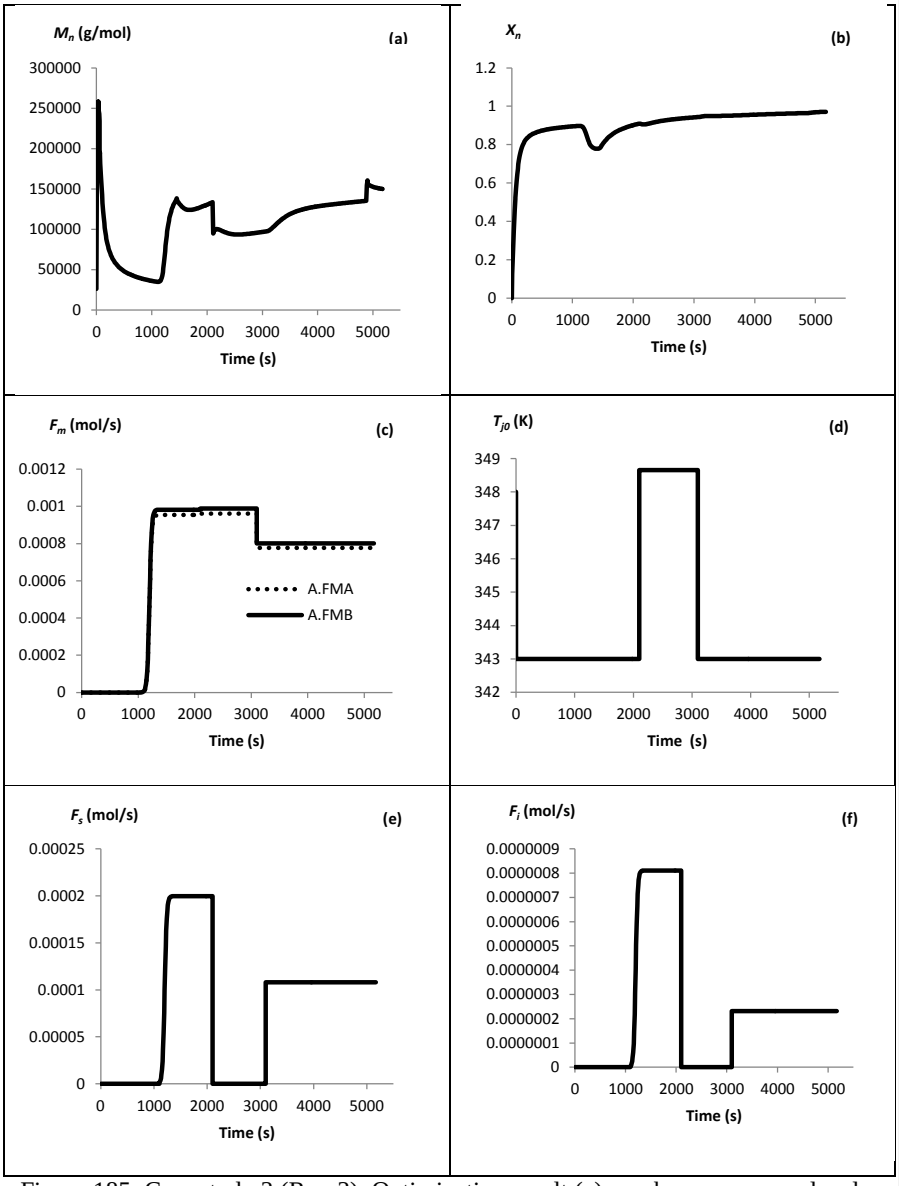

Figure 185: Case study 3 (Run 3); Optimization result (a) number average molecular weight (M_n); (b) overall conversion (X_n); (c) optimal profile of monomer flow rate [F_{mA} - styrene; F_{mB} - MMA]; (d) optimal profile of jacket temperature T_{j0}; (e) optimal profile of surfactant flow rate (F_S); (f) optimal profile of initiator flow rate (F_I)

APPENDIX 4

Optimal profile for case study 4

Case study 4: run 1

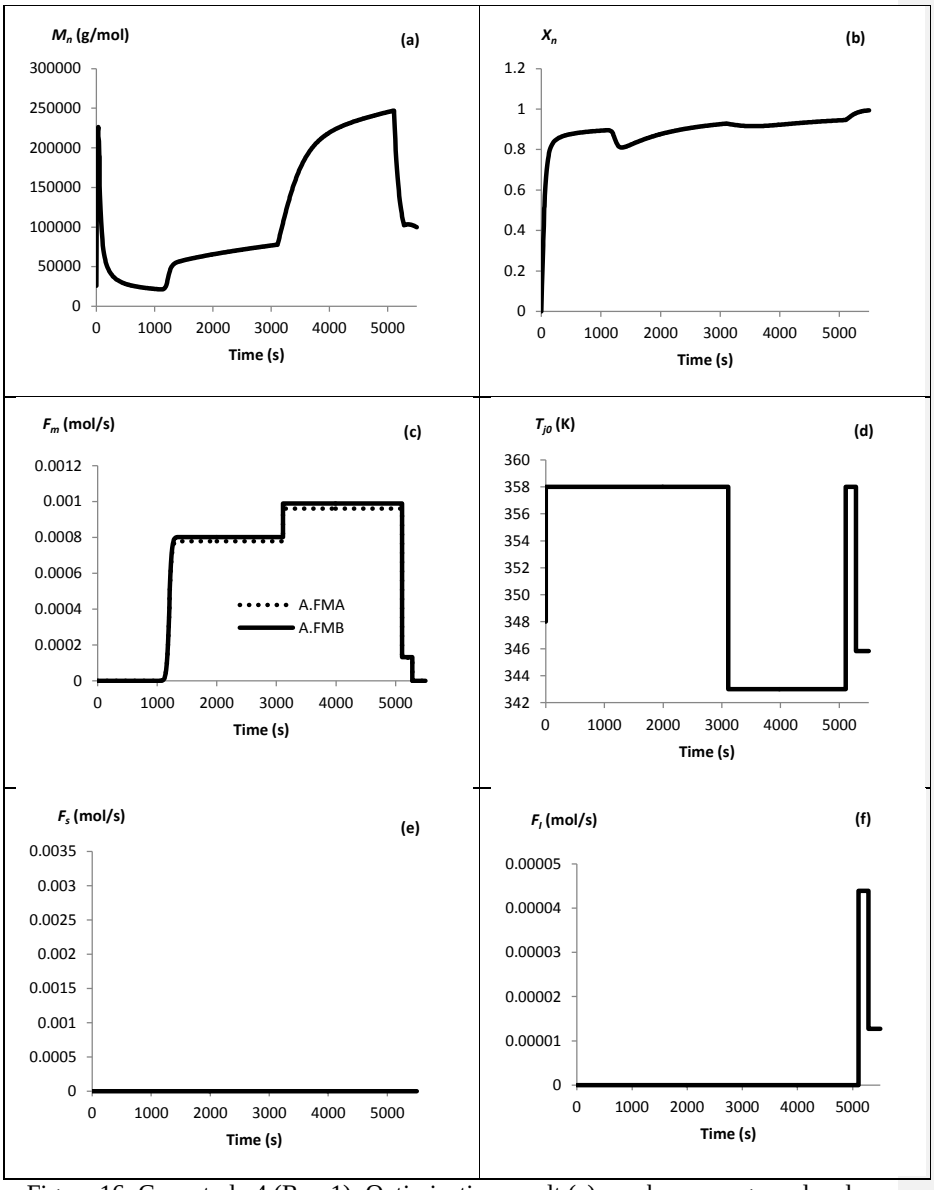

Figure 16: Case study 4 (Run 1); Optimization result (a) number average molecular weight (M_n); (b) overall conversion (X_n); (c) optimal profile of monomer flow rate [F_{mA} - styrene; F_{mB} - MMA]; (d) optimal profile of jacket temperature T_{j0}; (e) optimal profile of surfactant flow rate (F_S); (f) optimal profile of initiator flow rate (F_I)

Case study 4: run 2

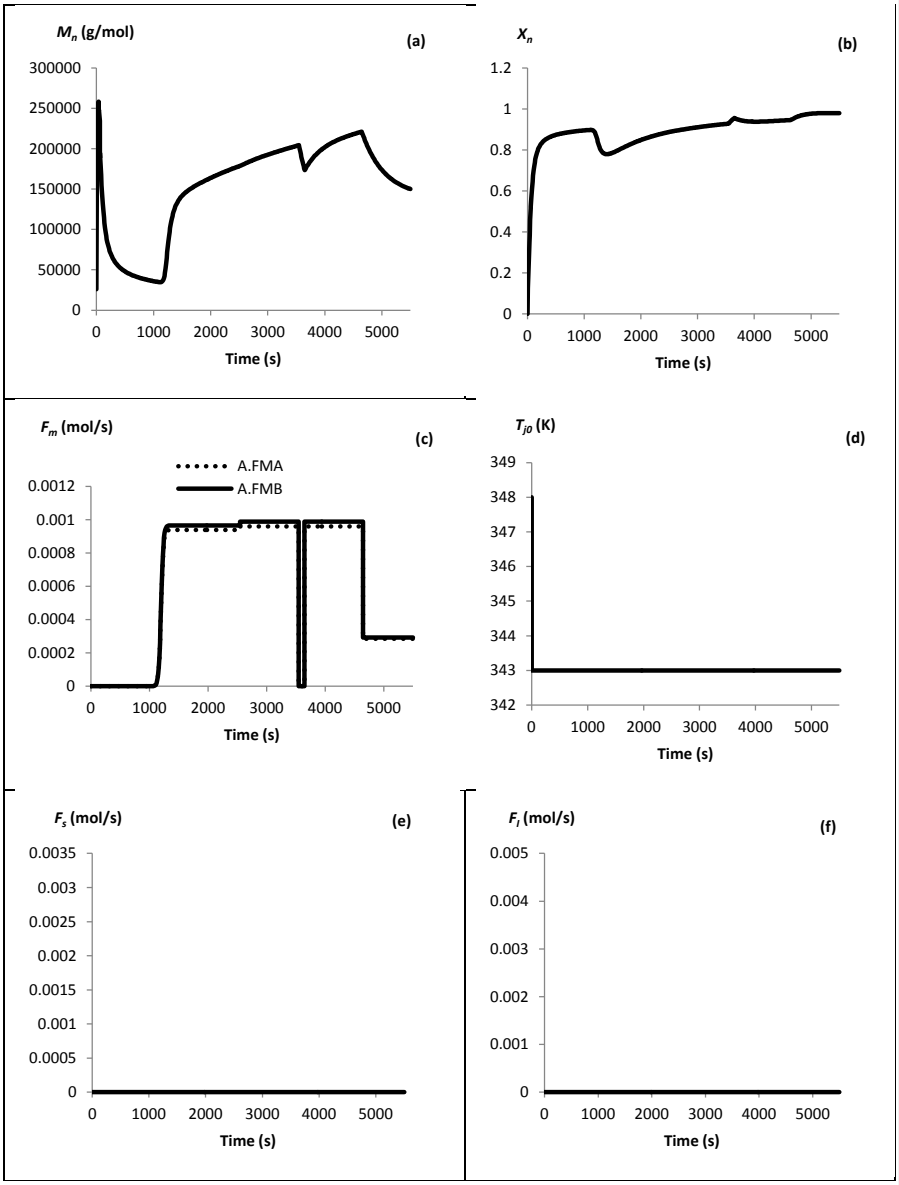

Figure 17: Case study 4 (Run 2); Optimization result (a) number average molecular weight (M_n); (b) overall conversion (X_n); (c) optimal profile of monomer flow rate [F_{mA} - styrene; F_{mB} - MMA]; (d) optimal profile of jacket temperature T_{j0}; (e) optimal profile of surfactant flow rate (F_S); (f) optimal profile of initiator flow rate (F_I)

Case study 4: run 3

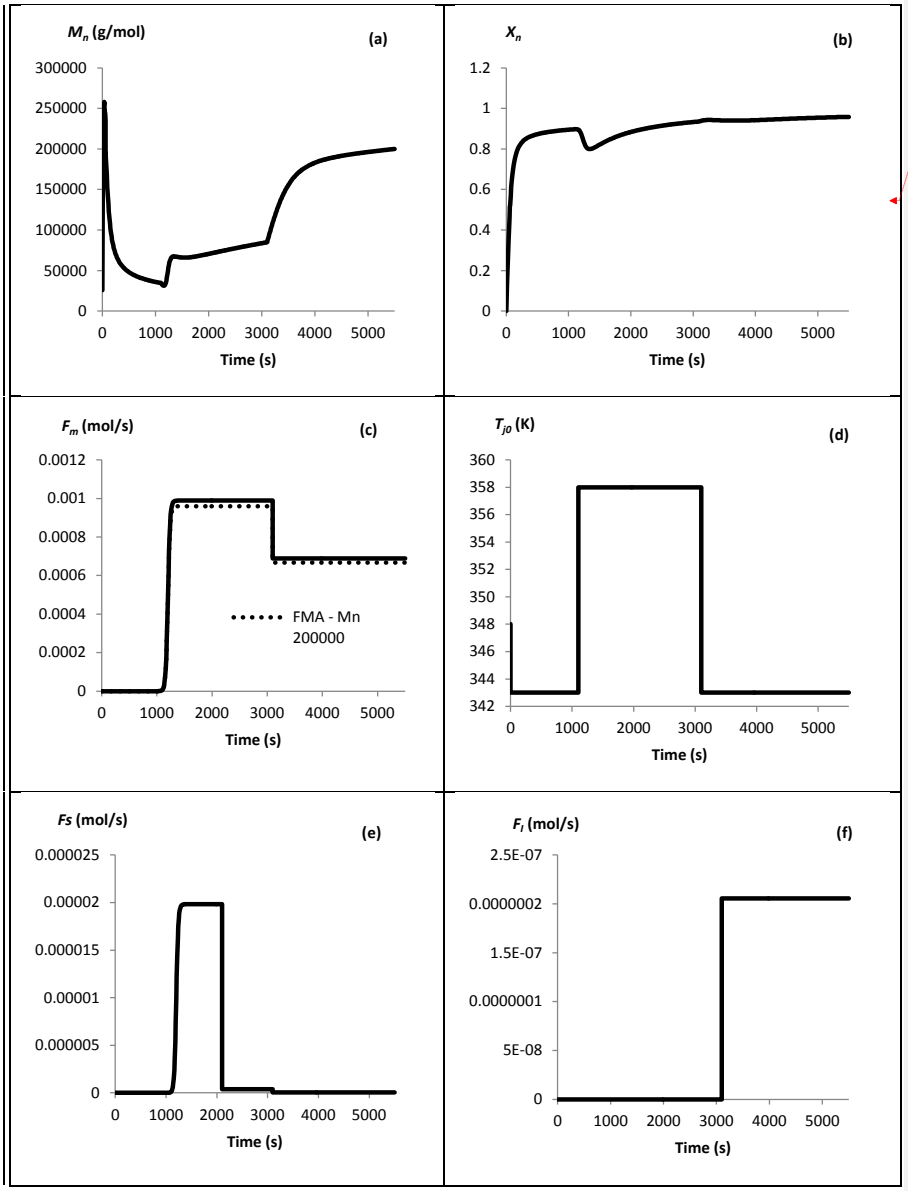

Figure 18: Case study 4 (Run 3); Optimization result (a) number average molecular weight (M_n); (b) overall conversion (X_n); (c) optimal profile of monomer flow rate [F_{mA} - styrene; F_{mB} - MMA]; (d) optimal profile of jacket temperature T_{j0}; (e) optimal profile of surfactant flow rate (F_S); (f) optimal profile of initiator flow rate (F_I)

Formatted Table

APPENDIX 5

Optimal profile for case study 5

Case study 5: run 2

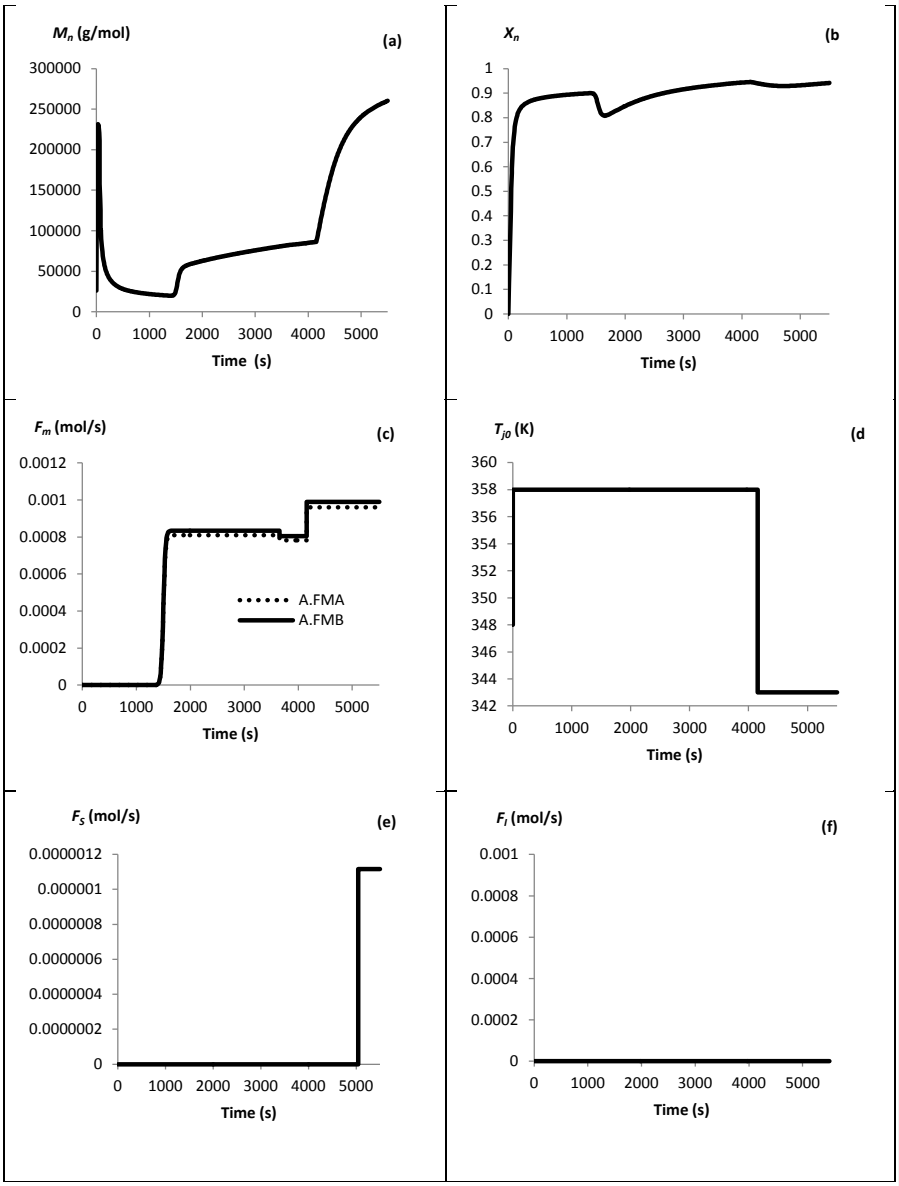

Figure 19: Case study 5 (Run 2); Optimization result (a) number average molecular weight (M_n); (b) overall conversion (X_n); (c) optimal profile of monomer flow rate [F_{mA} - styrene; F_{mB} - MMA]; (d) optimal profile of jacket temperature T_{j0}; (e) optimal profile of surfactant flow rate (F_S); (f) optimal profile of initiator flow rate (F_I)

Case study 5: run 3

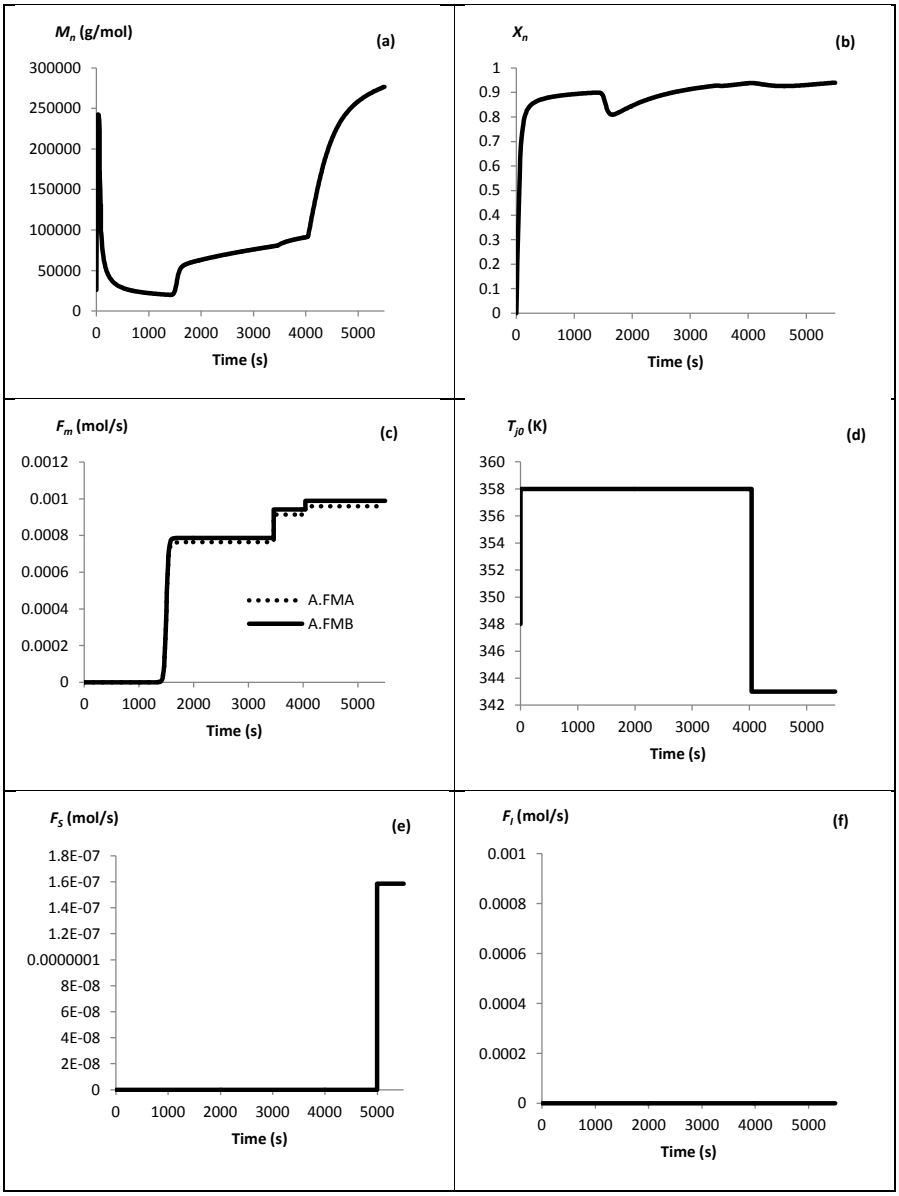

Figure 20: Case study 5 (Run 3); Optimization result (a) number average molecular weight (M_n); (b) overall conversion (X_n); (c) optimal profile of monomer flow rate [F_{mA} - styrene; F_{mB} - MMA]; (d) optimal profile of jacket temperature T_{j0}; (e) optimal profile of surfactant flow rate (F_S); (f) optimal profile of initiator flow rate (F_I)

Case study 5: run 4

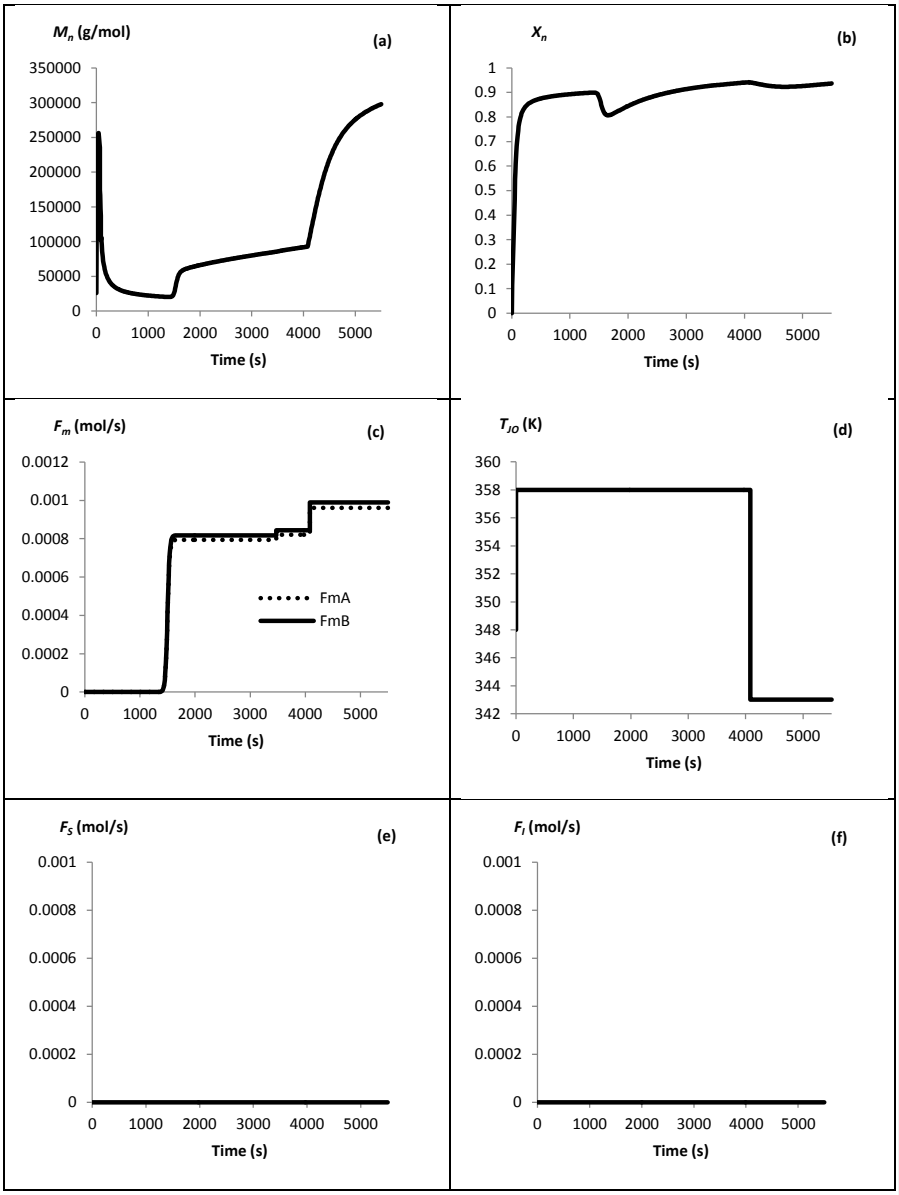

Figure 21: Case study 5 (Run 4); Optimization result (a) number average molecular weight (M_n); (b) overall conversion (X_n); (c) optimal profile of monomer flow rate [F_{mA} - styrene; F_{mB} - MMA]; (d) optimal profile of jacket temperature T_{j0}; (e) optimal profile of surfactant flow rate (F_S); (f) optimal profile of initiator flow rate (F_I)

Case study 5: run 5

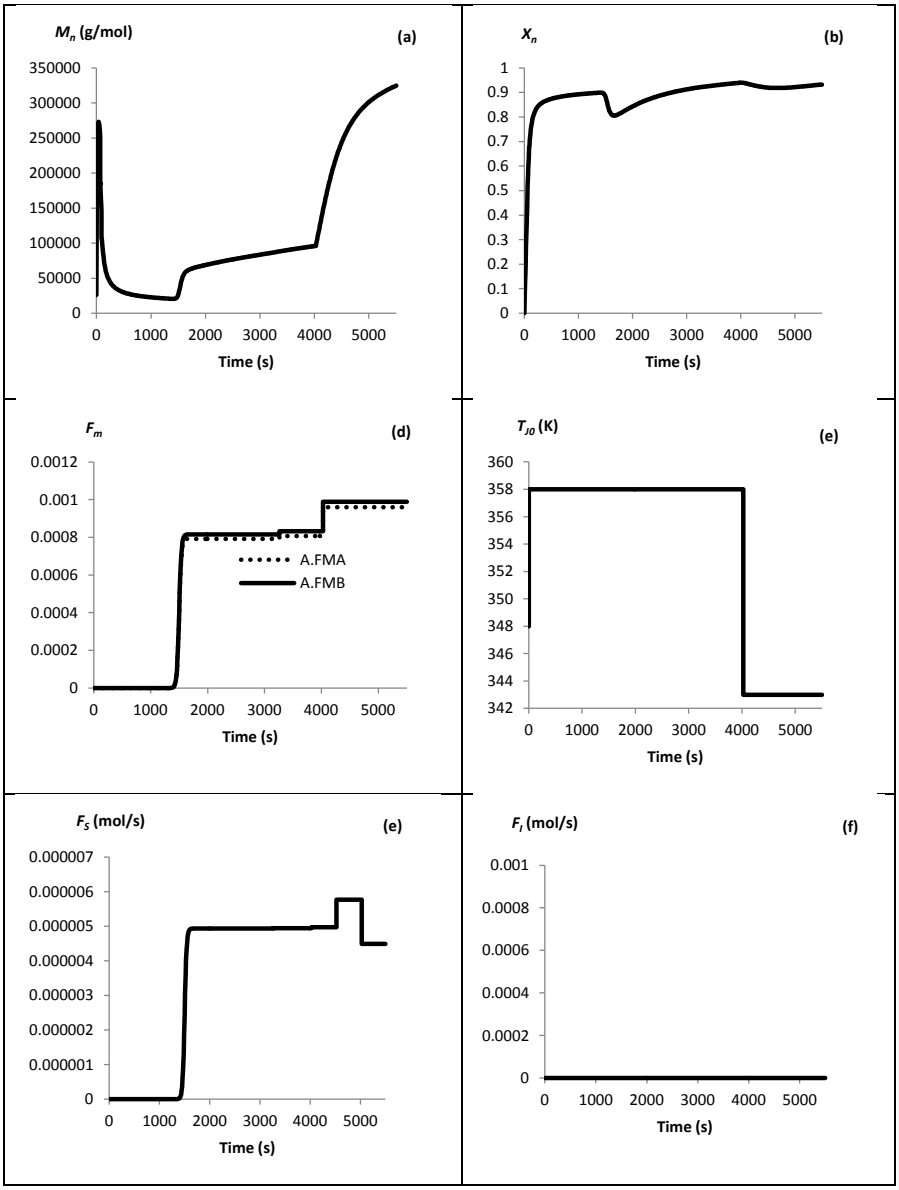

Figure 192: Case study 5 (Run 5); Optimization result (a) number average molecular weight (M_n); (b) overall conversion (X_n); (c) optimal profile of monomer flow rate [F_{mA} - styrene; F_{mB} - MMA]; (d) optimal profile of jacket temperature T_{j0}; (e) optimal profile of surfactant flow rate (F_S); (f) optimal profile of initiator flow rate (F_I)

APPENDIX 6

Optimal profile for case study 7

Case study 7: run 1

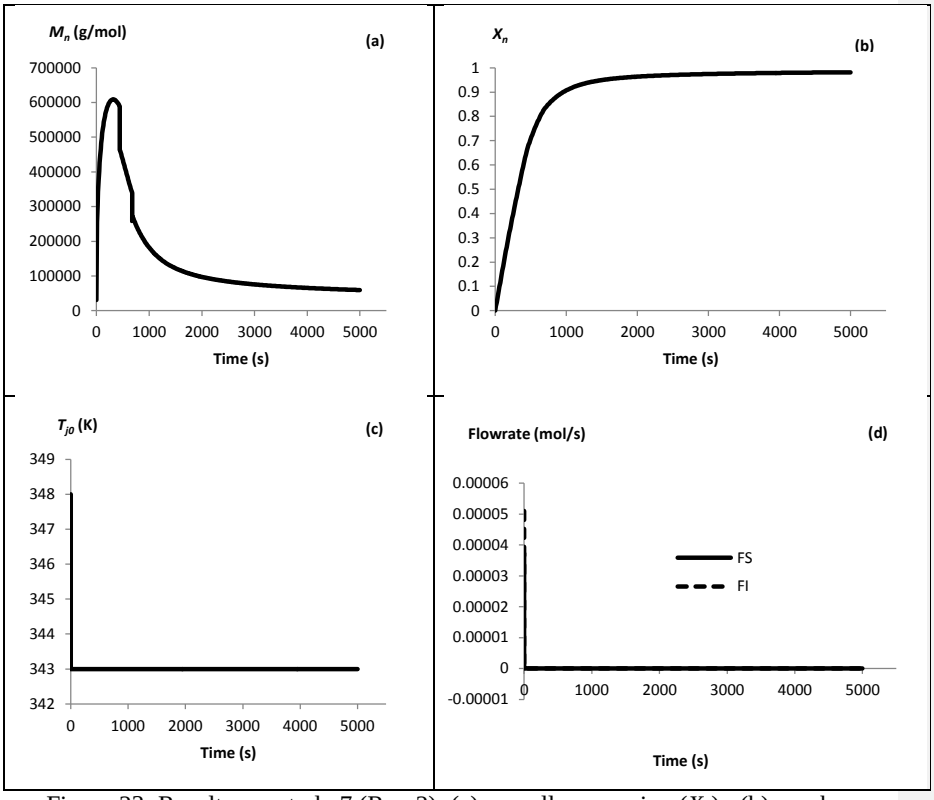

Figure 23: Result case study 7 (Run 2); (a) overall conversion (X_n); (b) number average molecular weight (M_n); (c) jacket temperature (T_{j0}); (d) optimal profile of surfactant flow rate (F_S) and optimal profile of initiator flow rate (F_I).

Case study 7: run 2

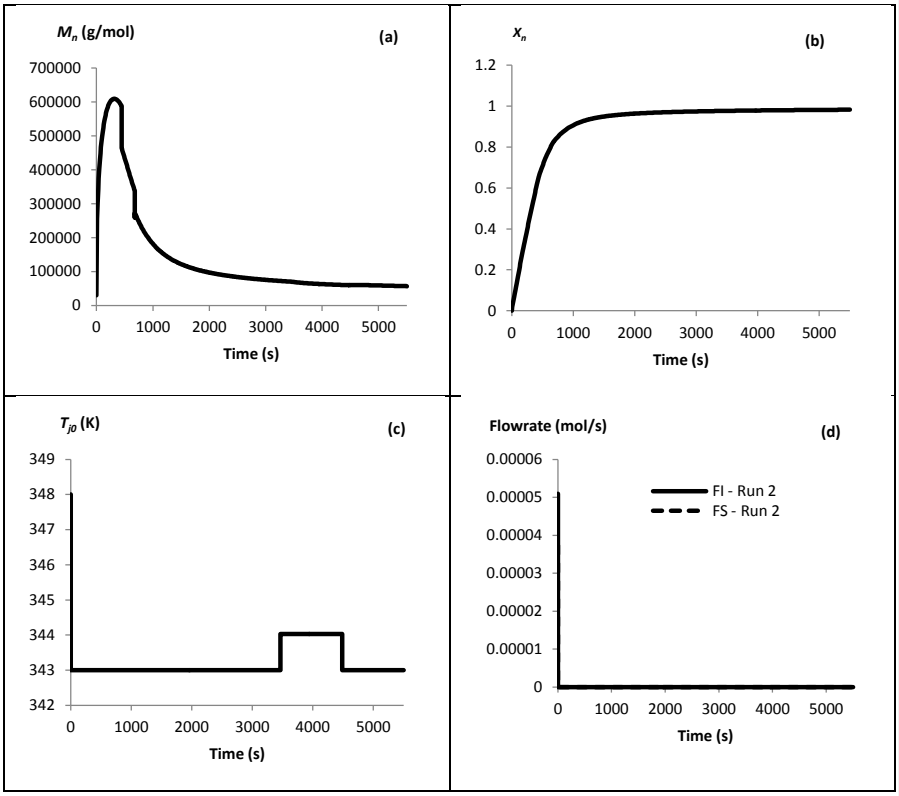

Figure 24: Result case study 7 (Run 2); (a) overall conversion (X_n); (b) number average molecular weight (M_n); (c) jacket temperature (T_{j0}); (d) optimal profile of surfactant flow rate (F_S) and optimal profile of initiator flow rate (F_I).

Case study 7: run 3

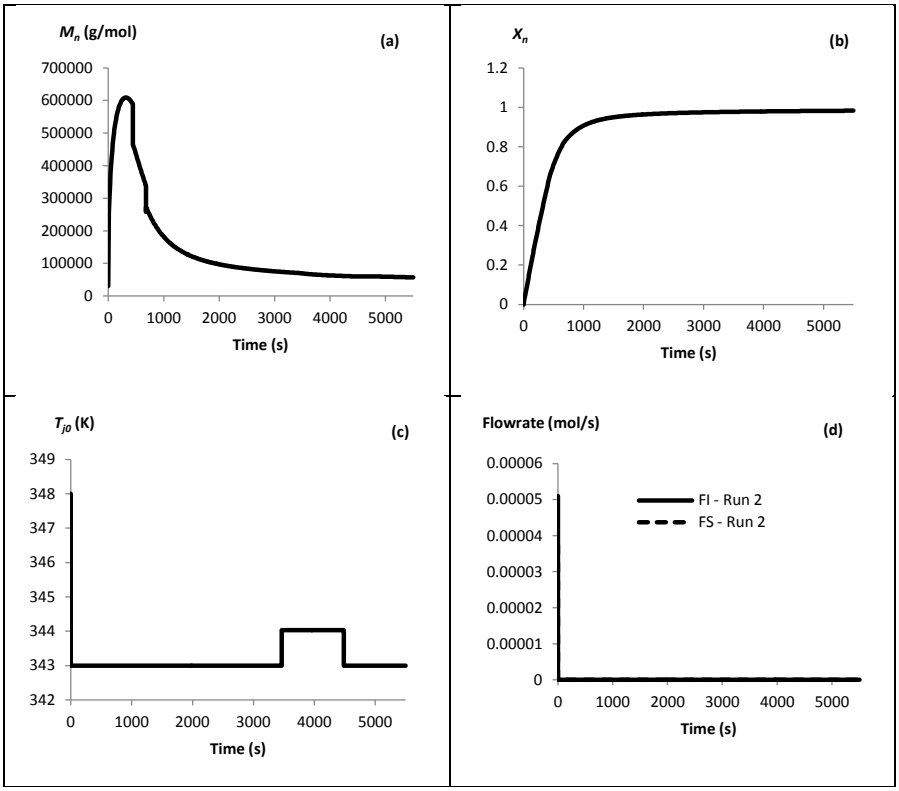

Figure 25: Result case study 7 (Run 2); (a) overall conversion (X_n); (b) number average molecular weight (M_n); (c) jacket temperature (T_{j0}); (d) optimal profile of surfactant flow rate (F_S) and optimal profile of initiator flow rate (F_I).

APPENDIX 7

Typical gPROMS Models

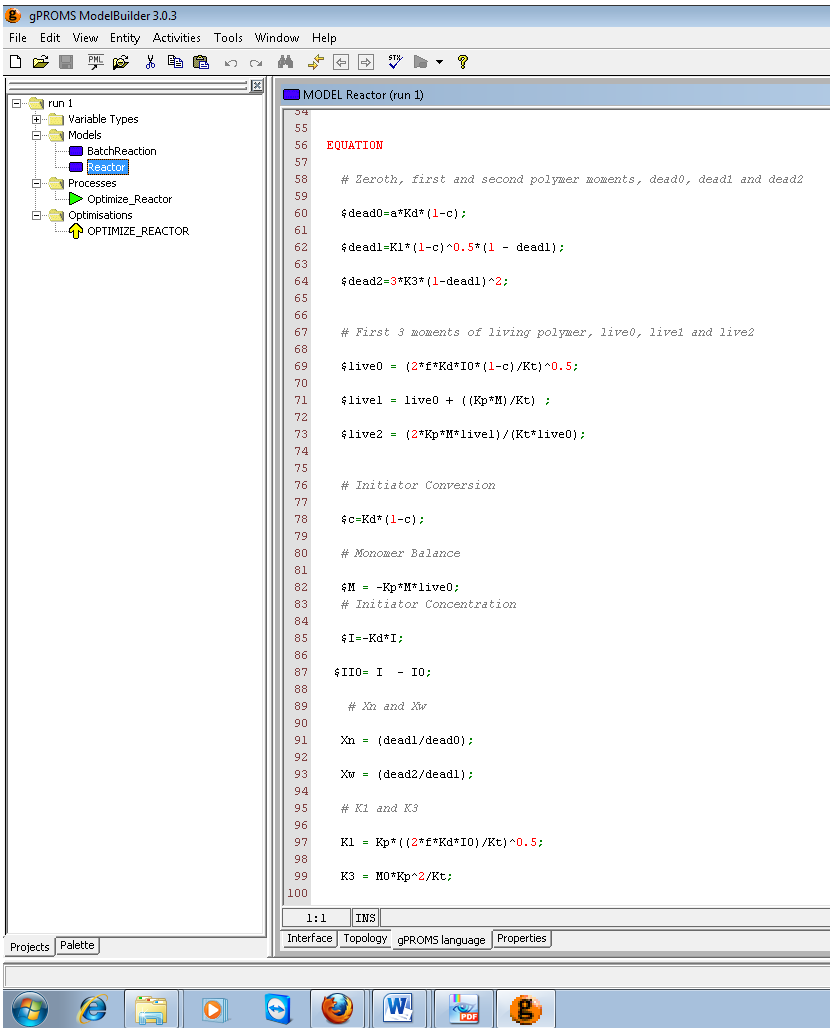

Figure 26: gPROMS Model Builder Window for bulk polymerization of styrene

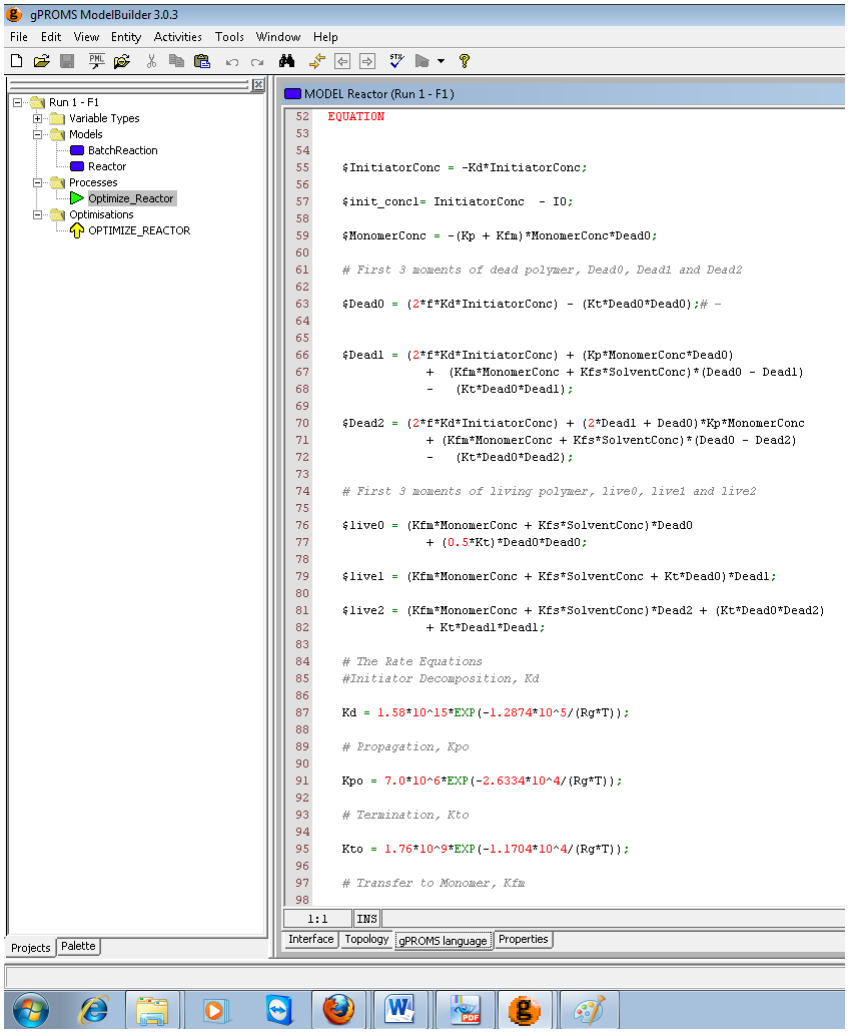

Figure 27: gPROMS Model Builder Window for solution polymerization of MMA

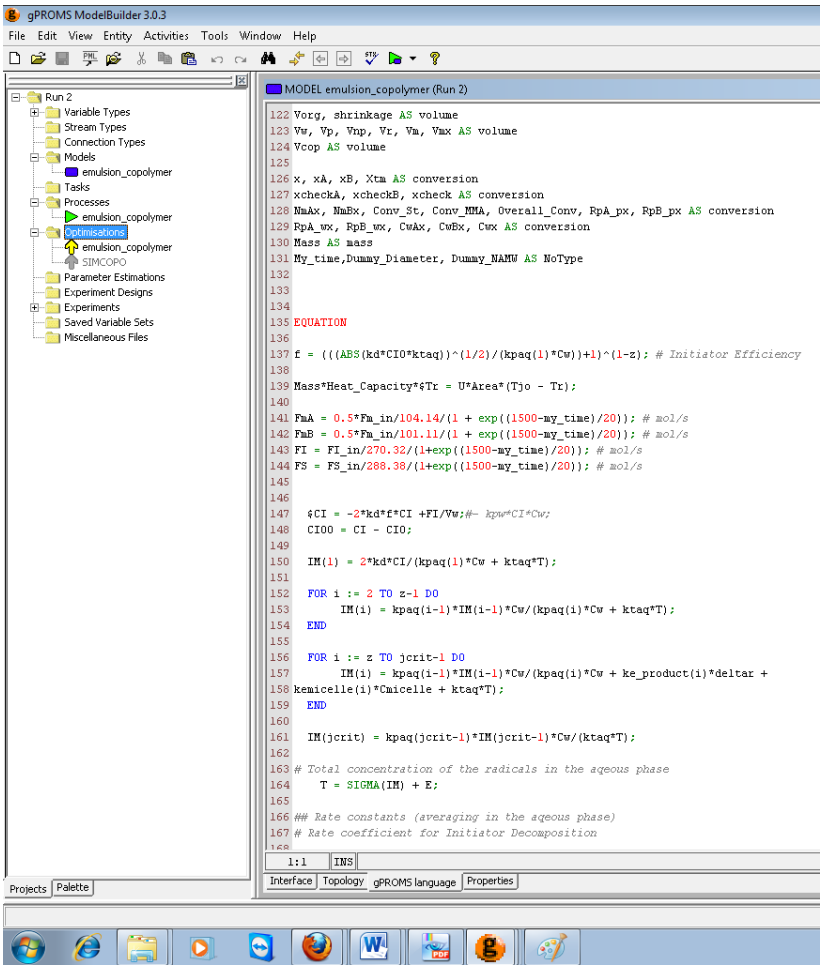

Figure 28: gPROMS Model Builder Window for emulsion copolymerization of styrene and MMA